Universidade de Aveiro Departamento de Biologia
2018

Cátia Sofia Silva Vieira

Antimicrobial photodynamic therapy potentiation by potassium iodide.

Potenciação da terapia fotodinâmica antimicrobiana por iodeto de potássio

DECLARAÇÃO

Declaro que este relatório é integralmente da minha autoria, estando devidamente referenciadas as fontes e obras consultadas, bem como identificadas de modo claro as citações dessas obras. Não contém, por isso, qualquer tipo de plágio quer de textos publicados, qualquer que seja o meio dessa publicação, incluindo meios eletrónicos, quer de trabalhos académicos.

Universidade de Aveiro Departamento de Biologia
2018

Cátia Sofia Silva Vieira

Antimicrobial photodynamic therapy potentiation by potassium iodide.

Potenciação da terapia fotodinâmica antimicrobiana por iodeto de potássio

Dissertação apresentada à Universidade de Aveiro para cumprimento dos requisitos necessários à obtenção do grau de Mestre em Microbiologia, realizada sob a orientação científica da Professora Doutora Maria Adelaide de Pinho Almeida, Professora Auxiliar com agregação do Departamento de Biologia da Universidade de Aveiro, e co-orientação da Professora Doutora Maria do Amparo Ferreira Faustino, Professora Associada com Agregação do Departamento de Química da Universidade de Aveiro.

This work was supported by funding FEDER through COMPETE – Programa Operacional Factores de Competitividade, and by National funding through Fundação para a Ciência e Tecnologia (FCT) and Marine Studies (CESAM).

Dedico este trabalho à minha mãe e irmãos.

o júri

presidente

Prof. Doutor Artur Jorge da Costa Peixoto Alves
Investigador Principal do Departamento de Biologia da Universidade de Aveiro

Prof. Doutora Maria Adelaide Pinho de Almeida (Orientadora)
Professora Auxiliar com Agregação do Departamento de Biologia da Universidade de Aveiro

Prof. Doutora Ana Cristina de Fraga Esteves
Professora Auxiliar Convidada do Instituto de Ciências da Saúde, Universidade Católica Portuguesa

agradecimentos

Esta seção foi reservada para agradecer a todos os que contribuíram de alguma forma para a realização deste trabalho.

À Professora Doutora Adelaide Almeida, pela orientação, ajuda, incentivo, apoio e paciência dedicados durante este trabalho.

Às Professoras Doutora Maria do Amparo Faustino e Maria da Graça Neves, pela orientação e auxílio na execução da dissertação.

Aos professores e alunos do grupo de Química Orgânica do Departamento de Química da Universidade de Aveiro pela cedência dos fotossensibilizadores usados neste trabalho, ajuda e prestabilidade. Faço um especial agradecimento à Mariana Mesquita, pela sua paciência e amabilidade.

Aos colegas do Laboratório de Microbiologia Aplicada que sempre estiveram disponíveis para aconselhar e auxiliar. Em especial à Sofia, à Vera, à Maria e à Lúcia, por todo apoio, orientação e incentivo que recebi durante este percurso.

À Ana Gomes pela ajuda preciosa na minha tese, pelas suas correções, orientação e conselhos.

À Adriele pelo acompanhamento, dedicação, companheirismo e docinhos. Sem si seria impossível realizar a segunda parte do trabalho.

Ao Miguel, pela paciência, carinho, apoio, e risadas que me permitiram continuar e concluir este trabalho.
À minha mãe, ao meu irmão Jorge e irmã Sandra, pela preocupação, apoio, e ajuda que me deram ao longo de toda a minha formação académica.

Aos meus amigos e família, que mesmo indiretamente fizeram parte deste percurso.

palavras- chave

Terapia fotodinâmica antimicrobiana, porfirinas catiónicas, corantes fotosensibilizadores, iodeto de potássio, *Escherichia coli*, *Staphylococcus aureus*, *Candida albicans*, Bacteriófago T4, células planctónicas, biofilmes

Resumo

O aumento e disseminação da resistência a antimicrobianos torna necessário o procura de novas estratégias para combater infeções não tratáveis e muitas vezes mortais, causadas por microrganismos quer na forma planctónica quer organizados em biofilmes. A terapia fotodinâmica antimicrobiana tem-se revelado uma alternativa capaz de inativar microrganismos, independentemente do seu perfil de resistência aos antimicrobianos convencionais. Contudo, a baixa eficácia de fotosensibilizadores (PS) neutros e aniónicos na inactivação de bactérias de gram-negativo e fungos, bem como os elevados custos de produção e purificação associados, tem exigido à comunidade científica encontrar moleculas ou coadjuvantes que permitam aumentar a fotoinactivação microbiana (aPDT) e com diminuição dos custos associados quer pela diminuição da quantidade de composto aplicado quer pela diminuição do tempo de tratamento.

Estudos recentes, demonstraram que o iodeto de potássio (KI), um sal inorgânico, é capaz de potenciar o efeito de alguns PS porfirínicos e não porfirínicos catiónicos e não catiónicos. Estes estudos mostraram sempre nos PS testados um efeito potenciador do KI. Assim, o presente trabalho teve como objectivo determinar as características dos PS que influenciam o efeito potenciador do KI, usando para tal PS com características diferentes. Para tal, foram realizados ensaios de aPDT usando como modelo uma estirpe de *Escherichia coli* bioluminescente. Nestes ensaios o KI (50 mM e 100 mM) foi testado na presença de diferentes PS porfirínicos catiónicos substituídos quer em posições *meso* (incluindo uma formulação constituída por uma mistura de cinco porfirinas - FORM) quer nas posições β-pirrólicas, e PS não porfirínicos [Azul de metileno (MB), Rosa Bengal (RB), Azul de Toluidina (TBO), Violeta Cristal (CV) e Verde de Malachita (MG)]. Os resultados evidenciam que o KI é capaz de potenciar o efeito antibacteriano da maior parte dos PS testados, permitindo reduzir ainda o tempo de irradiação necessário para produzir o efeito fotodinãmico desejado. Contudo, não se observa o efeito potenciador do KI quando combinado com todos os PS porfirínicos e não-porfirínicos. Uma comparação dos resultados obtidos com os da literatura permite confirmar que o efeito potenciador quando o sal KI é combinado com um PS depende da produção de oxigénio singleto ($^1O_2$) por parte do PS, da sua estrutura (número de cargas e a sua posição espacial), da sua tendência para agregar e da sua afinidade para com as estruturas externas dos microrganismos.

Resumo (continuação)

Na segunda fase do trabalho pretendeu-se avaliar a capacidade da formulação porfirínica (FORM, de fácil preparação e obtenção comparativamente com as respectivos constituintes puros), e da combinação da FORM com KI (100 mM) na inativação de vários microrganismos (bactérias e fungos) quer na forma planctónica quer em biofilmes. Para tal, foram realizados ensaios com os seguintes microrganismos: *E. coli* resistente ao clorofenicol e à ampicilina (bactéria de gram-negativo), *Staphyloccocus aureus* resistente à meticilina (bactéria de gram-positivo), o fungo *Candida albicans;* quer na forma livre quer em biofilmes; bem como um bacteriófago tipo T4, utilizado como modelo de vírus humano. Os resultados obtidos mostraram que a FORM isoladamente é eficaz na inativação de bactéias, fungos e vírus na sua forma planctónica, e quando usada em combinação com o KI o seu efeito antimicrobiano é intensificado.

A combinação da FORM com o KI foi também eficaz na destruição de biofilmes bacterianos e fúngicos, e evitou a formação de biofilmes bacterianos, o que não se verifica quando a FORM foi utilizada isoladamente.

A utilização da FORM combinada com KI em aPDT permitiu reduzir a concentração de PS e o tempo de tratamento o que facilitará possíveis aplicações quer na clínica quer no ambiente.

keywords

Antimicrobial photodynamic therapy, cationic porphyrins, photosensitizer, dyes, potassium iodide, *Escherichia coli*, *Staphylococcus aureus*, *Candida albicans*, Bacteriophage T4, planctonic cells, biofilms

Abstract

With the global increasing and spreading of antibiotic-resistant microorganisms, there is a need to develop strategies capable of inactivating plantonic and biofilm-forms of pathogenic microorganisms that causes untreatable and mortal infections. Antimicrobial photodynamic therapy (aPDT) is an alternative approach capable of combating microorganisms independently of their resistance profile. Althought this technique presents great results and advantages, the neutral and monocationic photosensitizers (PS) do not usually kill efficiently gram-negative bacteria and fungi, and their synthetic preparation are usually expensive and laborious. In this context, it is needed to develop new approaches that can improve the antimicrobial effect of a PS and simultaneously to allow the decrease of the applied PS concentration and also of the treatment time. Recent studies have reported a enhancer effect on antimicrobial photoinactivation by the combined used of some PS and potassium iodide (KI), an inorganic salt. These studies have always shown potentiating effect of KI for the tested PS. The main goal of this work was, in a first phase, to achieve an insight into the KI potentiation effect on diferent groups of PS; tetraarylporphyrins positively charged at *meso* (including a formulation consisting of five cationic porphyrins - FORM) or β-pyrrolic positions and non-porphyrinic dyes, using a bioluminescent *Escherichia coli* as bacterial model. The results of these studies pointing out that the presence of KI can enhance the aPDT killing effect of some PS, but this enhancement is not general for all PS. The comparison of the obtained results with the ones from the literature allowed to confirm that the enhance effect of KI is related to the generation of $^1O_2$ by PS, PS structure (charge number and charge position), aggregation behavior and its affinity for the external structures of the microorganisms.

In a second phase, the aPDT effect of the FORM (easy to prepare when compared with their corresponding porphyrins that constitute the mixture in the pure form) and of its combined effect with KI (100mM) on planktonic and biofilm forms of a broad-spectrum of microorganisms. Therefore, this study was performed on the free and biofilms forms of gram-negative and gram-positive bacteria: E. coli resistant to chloramphenicol and ampicillin, and Staphylococcus aureus resistant to methicillin (MRSA), of the fungi Candida albicans as well as on the free-form of a T4 like bacteriophage as a model of human viruses.

Abstract (continuation)

The results of these experiments demonstrated that FORM is efficient on inactivating planktonic forms of bacteria, fungi and viruses and that when combined with KI was clearly more effective to inactivate all the microorganisms. This combination allows also to destroy efficiently the preformed biofilms of bacteria and fungi and avoided also the formation of *E. coli* and *S. aureus* biofilms, contrarily to that observed with FORM but without KI. The use of FORM combined with KI allowed to reduce PS concentration and the treatment time which will promote to transpose the aPDT to the clinic or environment fields.

Contents

List of abreviations ..... i-ii
List of figures ..... iii – iv
List of tables v
Objectives and thesis outline 1
Manuscripts already published: .....
CHAPTER I – Introduction 5
1.1. Antimicrobial photodynamic therapy (aPDT) as alternative to antibiotics 8
1.2. Photodynamic Mechanism 10
1.3. aPDT - a board-spectrum microorganisms approach 11
1.4. Light sources 14
1.5. Photosensitizers 14
1.6. Potentiation of aPDT by KI 18
1.7. Mechanism of the combined approach – PS + KI 20
1.8. Objectives 21
1.9. References .....
CHAPTER II: An insight on aPDT efficacy of photosensitizers mediated by potassium iodide 35
2.1. Abstract 37
2.2. Introduction 38
2.3. Materials and Methods 45
2.3.1. Photosensitizers: stock solutions and UV-Vis spectra 45
2.3.2. Light sources 45
2.3.3. Bacterial strains and growth conditions 46
2.3.4. Antimicrobial Photodynamic Therapy (aPDT) Procedure 46
2.3.4.1. Bioluminescence monitoring 46
2.3.4.2. Evaluation of the inorganic salt effect on Tetra-Py(+)-Me photodynamic action 47
2.3.4.3. Evaluation of the antimicrobial effect in the presence of different PSs and KI 47
2.3.5. Detection of iodine formation 48
2.3.6. Statistical analysis 48
2.4. Results 49
2.4.1. Evaluation of the salt effect on Tetra-Py(+)-Me photodynamic efficiency. 49
2.4.2. Evaluation of the KI effect on the photodynamic action of *meso* tetraarylporphyrins bearing one to four positive charges 50

2.4.3. Evaluation of the KI effect on the photodynamic action of porphyrin derivatives bearing cationic imidazole units at the β-pyrrolic position 53
2.4.4. Evaluation of the KI effect in the photodynamic action of non-porphyrinic dyes 55
2.4.5. Detection of iodine formation mediated by the PS 56
2.5. Discussion 61
2.6. References 66
CHAPTER III: Advances in the photoinactivation by a cationic porphyrinic formulation with potassium iodide: effectiveness on planktonic and biofilm forms of bacteria, viruses and fungi. 75
3.1. Abstract: 77
3.2. Introduction 78
3.3. Material and methods 81
3.3.1. Photosensitizer and KI solution 81
3.3.2. Characterization of microbial strains 82
3.3.3. Microbial grown conditions 82
3.3.4. Light sources 83
3.3.5. Photodynamic inactivation essays 83
3.3.6. Planktonic cells Treatment 84
3.3.7. Formed Biofilm Cells Treatment 85
3.3.8. Biofilm Formation Cells Treatment 85
3.3.9. Statistics 86
3.4. Results and Discussion 86
3.4.1. Photoinactivation of planktonic cells with combinations of FORM and KI 86
3.4.2. Photoinactivation of biofilms with combinations of FORM and KI 93
3.4.3. Prevention of biofilms development through aPDT with combinations of FORM and KI 96
3.5. Conclusion 99
3.6. References 99
Chapter IV: General Conclusions and Future Perspectives 105
4.1. Conclusions 107
4.2. Future perspectives: 109
Appendix I 111

List of abbreviations

$^1O_2$	Oxygen Singlet
A. baumannii	*Acinetobacter baumannii*
Amp	Ampicillin
aPDT	Antimicrobial Photodynamic Therapy
CFU	Colony Forming Units
Cm	Chloramphenicol
CV	Crystal Violet
DC	Dark Control
Di-Py(+)-Me adj	5,15-bis(1-methylpyridinium-4-yl)-10,20-bis(pentafluorophenyl)porphyrin di-iodide
Di-Py(+)-Me opp	5,10-bis(1-methylpyridinium-4-yl)-15,20-bis(pentafluorophenyl)-porphyrin di-iodide
DMSO	Dimethyl sulfoxide
E. coli	*Escherichia coli*
EDTA	Ethylenediaminetetraacetic acid
$I_2^{\cdot -}$	Free Iodine radical
I_2/I_3^-	Iodine species
KI	Potassium Iodide
LC - Bacteria	Light Control – Bacteria
LC – KI	Light Control – Potassium Iodide
MB	Methylene Blue
MDR	Multidrug Resistant
MG	Malachite Green
Mono-Py(+)-Me	5-(1-methylpyridinium-4-yl)-10,15,20-tris(pentafluorophenyl)-porphyrin iodide
NMB	New Methylene Blue
$O_2^{\bullet -}$	Superoxide Anions
$OH^{\bullet}$	Hydroxyl Radicals
PBS	Phosphate Buffered Saline solution
PFU	Plaques Forming Units
PS	Photosensitiser
Psa	*Pseudomonas syringae* pv. a*ctinidiae*
RB	Rose Bengal
RLU	Relative Light Units
ROS	Reactive Oxygen Species
rpm	Revolutions per Minute
S. aureus	*Staphylococcus aureus*
TBO	Toluidine 0
Tetra-Py	5,10,15,20-tetra-(4-pyridyl)porphyrin
Tetra-Py(+)-Me	5,10,15,20-tetrakis(1-methylpyridinium-4-yl)porphyrin tetra-iodide

$TPPS_4$	5,10,15,20-tetrakis(4-sulfonatophenyl)porphyrin dihydrochloride
$TMPyP_4$	5,10,15,20-tetrakis(1-methylpyridinium4-yl)porphyrin tetratosylate
Tri-Py(+)-Me	5,10,15-tris(1-methylpyridinium-4-yl)-20-(pentafluorophenyl)porphyrin tri-iodide
TSA	Tryptic Soy Agar
TSB	Tryptic Soy Broth

List of figures

Figure 1.1. Jablonski diagram showing photodynamic mechanism and respective pathways 11

Figure 1.2. Cellular structure differences of three microorganisms: Gram- positive bacteria, Gram negative bacteria and Fungi. 13

Figure 1.3. Structure of three complex viruses: bacteriophage T4, adenovirus and human immunodeficiency virus (HIV).. 13

Figure 1.4. Hematoporphyrin and the general tetrapyrrolic structure of porphyrins, chlorins and phthalocyanines. 15

Figure 1.5. Structure of some non-porphyrinic dyes. Phenothiazinium: MB and TBO. Triarylmethane: CV and MG. Xanthene: Rose Bengal. 15

Figure 1.6. The porphyrin structure substituted at meso and beta–positions 16

Figure 1.7. Structure of porphyrins constituting FORM 17

Figure 1.8. Representation of the mechanism responsible for iodine reactive species formation 20

Figure 1.9. The distinct killing curve profiles produced by free iodine (I_2) and reactive iodine ($I2^{\bullet-}$) species. 21

Figure 2.1. Schematic representation of the decomposition of peroxyiodide

Figure 2.2. Structures and acronyms/abbreviations of the PSs used in this study... 44

Figure 2.3. Survival of bioluminescent *E. coli* during aPDT with Tetra-Py-(+)-Me and KI, NaI, KCl, NaCl, and NaBr..... 50

Figure 2.4. Survival of bioluminescent *E. coli* during aPDT assays in the presence of Mono-Py(+)-Me, Di-Py(+)-Me opp, Di-Py(+)-Me adj, Tetra-Py(+)-Me, Tri-Py(+)-Me, Form, and Tetra-Py 53

Figure 2.5. Survival of bioluminescent *E. coli* during aPDT assays in the presence of mono-cationic porphyrins β-ImiPhTPP, β-ImiPyTPP, and β-BrImiPyTPP 54

Figure 2.6. Survival of bioluminescent *E. coli* during aPDT assays in the presence of non-porphyrinic PSs: RB, TBO, MB, CV, and MG 56

Figure 2.7. Monitoring of the formation of iodine at 340 nm after different irradiation periods in the presence of each PS 57

Figure 2.8. Visual appearance of the starch solutions after different irradiation periods in the presence of each PS and KI. 60

Figure 3.1. Structure of porphyrin derivatives present in FORM. 81

Figure 3.2. Photodynamic inactivation of planktonic forms of *E. coli* by combination of KI and FORM 88

Figure 3.3. Photodynamic inactivation of planktonic forms of *S. aureus* by combination of KI and FORM 89

Figure 3.4. Photodynamic inactivation of planktonic forms of C. albicans by combination of KI and FORM. 91

Figure 3.5. Photodynamic inactivation of planktonic forms of bacteriophage T4 by combination of KI and FORM.. 92

Figure 3.6. Photodynamic inactivation of biofilms of *E. coli*, *S. aureus* or C. albicans by ii FORM and KI 96

Figure 3.7. - Inactivation of *E. coli* planktonic cells and prevention of biofilms formation by FORM and KI 97

Figure 3.8. - Inactivation of *S. aureus* planktonic cells and prevention of biofilms formation by FORM and KI 97

List of Tables

Table 1.1 - Results obtained in the photoinactivation of bioluminescent *E. coli* using combinations of tested PSs and KI. 62

Objectives and thesis outline

This dissertation describes the research work regarding the antimicrobial photodynamic therapy (aPDT) potentiation by potassium iodide, in order to decrease the PS costs and to improve the effectiveness of this approach on, gram-negative and -positive bacteria, fungi and viruses.

The document is divided into four parts.

The first part (Chapter I), consists in an introduction regarding the theme. In this section it will be described the state of art and the concepts about antimicrobial resistance (problem to solve), the antimicrobial therapy photodynamic (aPDT) (solution). Additionally, it will be discussed the recent achievements concerning the combined used of KI with PS, and also the type of PS usually used in aPDT. A special attention will be given to an efficient PS formulation (FORM, based on the non-separated mixture of porphyrins), due to its role on the development of this work; this PS can be obtained in high yield and with a reduced production time when compared with other efficient PS (method to improve the solution).

The second part (Chapter II), provides an insight on aPDT efficacy of photosensitizers mediated by potassium iodide. This chapter corresponds to an article already published (Vieira *et al.* 2018) where it is described the work performed during the dissertation, the experimental setup design and results which enabled to identify the main structural characteristics and properties of PS (porphyrinics and non-porphyrinics derivatives) needed to obtain the KI potentiation effect.

The third part (Chapter III), consists on a study regarding a new insight on the photoinactivation of an efficient formulation based on cationic porphyrins (FORM) and the potentiation effect by potassium iodide, that was performed for planktonic and biofilms forms of a gram-negative bacteria (*Escherichia coli*), a gram-positive bacterium (*Staphylococcus aureus*) and a fungus (*Candida albicans*), as well as for a T4 like bacteriophage. In this study, the prevention of biofilms formation was also evaluated. FORM was chosen according to the results of the second chapter, and its advantages compared to other PS. This third Chapter is presented as an article to be further submitted.

The fourth part (Chapter IV) describes the main conclusions obtained in this experimental work and the perspectives for future work.

During the dissertation period, it was performed the biological assays of a series of β-functionalized porphyrin derivatives just with one positive charge, towards *Escherichia coli*, that appears included in the manuscript already published (Moura *et al.* 2019). A copy of this manuscript is presented as Appendix I of this document.

Manuscripts already published:

Moura, N.M.M., Esteves, M., Vieira, C., Rocha, G.M.S.R.O., Faustino, M.A.F., Almeida, A., Cavaleiro, J.A.S., Lodeiro, C. and Neves, M.G.P.M.S., **2019**. Novel β-functionalized mono-charged porphyrinic derivatives: Synthesis and photoinactivation of *Escherichia coli*. *Dyes and Pigments*, 160, 361–371.

Vieira, C., Gomes, A.T.P.C., Mesquita, M.Q., Moura, N.M.M., Neves, M.G.P.M.S., Faustino, M.A.F., and Almeida, A., **2018**. An Insight Into the Potentiation Effect of Potassium Iodide on aPDT Efficacy. *Frontiers in Microbiology*, 9 (November), 1–16.

CHAPTER I – Introduction

In 1950's, the discovering of the antibiotics was received as a miracle that allowed to treat infectious diseases during the Second World War. However, the incorrect prescription of antimicrobials in the last half-century for therapeutic purposes, agriculture and animal husbandry, among others, has led to a rapid increasing rate of antimicrobial resistance to many chemicals, including the drugs used as last resort on hospitals (Tenover and McGowan 1940). The dissemination of this resistance genes due to the global trading makes impossible to control this situation, of which results many dead people annually.

The infections caused by resistant microbes have a fewer probability of an effective treatment, which is related to a higher morbidity, mortality and economic costs. World Health Organization (WHO) has stated that more than 20 thousand deaths occur annually in the United States and in the European Union (WHO 2017).

Although the free form of microorganisms cause severe diseases, namely when multidrug resistant (MDR) strains are involved, approximately 80% of the bacterial and fungal infections that affects human are caused by microorganisms organized in biofilms (Høiby 2017). They are responsible for diverse infections, such as gingivitis, caries, catheter infections, urinary tract infection, contact lenses, endocarditis and infections in cystic fibrosis (Mysorekar and Hultgren, 2006; Belibasakis, Thurnheer and Bostanci, 2014; Bao et al., 2015; Bispo, Haas and Gilmore, 2015; Wu et al., 2015).

Biofilm consist on a microbial community attached to a surface, which are embedded in a matrix constituted by water and extracellular polymeric substances produced by individual cells (Hall-stoodley *et al.* 2004). They present several advantages compared to their planktonic equivalents, as they have a higher virulence, structural stability and adherence to the various surfaces. The higher diversity of species in a biofilm also facilitates the horizontal gene transference occurrence, and thus the acquisition of resistant phenotypes (Lewis 2001; Burmølle *et al*. 2006; Madsen *et al*. 2012; Wolcott *et al*. 2013). Additionally, some biofilms can shelter "persistent cells" that presents a low metabolic rate allowing it to survive to antibiotic treatments, and after gain activity enabling the disease persistence (Hobby *et al*., 1942; Bigger, 1944; Shah et al. 2006; Kwan et al. 2013; Conlon et al., 2016). These characteristics are related with an increased

resistant to the host immune response, antimicrobials and biocides (Stewart 2003, Wolcott and Ehrlich 2008).

Staphylococcus aureus, *Escherichia coli* and *Candida albicans* are some of the many microorganisms that frequently form biofilms and which resistance to antimicrobials has been increasing and causing elevated mortality and economic costs (Laxminarayan *et al*. 2016; Renwick *et al*. 2016; Perlin *et al*. 2017).

Viruses are microorganisms that infect theirs hosts and are incapable of producing biofilms similar to those from bacteria and yeasts. However, they are responsible for causing severe infections, and can also contribute to the development of cancer such as Epstein–Barr virus, papillomavirus, hepatitis B and C viruses, human T-lymphotropic virus and Kaposi's sarcoma-associated herpes virus. Its rapid mutation associated with a high genetic flexibility has led to the devolvement of resistance to antiviral treatments (Pulitzer, Amin and Busam, 2009).

1.1. Antimicrobial photodynamic therapy (aPDT) as alternative to antibiotics

Due to the high incidence of MDR microorganisms, it is necessary to develop alternative approaches to combat infections. In this context, the antimicrobial photodynamic therapy, aPDT, arises as an alternative to chemotherapy.

In 1890, aPDT was discovered when the medical student Oscar Raab observed that *Paramecium* spp. stained with acridine orange (a dye) was destroyed when exposed to light but remained alive if they were kept in the dark. Afterward, his professor Von Tappeiner demonstrated that the oxygen is essential for this phenomenon and gave it the term "Photodynamic action" (Lobanovska and Pilla 2017).

Contrary to the expected, with the discover and commercialization of penicillinic antibiotics, there was a loss of interest on testing and applying PDT to combat microbial infections. Instead, this approach began firstly to be tested on tumoral cells. In fact, Thomas Dougherty and co-workers, published in 1978 the first article about PDT to treat cutaneous or subcutaneous malignant tumors by using hematoporphyrin derivative as

photosensitizer (PS) (Lobanovska and Pilla 2017). Some years latter a formulation based on this PS (Photofrin®) was approved for clinical use. Since that time, PDT has been applied to treat cancer diseases as actinic keratosis or basal cell carcinoma.

However, with a higher incidence and spreading of antimicrobial resistant microorganisms, this therapy re-emerged to combat microbial infections (Wainwright 2016, Wainwright *et al.* 2016). aPDI is an effective and non-evasive approach to inactivate a broad-spectrum of microorganisms such as bacteria, fungi, protozoa and viruses (Alves *et al.* 2008, Alves, Costa, *et al.* 2011, Costa, Faustino, *et al.* 2012, Costa, Gomes, *et al.* 2012, Wainwright 2016). It is based on a non-toxic dye, referred as the photosensitizer (PS), which after being activated in the presence of visible light is able to generate high cytotoxic reactive oxygen species (ROS) such as free radicals and singlet oxygen. These species are short-lived, whereby the killing effect only occurs during the illumination step. The oxidative damages promoted by ROS take place on the external and internal structure of microorganisms, occurring the oxidation of lipids, proteins, degradation of essential enzymes, and damage of the nucleic acids (DNA/RNA) that cause morphological changes and disturb its functionality (Zúpan *et al*. 2008; Calin and Parasca 2009; Alves *et al*. 2014; Almeida et al2015; Wainwright *et al*. 2016).

Comparatively to conventional antimicrobials, aPDT has many advantages. It is a safe approach capable of inactivate microorganisms independently of their resistance profile. This approach also displays fewer adverse and mutagenic effects, invasiveness and short time treatment when compared with the classical antimicrobial treatments. Being a multi-target therapy, affects several components of microbial external structure and it is efficient on a broad-range spectrum of microorganisms, such as bacteria, viruses, fungi and parasites. The multi target characteristic combined to the lack of protection against singlet oxygen, the most important ROS in aPDT, is related with a low probability of development of resistance after the treatment. (Wainwright *et al*, 2017; Alves, Faustino, Neves, Cunha, *et al*. 2014; Almeida *et al*. 2009). Even though the microbes can produce enzymes such as superoxide dismutase, catalase and peroxidase to protect them self from some ROS produced by mechanism type I, it was demonstrated that singlet

oxygen can inactivate these enzymes (Nitzan *et al.* 1989, Mtiller-breitkreutz *et al.* 1995, Hadjur *et al.* 1998, Wainwright and Crossley 2004, Maclean *et al.* 2008).

1.2. Photodynamic Mechanism

Firstly, the PS can have different excited states. In the dark, the PS remains in a singlet ground state (S_0), a state of lower energy. When exposed to light, the PS absorb photons and it is promoted to a higher energy level (S_n). Since this excited state is unstable and consequently have a short-lifetime (μs) can lose the excess of energy by emitting light (as fluorescence), as heat or can undergo an intersystem crossing process giving rise to an excited triplet-state (T_1) with longer-lifetime than the previous one (Ochsner 1996, Juzeniene and Moan 2007) (Figure 1.1). Afterwards, the photodynamic mechanism can occur by two distinct pathways; Type 1 and Type 2 (Figure 1.1).

Type 1: the PS in the triplet state reacts with a substrate by transferring a hydrogen atom or an electron to form free radicals. These free radicals can give origin to reactive oxygen species (ROS) by interacting with molecular oxygen (O_2). Posteriorly, hydrogen peroxide (H_2O_2) can be produced by the reaction between the superoxide anions ($O_2^{\bullet -}$) and water (Sharman *et al.* 1999, Takasaki *et al.* 2009).

Type 2: The PS in the triplet state reacts with the molecular oxygen (O_2), transferring energy to it and giving rise to singlet oxygen - $^1O_2$. This specie is the most important ROS produced by the photodynamic approach for which no mechanism of resistance has been reported. It is a highly reactive oxygen species that has a short-lifetime span, being its half-life time of approximately 40 ns, allowing its interaction with the surrounding in a short radius of ~ 20 nm (Moan and Berg 1991, Sharman *et al.* 1999).

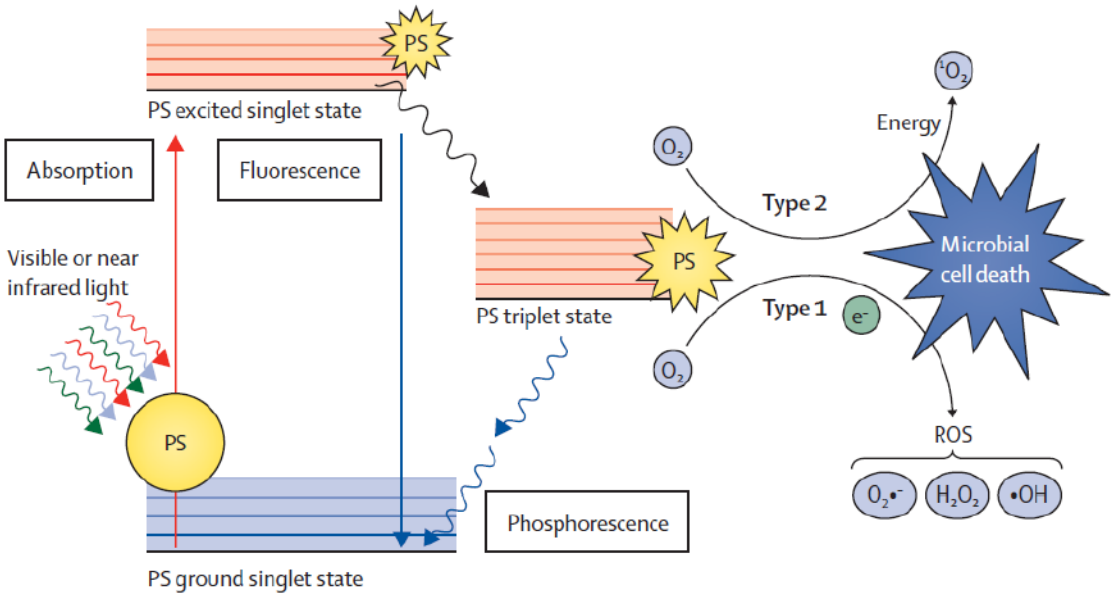

Figure. 1.1 – Jablonski diagram showing photodynamic mechanism and respective pathways (Type 1/I and 2/II) (adapted from Wainwright, 1998).

1.3. aPDT - a board-spectrum microorganisms approach

The distinct classes of microorganisms have a different cellular organization that influence the outcome of an aPDT treatment. For most of the microorganisms, the inactivation occurs when the PS adheres to the external structures as the cell membrane (bacteria, fungi and parasites) and protein capsid or envelope (viruses), and after can enter in the microorganism to create a continuous damage (Hamblin and Hasan 2004). However, the ligation of PS to the external components of Fungi is less important, because the free PS is capable of oxidize the cell membrane enabling its entrance with progressive aPDT action inside the cell (Zambotto *et al.* 1987, Kassab *et al.* 2003).

For bacteria, the differences between the cell walls of gram-positive and gram-negative bacteria have a high influence in the microbe vulnerability to aPDT (Figure 1.2 - A and B). The inactivation of gram-positive bacteria is easier due to their porous layer that gives it a higher permeability than the gram-negative cell (Minnock *et al.* 2000). The gram-positive and -negative bacteria both possess a cytoplasmatic membrane, that in the first case is surrounded by a thick and porous peptidoglycan layer, and in the second

presents a thin layer of peptidoglycan between the outer membrane and the cytoplasmatic membrane (Bourr *et al.* 2010, Sperandio *et al.* 2013). The double layer cell wall of the gram-negative bacteria makes these microbial more impermeable to chemicals than the cell walls of gram-positive bacteria. During an aPDT treatment, the binding of PS to the external cellular components is essential, and afterwards, it can penetrate it until arrive the cytosol.

Fungi have a different structure composed by an outer layer moderately porous of β- β-1,6 glucan and mannan polysaccharides and an inner layer of chitin, which gives it an intermediate permeability between gram-positive and gram-negative bacteria (Denis *et al.* 2011). However, Fungi are compartmented and have a larger size than bacteria which difficults their inactivation relatively to the bacteria (Demidova and Hamblin 2005) (Figure 1.2 C).

Viruses are surrounded by a protein capsid or by a lipidic envelope, which are attacked by ROS with leakage of viruses' components and/or the dysfunctionality of enzymes. It has been shown that the non-enveloped viruses are more resistant than the enveloped ones (Abe and Wagner 1995, Zúpan *et al.* 2008, Jori *et al.* 2011, Sieber 2014) (Figure 1.3).

Biofilms have less susceptibility to aPDT than their planktonic forms, with a higher PS quantity needed to achieve the inactivation. This is explained by its rapid cell growing and the existence of a polysaccharide intercellular adhesin (PIA) that acts as a barrier to the PS and light entry (Costerton *et al.* 1999, Usacheva *et al.* 2001, Gad *et al.* 2004, Zanin *et al.* 2006).

Depending on how the PS penetrated the biofilm, it can suffer matrix, membrane cellular or intercellular damage (Merchat *et al.* 1996, Soukos *et al.* 1998, Shrestha *et al.* 2010, Lam *et al.* 2011, Garcez *et al.* 2013, Luke-marshall *et al.* 2014, Nanoparticles *et al.* 2014).

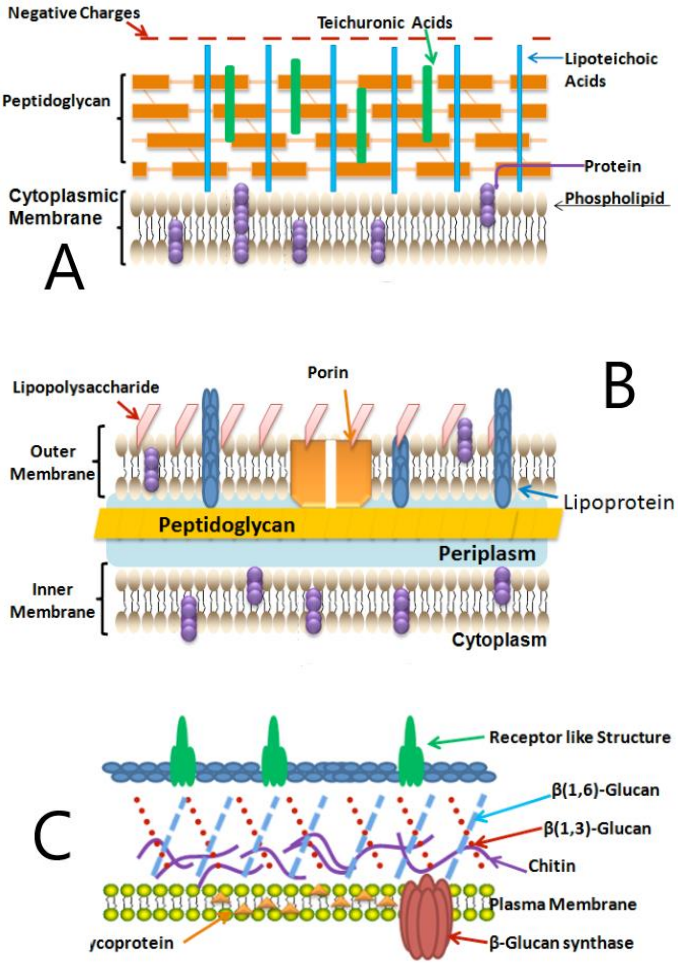

Figure 1.2. Cellular structure differences of three microorganisms: A) - Gram- positive bacteria; B) – Gram negative bacteria; C) – Fungi. (Kashef *et al.* 2017)

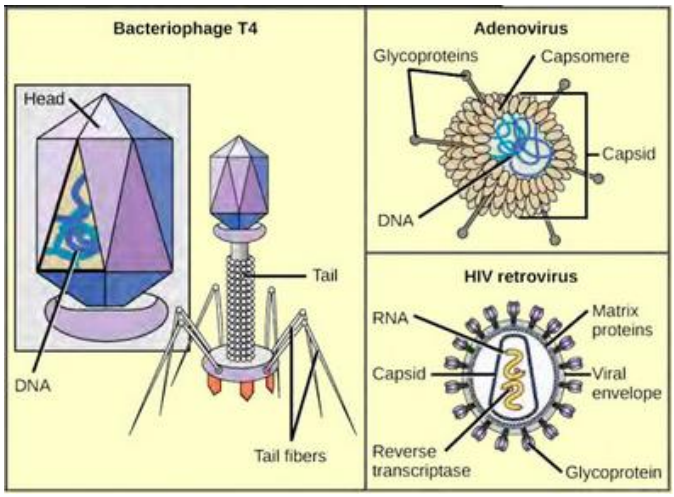

Figure 1.3. Structure of three complex viruses. A)- Bacteriophage (Phage) T4; B) – Adenovirus; C)- Human immunodeficiency virus (HIV).(Fowler *et al.* 2008)

1.4. Light sources

An aPDT treatment requires a light source with an emission spectrum adequate to the PS. The light induces PS photoactivation if its absorption peaks overlap with the spectrum of the light source. A light source must be selected considering the application, its advantages and limitations. Sunlight, halogen or fluorescent lamps, LEDs and lasers are common light sources applied on aPDT. As example, the sunlight is excellent to inactivate microbial cells in environmental applications. Halogen and fluorescent lamps as well as LEDs are cheaper light sources than lasers but due to the fact that are not monochromatic lights it is harder to control the effective light dose applied. The aPDT effects increase with the increase of irradiation time and intensity of light. When aPDT is applied on tissues a low potent light should be chosen, as a high level of energy can provoke thermogenesis (Castano, Demidova, and Hamblin 2005; Takasaki *et al*. 2009; Costa *et al*. 2010; Alves *et al*. 2014).

1.5. Photosensitizers

The first PS to be clinic used was hematoporphyrin derivative (Figure 1.4). Afterwards, this compound served as mould to the preparation of new PS namely for the tetrapyrrolic ones - porphyrins, chlorins, phthalocyanines, among others (Figure 1.4). However, well-known dyes of other classes as: phenothiazinium (methylene blue - MB), triarylmethane (e.g. malachite green - MG, crystal violet - CV) and xanthene (acridine orange - AO, rose bengal - RB) derivatives (Figure 1.5) are also meriting the attention of the scientific community in PDT applications (Derosa and Crutchley 2002, Flors and Nonell 2006, Almeida *et al.* 2011, Mizuno *et al.* 2011, Regensburger *et al.* 2011, Mesquita *et al.* 2013, Tortik and Plaetzer 2014, Spaeth *et al.* 2017).

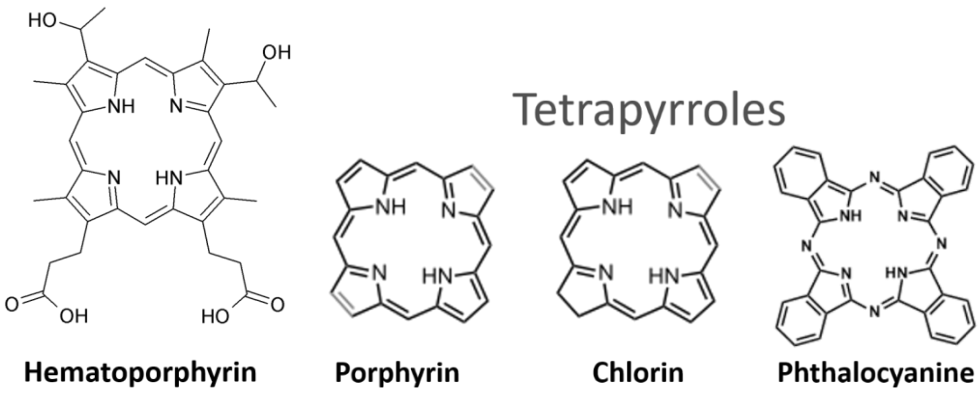

Figure 1.4 - Hematoporphyrin and the general tetrapyrrolic structure of porphyrins, chlorins and phthalocyanines.

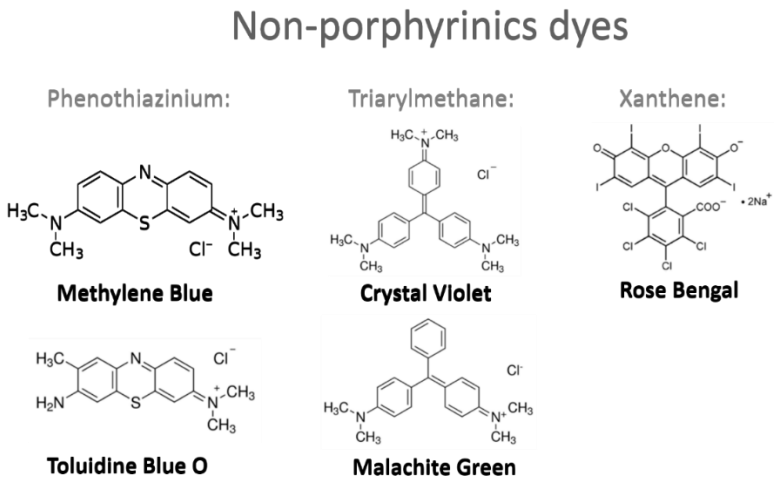

Figure 1.5 - Structure of some non-porphyrinic dyes. Phenothiazinium: MB and TBO. Triarylmethane: CV and MG. Xanthene: Rose Bengal.

The PS commonly used in aPDT are the MB and the TBO due to the fact they are very accessible. These phenothiazinium dyes have one positive charge and are constituted by a three-ring π-system with auxochromic side groups (Wainwright 1998, 2000, Gollmer 2014).

The tetrapyrrolic PS can be extracted from natural sources or synthetized in laboratory and are constituted by four pyrrole type units linked by methinic bridges (Fernandez *et al.* 1997). The tetrapyrrolic macrocycle like porphyrins can have substituents at the *meso*-positions and/or at *beta*–positions (Figure 1.6). The preparation of *beta*-substituted porphyrins can involve more synthetic steps than those conducting to the *meso*-substituted porphyrins (Li and Diau 2013).

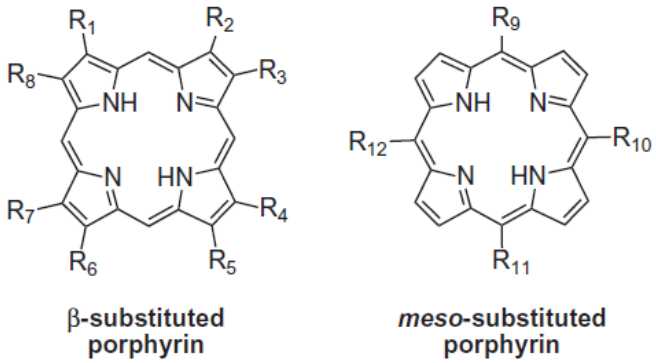

Figure 1.6 - The porphyrin structure substituted at *meso* and *beta*–positions.

A PS must accomplish some requirements in order to be applied in a aPDT treatment (Alves *et al.* 2009, Costa *et al.* 2010, Wainwright *et al.* 2016):

- It should be amphiphilic to have affinity to the bacteria and must not affect the host.
- It should not aggregate during the treatment. The solubility of the PS is a key feature for the successful of the photodynamic approach, as the aggregation of the PS impossibilities its binding to the microbial surfaces and reduce significantly the singlet oxygen production.
- It must be photostable and must not suffer degradation under the light action.
- The PS should have an absorption spectrum coincident with the light source emission spectrum and must be used in low concentrations to prevent the PS reaction with the skin/organs.
- The PS should photoinactivate a broad-range of microorganisms.
- The PS preparation or extraction must be easy, and the purification step should be not too laborious, and must be related with a low yield of production.

In fact, is well known that when an aPDT treatment is performed on gram-negative bacteria, positive charged PS should be preferentially chosen to be able to kill efficiently these bacteria, as their impermeable external membrane prevents the neutral

and anionic PS from entry into de cells. The application of cationic PS allows its entrance through the bacterial external structure by the "self-promoted uptake pathway" (Hancock *et al*. 1991; Merchat *et al*. 1996). To confront this problem, some adjuvants can be applied, such as poly-L-lysine, polyethylenimine, polymyxin B nonapeptide and ethylenediaminetetraacetic acid (EDTA). The combination of these compounds with neutral PS, or PSs with a few number of positive charges enhance the killing effect of pathogens, by causing its membrane disruption or by destabilizing its cell wall organization (Yoshimura and Nikaido 1985; Nitzan *et al*. 1992; Helander *et al*. 1997; Lounatmaa 1998; Soukos *et al*. 1998; Jori *et al*. 2006).

In addition, concerning the production and PS purification, by the Organic Chemistry Group of Department of Chemistry of University of Aveiro research group has published the aPDT effects of a new formulation based on cationic porphyrins - FORM, that is composed of a non-separated mixture of Mono-Py(+)-Me (19%), Di-Py(+)-Me opp and Di-Py(+)-Me adj (20%) Tri-Py(+)-Me (44%) and Tetra-Py(+)-Me (17%) obtained in two synthetic steps (Figure 1.7).

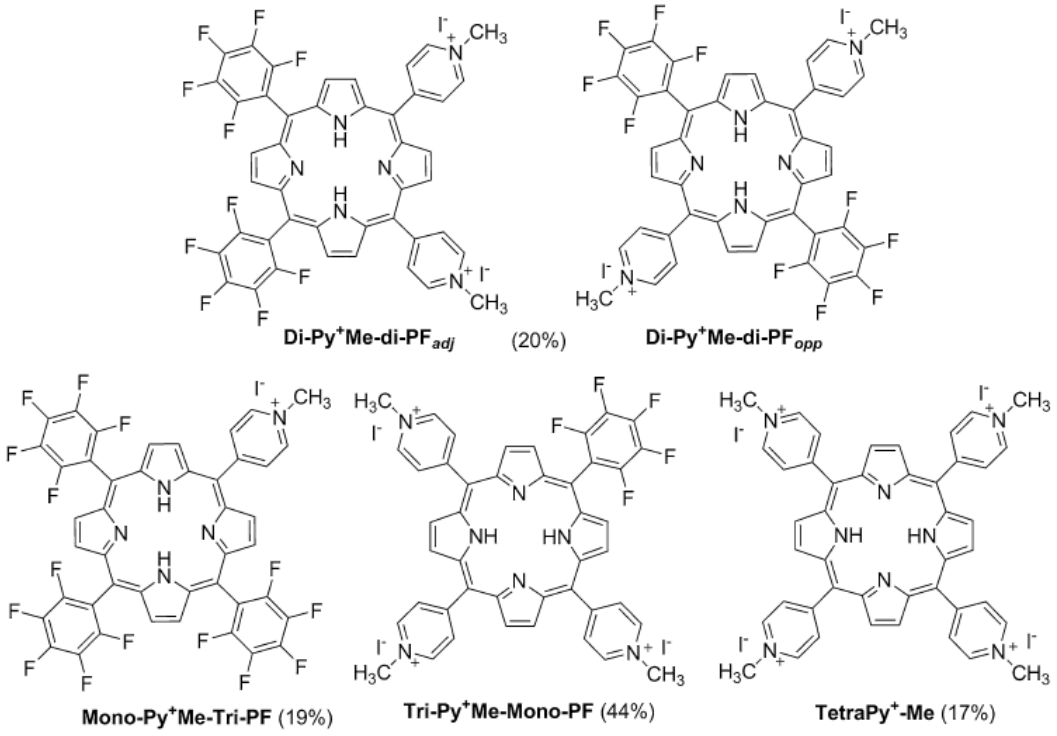

Figure 1.7 - Structure of porphyrins constituting FORM (Simões *et al*., 2016 ; Marciel *et al*., 2018 ; Martins *et al*., 2018).

Although FORM lacks the laborious separation and purification procedure after its synthesis, its killing efficiency is similar to that of Tri-Py(+)-Me (Marciel et al. 2018). In line with this main goal of cost reduction and efficiency increase, it is also important to use adjuvants that can enhance the photodynamic killing effect of different PS on distinct microorganisms, allowing the neutral PSs or cationic ones with few positive charges to efficiently inactivate gram-negative bacteria. This will possibly reduce the treatment time and the PS concentration and consequently to reduce the overall costs.

1.6. Potentiation of aPDT by KI

Various studies have demonstrated that different inorganic salts as sodium bromide (Wu *et al.* 2016) sodium azide (Huang *et al.* 2012), sodium thiocyanate (G St Denis *et al.* 2013) and potassium iodide (KI) can enhance aPDT efficiency of gram-negative and positive bacteria, and yeast. Of these four salts, sodium azide and sodium thiocyanate are toxic (Kasimova *et al*. 2014; Vecchio *et al*. 2015; Zhang *et al*. 2015; Freire *et al*. 2016; Y. Y. Huang *et al*. 2016; Hamblin 2017; Reynoso *et al*. 2017; Wen *et al*. 2017; L. Huang, *et al*. 2018a; L. Huang, *et al*. 2018b; Huang *et al*. 2018c).

In previous studies, sodium bromide (NaBr) was tested combined with different PS such as MB and RB and without inducing any improvement on aPDT efficiency (Wu *et al.* 2016). In this context, compared the others salts, the combination of KI and PS has been tested in several studies and seems to be the most promising one. This non-toxic salt is approved as an antifungal compound, capable of enhance the aPDT killing efficiency of titanium dioxide (TiO_2) and some neutral porphyrins, fullerenes and dyes such as MB and RB (Hamblin 2017). It was already stated that KI can potentiate the effect of different PS that acting through mechanism Type I and Type 2 (Wu *et al*., 2016; Huang *et al*., 2017; Hamblin and Abrahamse, 2018). Hamblin's research group has studied the combined effect between KI and TiO_2, a photocatalyst that acts by the Type I mechanism. With the addition of KI, the inactivation of fungi, gram-positive and negative bacteria increased in 6 log. Afterwards, they proved that two different species are produced as a consequence of

KI and TiO_2 combination: short-live iodine reactive species (IO^-, hypoiodite) and long-live oxidized iodine products (I_2/I_3^-). The first are responsible to destroy the bacteria during the irradiation, as the second continuously inactivate the cells after the irradiation time (in the dark). The results of inactivation depend on KI and TiO_2 concentration and light irradiance (Wu *et al.* 2016).

Other study showed that KI potentiated the photodynamic efficiency of a fullerene when excited by UVA light (360 nm), by facilitating electron transfer reactions from the photoexcited fullerene. *In vitro*, an increasing effect of 1-2 log was obtained on Gram-negative bacteria *Acinetobacter baumannii (A. baumannii)*, Gram-positive methicillin-resistant *Staphylococcus aureus (S. aureus)* and fungal yeast *Candida albicans (C. albicans),* when compared to the alone action of the fullerene. *In vivo*, allowed to treat efficiently a mouse abrasion infected with *A. baumannii* (Zhang *et al.* 2015).

It was also tested the combination of KI and a PS that acts by a Type II mechanism. When compared to MB control, the combination of MB at 50 µM and KI at 10 mM illuminated with red light achieved 3 log and 1-2 log of *S. aureus* and *E. coli* additional inactivation, respectively. *In vivo*, this combined approach was also able to reduce the murine burn infection caused by MRSA, when irradiated with a red light after a light dose of 150 J/cm^2 (Vecchio *et al.* 2015). The previous (MB+KI) was also applied in aPDT to treat mice with oral candidiasis. *In vitro*, the addition of KI allowed to reduce more 1-2 log of *C. albicans* than the MB alone. *In vivo*, the infection was irradiated after 5 days of treatment (Freire *et al.* 2016).

Afterwards, the addition of KI at 100 mM to Photofrin at 10 µM, a hematoporphyrin derivative that alone does not present a killing effect on gram-negative bacteria, produced the total inactivation of *E. coli*, *Pseudomonas aeruginosa*, *Klebsiella pneumoniae*, *Proteus mirabilis* and *A. baumannii*, when the samples were illuminated with blue light. This result indicate that KI can potentiate the killing effect of PS that alone does not photoinactivate gram-negative bacteria (Huang *et al*. 2017).

A similar study was performed with RB. In fact, the RB combined with KI were applied on a yeast (*C. albicans*), a gram-positive (methicillin resistant *S. aureus* - MRSA) and gram-negative bacteria (*E. coli* and *P. aeruginosa*) under green light irradiation. It was

observed that the treatment with green light and KI and RB induced the reduction of these microorganisms in more 6 logs than the RB alone. *In vivo* assays, the total eradication of *P. aeruginosa* was achieved on a partial thickness skin wound of a mouse (Wen *et al.* 2017).

1.7. Mechanism of the combined approach – PS + KI

The mechanism of KI action proposed in the literature evolve reactions that occur in parallel. Firstly, the KI reacts with singlet oxygen generated by the PS producing peroxyiodide ($HOOI^-$). Depending of the degree of PS binding to the pathogens cells, $HOOI^-$ can be decomposed by two distinct pathways (Vecchio *et al.* 2015, Zhang *et al.* 2015, Freire *et al.* 2016, Gsponer *et al.* 2016, Hamblin 2017, Huang *et al.* 2017, Kashef *et al.* 2017, Reynoso *et al.* 2017, Wen *et al.* 2017) (Figure 1.8):

Pathway a) – Free iodine (I_2/I_3^-) and hydrogen peroxide (H_2O_2) are formed. The first specie is long-lived and presents antimicrobial activity when its production reaches a concentration threshold. The amount of iodide anion (I^-) and of singlet oxygen ($^1O_2$) are factors that affect the quantity of free iodine produced.

Pathway b) – A homolytic cleavage process occur which produces reactive iodine radicals ($I_2^{\bullet -}$). This species are short-lives and have a short radius of action.

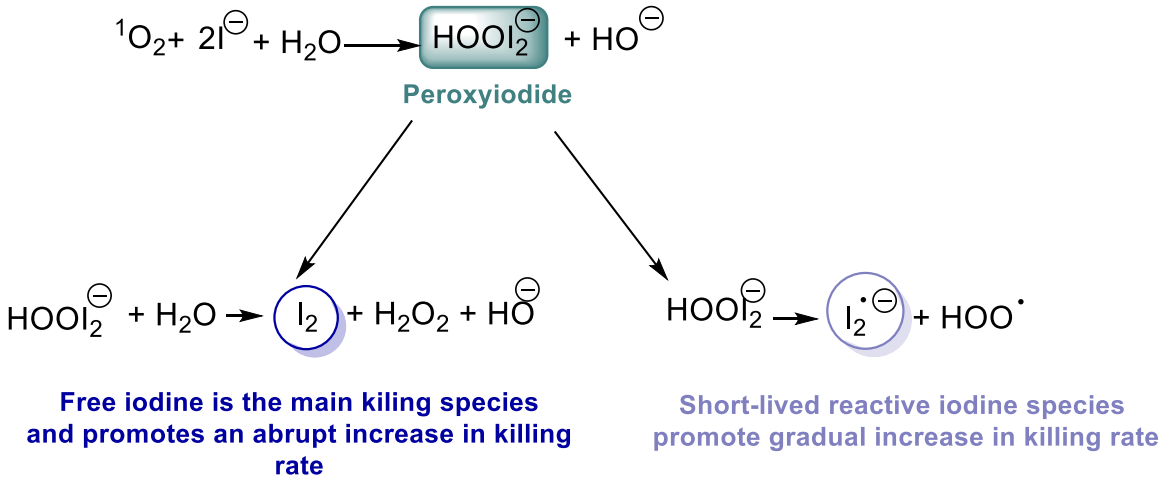

Figure 1.8 – Representation of the mechanism responsible for iodine reactive species formation.

The importance of each specie (I_2 or $I_2^{\bullet-}$) in the microbial inactivation can be assigned by the killing curve profile produced (L. Huang, *et al*. 2018b).

When the inactivation curves shows an abrupt decline, means that the free iodine (I_2) as reached a threshold of concentration that induce the abrupt microbial death (L. Huang, *et al*. 2018b).

In the killing curves that have a low decline of inactivation, the effect of PS in addition with KI was gradual and so the main responsible were the reactive iodide species ($I_2^{\bullet-}$) (Figure 1.9).

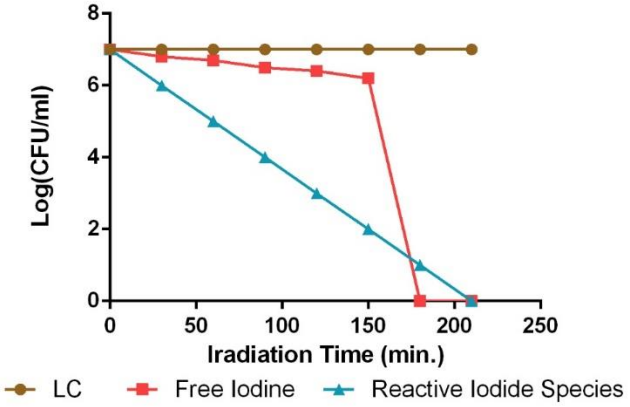

Figure 1.9. The distinct killing curve profiles produced by free iodine (I_2) and reactive iodine ($I_2^{\bullet-}$) species, compared to the bacteria control (Light control - LC).

1.8. Objectives

Previous studies have focused on positive potentiation of KI on PS effect, however the doubt remains if this potentiation can be observed for all the PSs. This missing information is essential to understand the factors responsible for influencing the potentiation occurrence.

In this context, our first goal consisted on gaining an insight into the potentiation effect of KI on different PSs. To achieve this objective, we tested the combination of KI at 50 mM and 100 mM with *meso*-substituted porphyrins, beta-substituted porphyrins, and non-porphyrinic dyes at 5.0 µM. The bioluminescent *E. coli* strain as a gram-negative

bacterial model was used on the aPDT assays. This bacterium was chosen considering the increased difficult to inactivate gram-negative bacteria compared to the gram-positive and yeasts, as well as the numerous assays needed to perform the proposed plan. The bioluminescent technique allows to detect with a high sensitivity the viability of the bacteria in real-time. Additionally, the luminescence produced by the bacteria is strongly correlated with colony-forming unit, CFU (Alves *et al*. 2008; Alves, *et al*. 2011a; Alves, *et al*. 2011b).

Our second goal consisted on a continuation of the previous study. For achieving it, we evaluated *in vitro* the aPDT of effect of FORM and the potentiation effect of its combination with KI to inactivate a broad-spectrum of microorganism and to prevent the formation of biofilms. Moreover, considering a creation of a feasible protocol to be *in vivo* tested in the future, in this work we wanted to evaluate the effect of low concentrations of PS in order to diminish the treatment costs and host adverse effects. To accomplish it, we tested various concentrations of FORM and FORM + KI at 100 mM on a T4 like bacteriophage (a model of mammalian viruses) and on planktonic and biofilms of a *E. coli* bioluminescent (a gram-negative bacterium resistant to ampicillin and chloramphenicol), a MRSA (a gram-positive bacteria), *C. albicans* (a yeast) and on. The prevention of *E. coli* and *S. aureus* biofilms formation was also assessed.

To perform this study, we have chosen FORM for two main reasons. Firstly, it exhibits a great killing effect on *E. coli*, *S. aureus* and *Pseudomonas syringae pv. actinidiae,* and a significantly cheaper production cost when compared with the single cationic porphyrinic PS including the tricationic porphyrin (Tri-Py(+)-Me) which has been effective to inactivate a wide broad-range of microorganisms efficiently (Marciel *et al.* 2018). Also, it was described in our previous work that FORM aPDT effect on *E. coli* is highly potentiated by KI.

1.9. References

Abe, H. and Wagner, S.J.,1995. Analysis of Viral Dna, Protein and Envelope Damage After Methylene Blue, Phthalocyanine Derivative or Merocyanine 540 Photosensitization. Photochemistry and Photobiology, 61 (4), 402–409.

Almeida, A., Cunha, A., Faustino, M.A.F., Neves, M.G.P.M.S., and Tomé, A.C., 2011. Porphyrins as Antimicrobial Photosensitizing Agents, 11, 83-160.

Almeida, A., Cunha, Â., Gomes, N.C.M., Alves, E., and Costa, L., 2009. Phage Therapy and Photodynamic Therapy : Low Environmental Impact Approaches to Inactivate Microorganisms in Fish Farming Plants. Marine Drugs, 7, 268–313.

Almeida, A., Faustino, M.A., and Tomé, J.P.C., 2015. Photodynamic inactivation of bacteria: finding the effective targets. Future Medicinal Chemistry, 7, 1221–1224.

Alves, E., Carvalho, C.M.B., Tomé, J.P.C., Faustino, M.A.F., Neves, M.G.P.M.S., Tomé, A.C., Cavaleiro, J.A.S., Cunha, Â., Mendo, S., and Almeida, A., 2008. Photodynamic inactivation of recombinant bioluminescent *Escherichia coli* by cationic porphyrins under artificial and solar irradiation. Journal of Industrial Microbiology and Biotechnology, 35 (11), 1447–1454.

Alves, E., Costa, L., Carvalho, C.M., Tomé, J.P., Faustino, M.A., Neves, M.G., Tomé, A.C., Cavaleiro, J.A., Cunh, A., and Almeida, A., 2009. Charge effect on the photoinactivation of gram-negative and gram-positive bacteria by cationic meso-substituted porphyrins. BMC Microbiology, 9, 1–13.

Alves, E., Costa, L., Cunha, Â., Faustino, M.A.F., Neves, M.G.P.M.S., and Almeida, A., 2011. Bioluminescence and its application in the monitoring of antimicrobial photodynamic therapy. Applied Microbiology and Biotechnology, 92 (6), 1115–1128.

Alves, E., Faustino, M.A., Neves, G.M., Cunha, A., Tomé, J., and Almeida, A., 2014. An insight on bacterial cellular targets of photodynamic inactivation. Future Medicinal Chemistry, 141–164.

Alves, E., Faustino, M.A.F., Neves, M.G.P.M.., Angela, C., Helena, N., and Adelaide, A., 2014. Potential applications of porphyrins in photodynamic inactivation beyond the medical scope. Journal of Photochemistry and Photobiology, 22, 34-57.

Alves, E., Faustino, M.A.F., Tomé, J.P.C., Neves, M.G.P.M.S., Tomé, A.C., Cavaleiro, J.A.S.,

Cunha, Â., Gomes, N.C.M., and Almeida, A., 2011. Photodynamic antimicrobial chemotherapy in aquaculture: Photoinactivation studies of *Vibrio fischeri*. PLoS ONE, 6 (6), 1-9.

Beirão, S., Fernandes, S., Coelho, J., Faustino, M.A.F., Tomé, J.P.C., Neves, M.G.P.M.S., Tomé, A.C., Almeida, A., and Cunha, A., 2014. Photodynamic inactivation of bacterial and yeast biofilms with a cationic porphyrin. Photochemistry and Photobiology, 90 (6), 1387–1396.

Bourr, L., Giuntini, F., Eggleston, I.M., Mosse, C.A., Macrobert, J., and Wilson, M., 2010. Effective photoinactivation of Gram-positive and Gram-negative bacterial strains using an HIV-1 Tat peptide – porphyrin conjugate. Photochemical and Photobiological Sciences, 9, 1613–1620.

Calin, M.A. and Parasca, S. V, 2009. Light sources for photodynamic inactivation of bacteria. Lasers in Medical Science, 24, 453–460.

Castano, A.P., Demidova, T.N., and Hamblin, M.R., 2005. Mechanisms in photodynamic therapy : part one —– photosensitizers , photochemistry and cellular localization. Elsevier, 1, 279—293.

Chambers, H.F. and DeLeo, F.R., 2009. Waves of Resistance: *Staphylococcus aureus* in the Antibiotic Era. Nature Reviews Microbiology, 7 (9), 629–641.

Cieplik, F., Deng, D., Crielaard, W., Buchalla, W., Hellwig, E., Al-Ahmad, A., and Maisch, T., 2018. Antimicrobial photodynamic therapy–what we know and what we don't. Critical Reviews in Microbiology, 44 (5), 571–589.

Costa, D.C.S., Gomes, M.C., Faustino, M.A.F., Neves, M.G.P.M.S., Cunha, Â., Cavaleiro, J.A.S., Almeida, A., and Tomé, J.P.C., 2012. Comparative photodynamic inactivation of antibiotic resistant bacteria by first and second generation cationic photosensitizers. Photochemical and Photobiological Sciences, 11 (12), 1905–1913.

Costa, L., Alves, E., Carvalho, C.M.B., Tomé, J.P.C., Faustino, M.A.F., Neves, M.G.P.M.S., Tomé, A.C., Cavaleiro, J.A.S., Cunha, Â., and Almeida, A., 2008. Sewage bacteriophage photoinactivation by cationic porphyrins: A study of charge effect. Photochemical and Photobiological Sciences, 7 (4), 415–422.

Costa, L., Carvalho, C.M.B., Faustino, M.A.F., Neves, M.G.P.M.S., Tomé, J.P.C., Tomé, A.C.,

Cavaleiro, J.A.S., Cunha, Â., and Almeida, A., 2010. Sewage bacteriophage inactivation by cationic porphyrins: Influence of light parameters. Photochemical and Photobiological Sciences, 9 (8), 1126–1133.

Costa, L., Faustino, M.A.F., Neves, M.G.P.M.S., Cunha, Â., and Almeida, A., 2012. Photodynamic inactivation of mammalian viruses and bacteriophages. Viruses, 4 (7), 1034–1074.

Costerton, J.W., Stewart, P.S., and Greenberg, E.P., 1999. Bacterial Biofilms : A Common Cause of Persistent Infections. Science, 1318.

DeLeo, F.R., Otto, M., Kreiswirth, B.N., and Chambers, H.F., 2010. Community-associated methicillin-resistant *Staphylococcus aureus*. The Lancet, 375 (9725), 1557–1568.

Demidova, T.N. and Hamblin, M.R., 2005. Effect of Cell-Photosensitizer Binding and Cell Density on Microbial Photoinactivation. Antimicrob Agents Chemother, 49 (6), 2329–2335.

Denis, T.G.S., Dai, T., Izikson, A., Astrakas, C., Anderson, R.R., and Hamblin, M.R., 2011. All you need is light: antimicrobial photoinactivation as an evolving and emerging discovery strategy against infectious disease, Virulence, 2:6, 1-12.

Derosa, M.C. and Crutchley, R.J., 2002. Photosensitized singlet oxygen and its applications. Elsevier, 233-234, 351-371.

Donnelly, R.F., McCarron, P.A., and Tunney, M.M., 2008. Antifungal photodynamic therapy. Microbiological Research, 163 (1), 1–12.

Fernandez, J.M., Bilgin, M.D., and Grossweiner, L.I., 1997. Singlet oxygen generation by photodynamic agents. Journal of Photochemistry and Photobiology, 37, 131-140.

Flors, C. and Nonell, S., 2006. Light and Singlet Oxygen in Plant Defense Against Pathogens: Phototoxic Phenalenone Phytoalexins. Accounts of Chemical Research, 39 (5), 293–300.

Fowler, S., Roush, R., and Wise, J., 2008. Concepts of Biology. Biomaterials, 29, 450-468.

Freire, F., Ferraresi, C., Jorge, A.O.C., and Hamblin, M.R., 2016. Photodynamic therapy of oral Candida infection in a mouse model. Journal of Photochemistry and Photobiology B: Biology, 159, 161–168.

G St Denis, T., Vecchio, D., Zadlo, A., Rineh, A., Sadasivam, M., Avci, P., Huang, L.,

Kozinska, A., Chandran, R., Sarna, T., and Hamblin, M., 2013. Thiocyanate Potentiates Antimicrobial Photodynamic Therapy: In Situ Generation of the Sulfur Trioxide Radical Anion by Singlet Oxygen. Free Radical Biol Med, 65, 800–810.

Gad, F., Zahra, T., Hasan, T., and Hamblin, M.R., 2004. Effects of Growth Phase and Extracellular Slime on Photodynamic Inactivation of Gram-Positive Pathogenic Bacteria. Antimicrobial Agents and Chemotherapy, 48 (6), 2173–2178.

Garcez, A.S., Núnez, S.C., Azambuja, N., MSc, J., Fregnani, E.R., Rodriguez, H.M.H., Hamblin, M.R., Suzuki, H., and Ribeiro, M.S., 2013. Effects of Photodynamic Therapy on Gram-Positive and Gram-Negative Bacterial Biofilms by Bioluminescence Imaging and Scanning Electron Microscopic Analysis. Photomedicine and Laser Surgery, 31, 519-525.

Gsponer, N.S., Agazzi, M.L., Spesia, M.B., and Durantini, E.N., 2016. Approaches to unravel pathways of reactive oxygen species in the photoinactivation of bacteria induced by a dicationic fulleropyrrolidinium derivative. Methods, 109, 167–174.

Hadjur, C., Lange, N., Rebstein, J., Monnier, P., and Bergh, H. Van Den, 1998. Spectroscopic studies of photobleaching and photoproduct formation of meta (tetrahydroxyphenyl) chlorin (m-THPC) used in photodynamic therapy . The production of singlet oxygen by m-THPC. Journal of Photochemistry & Photobiology, B:Biology, 451, 170-178.

Hall-stoodley, L., Costerton, J.W., and Stoodley, P., 2004. Bacterial biofilms: From the natural environment to infectious diseases. Nature Reviews Microbiology, 2, 95-108.

Hamblin, M.R., 2017. Potentiation of antimicrobial photodynamic inactivation by inorganic salts. Expert Review of Anti-Infective Therapy, 15 (11), 1059–1069.

Hamblin, M.R., 2018. Upconversion in photodynamic therapy: Plumbing the depths. Dalton Transaction*s*, 47 (26), 8571–8580.

Hamblin, M.R. and Hasan, T., 2004. Photodymamic therapy: a new antimicrobial approach to infectious disease? Photochem Photobiol Sci., 3 (5), 436–50.

Helander, I.M., Alakomi, H.L., Latva-Kala, K., and Koski, P., 1997. Polyethyleneimine is an effective permeabilizer of Gram-negative bacteria. Microbiology, 143 (10), 3193–3199.

Høiby, N., 2017. A short history of microbial biofilms and biofilm infections, 125 (6), 272–275.

Hu, X., Huang, Y.Y., Wang, Y., Wang, X., and Hamblin, M.R., 2018. Antimicrobial photodynamic therapy to control clinically relevant biofilm infections. Frontiers in Microbiology, 9 (JUN), 1–24.

Huang, L., Bhayana, B., Xuan, W., Sanchez, R.P., McCulloch, B.J., Lalwani, S., and Hamblin, M.R., 2018. Comparison of two functionalized fullerenes for antimicrobial photodynamic inactivation: Potentiation by potassium iodide and photochemical mechanisms. Journal of Photochemistry and Photobiology B: Biology, 186, 197–206.

Huang, L., St. Denis, T.G., Xuan, Y., Huang, Y.Y., Tanaka, M., Zadlo, A., Sarna, T., and Hamblin, M.R., 2012. Paradoxical potentiation of methylene blue-mediated antimicrobial photodynamic inactivation by sodium azide: Role of ambient oxygen and azide radicals. Free Radical Biology and Medicine, 53 (11), 2062–2071.

Huang, L., El-Hussein, A., Xuan, W., and Hamblin, M.R., 2018. Potentiation by potassium iodide reveals that the anionic porphyrin TPPS4 is a surprisingly effective photosensitizer for antimicrobial photodynamic inactivation. Journal of Photochemistry and Photobiology B: Biology, 178, 277–286.

Huang, L., Szewczyk, G., Sarna, T., and Hamblin, M.R., 2017. Potassium Iodide Potentiates Broad-Spectrum Antimicrobial Photodynamic Inactivation Using Photofrin. *ACS* Infectious Diseases, 3 (4), 320–328.

Huang, Y.-Y., Wintner, A., Seed, P.C., Brauns, T., Gelfand, J.A., and Hamblin, M.R., 2018. Antimicrobial photodynamic therapy mediated by methylene blue and potassium iodide to treat urinary tract infection in a female rat model. Scientific Reports, 8 (1), 7257.

Huang, Y.Y., Choi, H., Kushida, Y., Bhayana, B., Wang, Y., and Hamblin, M.R., 2016. Broad-spectrum antimicrobial effects of photocatalysis using titanium dioxide nanoparticles are strongly potentiated by addition of potassium iodide. Antimicrobial Agents and Chemotherapy, 60 (9), 5445–5453.

Jori, G., Camerin, M., Soncin, M., Guidolin, L., and Coppellotti, O., 2011. Antimicrobial Photodynamic Therapy: Basic Principles. The Royal Society of Chemistry, 11, 1–18.

Juzeniene, A. and Moan, J., 2007. The history of PDT in Norway. Part one: Identification of basic mechanisms of general PDT. Photodiagnosis and Photodynamic Therapy, 4 (1), 3–11.

Kashef, N., Huang, Y.Y., and Hamblin, M.R., 2017. Advances in antimicrobial photodynamic inactivation at the nanoscale. Nanophotonics, 6 (5), 853–879.

Kasimova, K.R., Sadasivam, M., Landi, G., Sarna, T., and Hamblin, M.R., 2014. Potentiation of photoinactivation of Gram-positive and Gram-negative bacteria mediated by six phenothiazinium dyes by addition of azide ion. Photochemical and Photobiological Sciences, 13 (11), 1541–1548.

Kassab, K., Dei, D., Roncucci, G., and Coppellotti, O., 2003. Phthalocyanine-photosensitized inactivation of a pathogenic protozoan, *Acanthamoeba palestinensis*. Photochemical and Photobiological Sciences, 2, 668–672.

Lam, M., Jou, P.C., Lattif, A.A., Lee, Y., Malbasa, C.L., Mukherjee, P.K., Oleinick, N.L., Ghannoum, M.A., Cooper, K.D., and Baron, E.D., 2011. Photodynamic Therapy with Pc 4 Induces Apoptosis of *Candida albicans*, Photochemistry and Photobiology, 87, 904–909 .

Li, L.L. and Diau, E.W.G., 2013. Porphyrin-sensitized solar cells. Chemical Society Reviews, 42 (1), 291–304.

Liu, Y., Qin, R., Zaat, S.A.J., Breukink, E., and Heger, M., 2015. Antibacterial photodynamic therapy: overview of a promising approach to fight antibiotic-resistant bacterial infections. Journal of Clinical and Translational Research, 1 (3), 140–167.

Lobanovska, M. and Pilla, G., 2017. Penicillin ' s Discovery and Antibiotic Resistance : Lessons for the Future ?. Yale Journal of Biology and Medicine, 90, 135–145.

Lounatmaa, I.M.H.K.L.-K.K., 1998. Permeabilizing action of polyethyleneimine on 90 Printed in Great Britain Permeabilizing action of polyethyleneimine on *Salmonella typhimurium* involves disruption of the outer membrane and interactions with lipopolysaccharide. Microscopy, Electron, 144 (1 998), 385–390.

Luke-marshall, N.R., Mang, T.S., Hansen, L.A., and Campagnari, A.A., 2014. Moraxella catarrhalis is Susceptible to Antimicrobial Photodynamic Therapy With Photofrin. Lasers in Surgery and Medicine, (July), 1–6.

Maclean, M., Macgregor, S.J., Anderson, J.G., and Woolsey, G.A., 2008. The role of oxygen in the visible-light inactivation of *Staphylococcus aureus*. Journal of Photochemistry and Photobiology B : Biology, 92, 180–184.

Maisch, T., Eichner, A., Spath, A., Gollmer, A., Konig, B., Regensburger, J., and Baumler, W., 2014. Fast and Effective Photodynamic Inactivation of Multiresistant Bacteria by Cationic Riboflavin Derivatives. PLoS ONE, 9, e111792.

Marciel, L., Mesquita, M.Q., Ferreira, R., Moreira, B., Neves, M.G.P.M.S., Faustino, M.A.F., and Almeida, A., 2018. An efficient formulation based on cationic porphyrins to photoinactivate *Staphylococcus aureus* and *Escherichia coli*. Future Medicinal Chem, 10, 1821–1833.

Martins, D., Mesquita, M.Q., Neves, M.G.P.M.S., Faustino, M.A.F., Reis, L., Figueira, E., and Almeida, A., 2018. Photoinactivation of *Pseudomonas syringae pv. actinidiae* in kiwifruit plants by cationic porphyrins. Planta, 248 (2), 409–421.

Merchat, M., Bertolini, G., Giacomini, P., Villanueva, A., and Jori, G., 1996. Meso-substituted cationic porphyrins as efficient photosensitizers of gram-positive and gram-negative bacteria. Journal of Photochemistry and Photobiology B: Biology, 32 (3), 153–157.

Mesquita, M.Q., Menezes, J.C.J.M.D.S., Neves, G.P.M.. M., Tomé, A.C., Cavaleiro, J.A.S., Cunha, Â., Almeida, A., Hackbarth, S., Röder, B., and Faustino, M.A.F., 2013. Photodynamic inactivation of bioluminescent *Escherichia coli* by neutral and cationic pyrrolidine-fused chlorins and isobacteriochlorins. Bioorganic & Medicinal Chemistry Letters, 24, 808-812,.

Minnock, A., Vernon, D.I., Schofield, J., Parish, J.H., and Brown, S.B., 2000. Mechanism of Uptake of a Cationic Water-Soluble Pyridinium Zinc Phthalocyanine across the Outer Membrane of *Escherichia coli* Mechanism of Uptake of a Cationic Water-Soluble Pyridinium Zinc Phthalocyanine across the Outer Membrane of *Escherichia coli*. Antimicrobial Agents and Chemotherapy, 44 (3), 522–527..

Mizuno, K., Zhiyentayev, T., Huang, L., Khalil, S., and Nasim, F., 2011. Antimicrobial photodynamic therapy with functionalized Fullerenes: quantitative structure-activity relationships, J Nanomed Nanotechnol, 2 (2), 1–9.

Moan, J. and Berg, K., 1991. Research note the photodegradation of porphyrins in cells can be used to estimate the lifetime of singlet oxygen. Photochemistry and Photobiology 53 (4). 549–553.

Moura, N.M.M., Esteves, M., Vieira, C., Rocha, G.M.S.R.O., Faustino, M.A.F., Almeida, A., Cavaleiro, J.A.S., Lodeiro, C., and Neves, M.G.P.M.S., 2019. Novel β-functionalized mono-charged porphyrinic derivatives: Synthesis and photoinactivation of *Escherichia coli*. Dyes and Pigments, 160, 361–371.

Mtiller-breitkreutz, K., Mohr, H., Briviba, K., and Sies, H., 1995. Inactivation of viruses by chemically and photochemically generated singlet molecular oxygen, Journal of Photochemistry and Photobiology B: Biology, 30, 63–70 .

Nanoparticles, B., Shrestha, A., and Kishen, A., 2014. Antibiofilm Efficacy of Photosensitizer-functionalized. Journal of Endodontics, 1–7.

Nitzan, Y., Gutterman, M., Malik, Z., and Ehrenberg, B., 1992. Inactivation of Gram Negative Bacteria By Photosensitized Porphyrins. Photochemistry and Photobiology, 55 (1), 89–96.

Nitzan, Y., Shainberg, B., and Malik, Z., 1989. Microbiology The Mechanism of Photodynamic Inactivation of *Staphylococcus aureus* by Deuteroporphyrin. Current Microbiology, 19, 265–266.

Ochsner, M., 1996. Light scattering of human skin: a comparison between zinc(II)-phthalocyanine and Photofrin II ®. JournaJ of Photochemistry and Photobiology B: Biology 32 , 3–9.

Regensburger, J., Knak, A., Maisch, T., Landthaler, M., and Ba, W., 2011. Fatty acids and vitamins generate singlet oxygen under UVB irradiation. Experimental Dermatology, 04 (21), 135–139.

Reynoso, E., Quiroga, E.D., Agazzi, M.L., Ballatore, M.B., Bertolotti, S.G., and Durantini, E.N., 2017. Photodynamic inactivation of microorganisms sensitized by cationic BODIPY derivatives potentiated by potassium iodide. Photochemical and Photobiological Science*s*, 16 (10), 1524–1536.

Sharman, W.M., Allen, C.M., and Lier, J.E. Van, 1999. Photodynamic therapeutics : basic principles and clinical applications. Drug Discov Today, 4 (11), 507–517.

Shrestha, A., Zhilong, S., Gee, N.K., and Kishen, A., 2010. Nanoparticulates for Antibiofilm Treatment and Effect of Aging on Its Antibacterial Activity. Journal of Endodontics, 36 (6), 1030–1035.

Sieber, F., 2014. Merocyanine-sensitized photoinactivation of enveloped viruses. Blood Cells, 18:117-128.

Silva, Y.J., Costa, L., Pereira, C., Cunha, Â., Calado, R., Gomes, N.C.M., and Almeida, A., 2014. Influence of environmental variables in the efficiency of phage therapy in aquaculture. Microbial Biotechnology, 7 (5), 401–413.

Simões, C., Gomes, M.C., Neves, M.G.P.M.S., Cunha, Â., Tomé, J.P.C., Tomé, A.C., Cavaleiro, J.A.S., Almeida, A., and Faustino, M.A.F., 2016. Photodynamic inactivation of *Escherichia coli* with cationic meso-tetraarylporphyrins - The charge number and charge distribution effects. Catalysis Today, 266, 197–204.

Soukos, N.S., Ximenez-Fyvie, L.A., Hamblin, M.R., Socransky, S.S., and Hasan, T., 1998. Targeted antimicrobial photochemotherapy. Antimicrobial Agents and Chemotherapy, 42 (10), 2595–2601.

Spaeth, A., Graeler, A., Maisch, T., and Plaetzer, K., 2017. AC SC. European Journal of Medicinal Chemistry, 5, 423-440.

Sperandio, F.F., Huang, Y., Hospital, M.G., Hamblin, M., and Hospital, M.G., 2013. Antimicrobial Photodynamic Therapy To Kill Gram-Negative Bacteria. Recent Patents on Anti-Infective Drug Discovery, 8, 108-120.

Stewart, S.P., 2003. New ways to stop biofilm infections Diagnosing smallpox in possible bioterrorist attack For personal use . Only reproduce with permission from The Lancet Publishing Group . The Lancet, 361, 130.

Takasaki, A.A., Aoki, A., Mizutani, K., Schwarz, F., Sculean, A., Wang, C.-Y., Koshy, G., Romanos, G., Shikawa, I., and Zumi, Y., 2009. Application of antimicrobial photodynamic therapy in periodontal and peri-implant diseases. European Journal of Medicinal Chemistry, 51, 109–140.

Tavares, A., Carvalho, C.M.B., Faustino, M.A., Neves, M.G.P.M.S., Tomé, J.P.C., Tomé, A.C., Cavaleiro, J.A.S., Cunha, Â., Gomes, N.C.M., Alves, E., and Almeida, A., 2010. Antimicrobial Photodynamic Therapy: Study of Bacterial Recovery Viability and

Potential Development of Resistance after Treatment. Marine Drugs, 8 (12), 91–105.

Tenover, C.F. and McGowan, E.J., 1940. Reasons for the emergence of antibiotic resistance. The American Journal of the Medical Sciences, 311 (1), 9–16.

Tortik, N. and Plaetzer, K., 2014. Photodynamic decontamination of foodstuff from *Staphylococcus aureus* based on novel formulations of curcumin. Photochem. Photobiol. Sci., 13, 1402–1409.

Usacheva, M.N., Teichert, M.C., and Biel, M.A., 2001. Comparison of the Methylene Blue and Toluidine Blue Photobactericidal Eficacy Against Gram-Positive and Gram-Negative Microorganisms. Lasers in Surgery and Medicine, 29:165-173.

Vecchio, D., Gupta, A., Huang, L., Landi, G., Avci, P., Rodas, A., and Hamblina, M.R., 2015. Bacterial photodynamic inactivation mediated by methylene blue and red light is enhanced by synergistic effect of potassium iodide. Antimicrobial Agents and Chemotherapy, 59 (9), 5203–5212.

Vieira, C., Gomes, A.T.P.C., Mesquita, M.Q., Moura, N.M.M., Neves, M.G.P.M.S., Faustino, M.A.F., and Almeida, A., 2018. An Insight Into the Potentiation Effect of Potassium Iodide on aPDT Efficacy. Frontiers in Microbiology, 9 (November), 1–16.

Vilela, S.F.G., Junqueira, J.C., Barbosa, J.O., Majewski, M., Munin, E., and Jorge, A.O.C., 2012. Photodynamic inactivation of *Staphylococcus aureus* and *Escherichia coli* biofilms by malachite green and phenothiazine dyes: An in vitro study. Archives of Oral Biology, 57 (6), 704–710.

Wainwright, M., 1998. Review Photodynamic antimicrobial chemotherapy (PACT). *Journal of* Antimicrobial Chemotherapy, 13–28.

Wainwright, M., 2000. Methylene blue derivatives — suitable photoantimicrobials for blood product disinfection? Jornal of Antimicrobial Agents, 16, 381–394.

Wainwright, M., 2016. Dyes, flies, and sunny skies: photodynamic therapy and neglected tropical diseases. Coloration Technology, 3–14.

Wainwright, M. and Crossley, K.B., 2004. Photosensitising agents — circumventing resistance and breaking down biofilms : a review. International Biodeterioration & Biodegradation, 53, 119–126.

Wainwright, M., Maisch, T., Nonell, S., Plaetzer, K., Almeida, A., Tegos, G.P., and Hamblin,

M.R., 2016. Photoantimicrobials — are we afraid of the light? The Lancet, 3099 (16), 1–7.

Wen, X., Zhang, X., Szewczyk, G., El-Hussein, A., Huang, Y.Y., Sarna, T., and Hamblin, M.R., 2017. Potassium iodide potentiates antimicrobial photodynamic inactivation mediated by Rose bengal in in vitro and in vivo studies. Antimicrobial Agents and Chemotherapy, 61 (7), e00467-17.

WHO, 2017. Antimicrobial Resistance. Fach sheets on sustainable development goals: health targets, 1–7.

Wolcott, R.D. and Ehrlich, D.G., 2008. Biofilms and Chronic Infections. JAMA, 299, 2682–2684.

Wu, X., Huang, Y.Y., Kushida, Y., Bhayana, B., and Hamblin, M.R., 2016. Broad-spectrum antimicrobial photocatalysis mediated by titanium dioxide and UVA is potentiated by addition of bromide ion via formation of hypobromite. Free Radical Biology and Medicin*e*, 95, 74–81.

Zambotto, F., Conventi, L., and Reddi, E., 1987. Role of the specific cellular targets in the hematoporphyrin-sensitized photoinactivation of microbial cells. Photochemistry and Photobiology, 46 (5), 695–698.

Zanin, I., Lobo, M., Rodrigues, L., Pimenta, L., Hofling, J., and Gonçalves, R., 2006. Photosensitization of in vitro biofilms by toluidine blue O combined with a light-emitting diode. *European Jornal of* Oral Sciences, (II), 64–69.

Zhang, Y., Dai, T., Wang, M., Vecchio, D., Chiang, L.Y., and Hamblin, M.R., 2015. Potentiation of antimicrobial photodynamic inactivation mediated by a cationic fullerene by added iodide: In vitro and in vivo studies. Nanomedicine, 10 (4), 603–614.

Zúpan, K., Egyeki, M., Tóth, K., Fekete, A., Herényi, L., Módos, K., and Csík, G., 2008. Comparison of the efficiency and the specificity of DNA-bound and free cationic porphyrin in photodynamic virus inactivation. Journal of Photochemistry and Photobiology B: Biology, 90, 105–112.

An insight on aPDT efficacy of photosensitizers mediated by potassium iodide

Cátia Vieira[1], Ana T. P. C. Gomes[1], Mariana Q. Mesquita[2], Nuno M. M. Moura[2], M. Graça P. M. S. Neves[2], M. Amparo F. Faustino[2], Adelaide Almeida[1]

[1] Department of Biology and CESAM, University of Aveiro, 3810-193 Aveiro, Portugal

[2] Department of Chemistry and QOPNA, University of Aveiro, Aveiro, Portugal

Keywords: Antimicrobial Photodynamic Therapy, Cationic Porphyrins, Phenothiazines, Xanthenes, bioluminescent *E. coli*

CHAPTER II

2.1. Abstract

Antimicrobial photodynamic therapy (aPDT) is gaining a special importance as an effective approach against multidrug-resistant strains responsible of fatal infections. The addition of potassium iodide (KI), a non-toxic salt, is recognized to increase the aPDT efficiency of some photosensitizers (PSs) on a broad-spectrum of microorganisms. As the reported cases only refer positive aPDT potentiation results, in this work we selected a broad range of porphyrinic and non-porphyrinic PSs in order to gain a more comprehensive knowledge about this aPDT potentiation by KI. For this evaluation were selected a series of meso-tetraarylporphyrins positively charged at meso positions or at β-pyrrolic positions and the non-porphyrinic dyes Methylene blue, Rose Bengal, Toluidine Blue O, Malachite Green and Crystal Violet; the assays were performed using a bioluminescent *E. coli* strain as a model. The results indicate that KI has also the ability to potentiate the aPDT process mediated by some of the cationic PSs (**Tri-Py(+)-Me**, **Tetra-Py(+)-Me**, **Form**, **RB**, **MB**, **Mono-Py(+)-Me**, **β-ImiPhTPP**, **β-ImiPyTPP** and **β-BrImiPyTPP**) allowing a drastic reduction of the treatment time as well as of the PS concentration. However, the efficacy of some porphyrinic and non-porphyrinic PSs (**Di-Py(+)-Me *opp***, **Di-Py(+)-Me *adj***, **Tetra-Py**, **TBO**, **CV** and **MG**) was not improved by the presence of the coadjuvant. For the PSs tested in this study, the ones capable to decompose the peroxyiodide into iodine (easily detectable by spectroscopy or by the visual appearance of a blue colour in the presence of amylose) were the most promising ones to be used in combination with KI. Although these studies confirmed that the generation of $^1O_2$ is an important fact in this process, the PS structure (charge number and charge position), aggregation behavior and affinity for the cell membrane are also important features to be taken in account.

2.2. Introduction

Antibiotics are among the most commonly prescribed drugs used in both human medicine and in farm animals, resulting in the selection of multiple drugs resistant (MDR) bacteria (Economou and Gousia, 2015; O'Neill 2016). Infections with resistant bacteria are difficult to treat, causing severe illness and requiring costly and sometimes toxic alternatives, such as antibiotics of last resort. Drugs of last resort, such as vancomycin against Gram-positive bacteria and colistin against Gram-negative bacteria, have been the most reliable therapeutic agents against MDR bacteria. However, bacterial strains resistant to these antibiotics have been isolated worldwide (Levine 2006; Wang *et al*. 2018). This resistance can result from a chromosomal gene mutation, but comes mainly from horizontal transfer from external gene sources (Chambers and DeLeo, 2009; DeLeo et al., 2010; Gardete and Tomasz, 2014; Gao et al., 2016). The development of novel, antibiotics is not likely to solve the problem and it is probably only a matter of time until they will be also ineffective. Bacteria will inevitably find ways of resisting to the conventional antibiotics, which is why alternative approaches are urgent.

Antimicrobial photodynamic therapy (aPDT) can be a very promising alternative to antibiotic treatment namely in localized infections (Dai *et al*., 2010). aPDT involves the use of a photosensitizer (PS) which in the presence of visible light and oxygen produces reactive oxygen species (ROS), such as singlet oxygen ($^1O_2$). These species are responsible for the oxidation of several cellular components conducting to rapid cell inactivation. This approach presents some advantages when compared with the use of antibiotics, such as being efficient independently of the microorganism antibiotic resistance profile (Jori *et al*., 2011), does not induce the development of resistance, even after several cycles of treatment (Giuliani *et al*. 2010; Tavares *et al*. 2010; Costa *et al*. 2011) and can be applied with efficacy against Gram-negative and Gram-positive bacteria.

aPDT is considered more effective against Gram-positive bacteria due to their highly permeable cell walls allowing the easy diffusion of neutral, positive and negative charged PS into the cell. However, the impermeable external membrane of Gram-negative bacteria cell wall limits the anionic or neutral-charge PSs entrance (Minnock *et al*. 2000). This limitation is overcome by the use of cationic PS. These PSs are able to bind

and penetrate into the cell wall by the "self-promoted uptake pathway" (Hancock *et al*. 1991; Merchat *et al*. 1996). Nevertheless, neutral PSs or PSs with low number of charges can be effective against this type of bacteria by coupling or combining them with positively charged entities such as poly-L-lysine, polyethylenimine and polymyxin B nonapeptide that act as membrane disruptors (Nitzan *et al.* 1992, Helander *et al.* 1997, Lounatmaa 1998, Soukos *et al.* 1998). Ethylenediaminetetraacetic acid (EDTA) is also commonly used to destabilize the native organization of Gram-negative wall (Yoshimura and Nikaido 1985; Jori *et al*. 2006).

It has also been shown that different organic salts can improve the efficiency of aPDT against Gram-negative bacteria (L. Huang *et al*. 2012; Kasimova *et al*. 2014). Recently, some studies have demonstrated that aPDT can be potentiated by addition of several different inorganic salts, such as sodium bromide (Wu *et al*., 2016) sodium azide (Huang *et al*., 2012, Kasimova *et al*., 2014), sodium thiocyanate ((St Denis *et al*., 2013) and potassium iodide (Zhang *et al*., 2015, Freire *et al*., 2016, Huang *et al*., 2016, Hamblin, 2017, Huang *et al*., 2017, Reynoso *et al*., 2017, Wen *et al*., 2017, Huang, 2018, Huang *et al*., 2018b, Huang *et al*., 2018c, Vecchio *et al*., 2015).

In fact, the addition of iodide has been shown to improve the efficiency of aPDT in several animal models of localized infection. This salt is non-toxic and is an approved drug for antifungal therapy (Hamblin, 2017). The studies involving the use of KI demonstrate that the combination of this salt with neutral porphyrins, fullerenes and other dyes gives rise to higher microbial inactivation rates when are compared to the use of the PSs alone. KI was firstly studied as potentiator of aPDT mediated by a C_{60} fullerene bisadduct (Zhang *et al*., 2015). The results showed that KI potentiated the ultraviolet A (UVA) or the white light-mediated killing of Gram-negative bacteria *Acinetobacter baumannii*, Gram-positive methicillin-resistant *Staphylococcus aureus* and fungal yeast *Candida albicans* increasing the effect in 1–2 logs. This extra killing effect was also observed *in vitro* and *in vivo* using a mouse model with an infected skin abrasion (Zhang *et al*., 2015). These promising results conducted to new studies concerning the mechanism of action involved. The KI effect using Methylene Blue (MB) as PS in the photoinactivation of *E. coli* and *S. aureus* was also evaluated (Vecchio *et al*., 2015). The results showed that the addition of KI increased the

bacterial killing in 4 and 2 logs for *S. aureus* and *Escherichia coli* respectively, in a dose-dependent manner. The authors also affirmed that the KI potentiator effect in these aPDT studies mediated by MB was probably due to the formation of reactive iodine species that were quickly produced with a short lifetime (Vecchio *et al*., 2015). Since then, some other examples of the potentiation of aPDT effect using combinations of PSs and KI were reported. For instance, MB and new methylene blue (NMB) were studied in the photoinactivation of oral *Candida albicans* infection in a mouse model (Freire *et al*., 2016), Photofrin in the photoinactivation of several Gram-negative bacteria (Huang *et al*., 2017), BODIPY dyes in the photoinactivation of *S. aureus*, *E. coli* and *C. albicans* (Reynoso *et al*., 2017). This approach was also efficient in aPDT of Gram-negative and Gram-positive bacteria mediated by Rose Bengal (Wen *et al*., 2017) and fullerenes (Huang *et al*., 2018a). Interestingly, an anionic porphyrin in the presence of KI was able to photoinactivate *E. coli* (Huang *et al*., 2018b). The combination of MB and KI was also efficient to treat an urinary tract infection in a female rat model (Huang *et al*., 2018c). All these reports helped to elucidate the mechanism of action of KI potentiation. It was proposed that the extra killing effect is caused by several parallel reactions initiated by the reaction of $^1O_2$ with KI producing peroxyiodide (Figure 2.1), that can suffer further decomposition by two different pathways, which are dependent on the degree of binding of the PS to the microbial cells (Zhang *et al*. 2015; Reynoso *et al*. 2017; Vecchio *et al*. 2015; Gsponer *et al*. 2016; Freire *et al*. 2016; Wen *et al*., 2017; Kashef *et al*.,2017; Hamblin, 2017; Huang *et al*. 2017, 2018). One of the pathways involves the formation of free iodine (I_2/I_3^-) and hydrogen peroxide (H_2O_2). Free iodine can kill microbial cells when generated in solution but needs to reach a sufficient threshold concentration to be microbicidal. The amount of free iodine produced depends on the amount of $^1O_2$ produced, but also on the concentration of iodide anion present in solution (Figure 2.1). The other one involves a homolytic cleavage process producing reactive iodine radicals ($I_2^{\cdot-}$), which are much more toxic if generated very close to the target cells since these radicals have short diffusion distance (Figure 2.1).

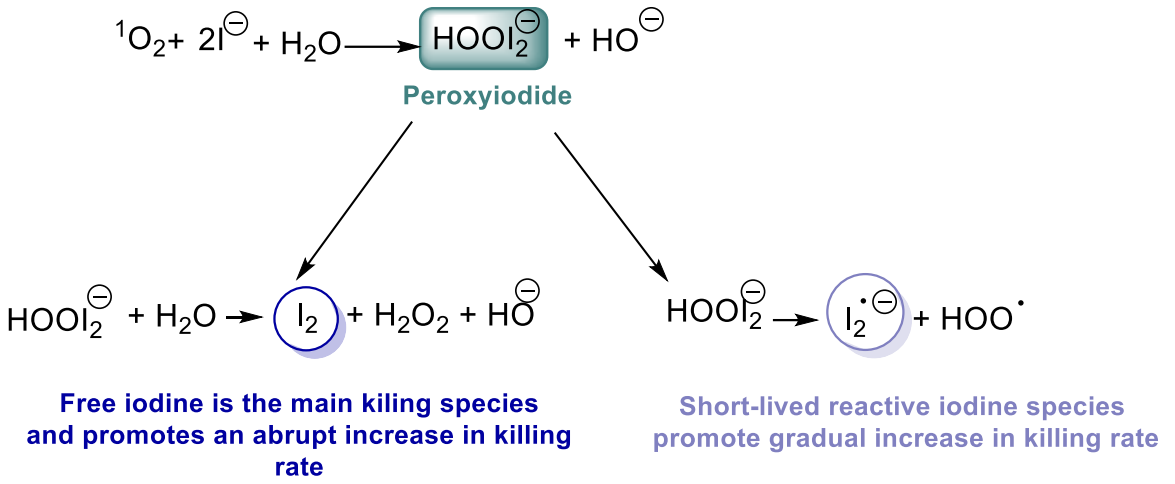

Figure 2.1. Schematic representation of the decomposition of peroxyiodide produced by the reaction of $^1O_2$ and KI (elaborated according with the literature - Zhang *et al*. 2015; Reynoso *et al*. 2017; Vecchio *et al*. 2015; Gsponer *et al*. 2016; Freire *et al*. 2016; Wen *et al*. 2017; Kashef *et al*. 2017; Hamblin, 2017; Huang *et al*. 2017, 2018).

The microbial killer role of the two species can be distinguished by observing the killing microbial curve profile. When the principal contribution for the killing is the free iodine, the curves assumes an abrupt threshold value. On the other hand, a gradual killing curve can be observed when the short-lived reactive iodine species are the mainly killing species (Huang *et al*. 2018).

Until now, the literature survey only reported combinations of PSs and KI with a positive aPDT potentiation. Additionally, the possibility of extending the approach to cationic porphyrins was not evaluated. Consequently, in this work, in order to gain a more comprehensive knowledge about this type of potentiation, we decided to assess the effect of KI in the presence of a broad range of cationic porphyrinic and non-porphyrinic dyes as PSs (Figure 2.2). To achieve this objective and considering the high number of assays required to evaluate the different combinations of PSs with KI, the assays were performed using a bioluminescent *E. coli* strain as a bacterial model. It is well known that the bioluminescence approach can provide a sensitive and innocuous way to detect the viability state of microorganisms. Compared to the conventional plating count methodology, the use of bioluminescent strains in aPDT allows to monitor the process in real-time and it is a sensitive and cost-effective methodology to evaluate this effect. Moreover, the strong correlation between CFU and bioluminescent signal of the

bioluminescent *E. coli* used in this work has already been proved and described (Alves *et al*., 2008, Alves *et al*., 2011a, Alves *et al*., 2011b)

The structures of the selected PSs summarized in Figure 2.2 comprise: i) the five structural related *meso*-tetraarylporphyrins with one [**Mono-Py(+)-Me**], two [**Di-Py(+)-Me *opp***, **Di-Py(+)-Me *adj***], three [**Tri-Py(+)-Me**] and four [**Tetra-Py(+)-Me**] positives charges and a formulation (**Form**) based on these porphyrins; ii) the three β-substituted porphyrins **β-ImiPhTPP**, **β-ImiPyTPP** and **β-BrImiPyTPP** bearing positively charged imidazole units; and iii) the non-porphyrinic dyes - methylene blue (**MB**), Rose Bengal (**RB**) and Toluidine Blue O (**TBO**), crystal violet (**CV**) and malachite green (**MG**).

In the selection of these three series of PSs was considered their different photoinactivation profile towards *E. coli* and their mechanism of action (Type I and Type II).

For the *meso*-tetraarylporphyrins with positive charges at the *meso* position the studies already performed demonstrated that their photodynamic efficiency was dependent on charge number, charge distribution, aggregation behavior and molecular amphiphilicity and the order of their efficacy was: **Mono-Py(+)-Me** < **Di-Py(+)-Me *opp*** < **Di-Py(+)-Me *adj*** < **Tetra-Py(+)-Me** < **Tri-Py(+)-Me**. Additionally, a formulation (**Form**) constituted by a non-separated mixture of Mono-Py(+)-Me (19%), Di-Py(+)-Me *opp* and Di-Py(+)-Me *adj* (20%) Tri-Py(+)-Me (44%) and Tetra-Py(+)-Me (17%) was also studied. This mixture has already proved to be efficient in the photoinactivation of *S. aureus*, *E. coli* and *Pseudomonas syringae pv. actinidiae* and is considered an excellent alternative to the highly efficient **Tri-Py(+)-Me** since the production costs and also the production time was reduced significantly (Martins *et al*., 2018; Marciel *et al*., 2018). The neutral 5,10,15,20-tetra-(4-pyridyl)porphyrin (**Tetra-Py**) precursor of the positively charged **Tetra-Py(+)-Me** was also included.

For the *meso*-tetraarylporphyrins with a positive charge at the *beta*-pyrrolic position (**β-ImiPhTPP**, **β-ImiPyTPP** and **β-BrImiPyTPP**) a different efficacy profile in photoinactivation of *E. coli* at concentrations of 20 μM was observed in previous studies; however, at 5.0 μM none of the three PSs caused a significant decrease in bacterial activity (Moura *et al*., 2019).

Although porphyrins and porphyrins analogues comprise most of the PSs used in aPDT, several non-porphyrinic chromogens exhibit photodynamic activity (Ormond and Freeman 2013). Thus, for this study were selected good $^1O_2$ generators with positive charges that already proved their photodynamic efficiency in clinical trials such as the phenothiazinium salts **MB** and **TBO** (Abrahamse and Hamblin 2016). In this study were also included two photoactive dyes that act mainly through type I mechanism (with lower $^1O_2$ production rates), the **CV** and **MG**. In this evaluation the study was extended to the xanthene derivative **RB**. Combinations of KI with **RB** and with **MB** were already studied and were introduced in this work to corroborate our results (Wen *et al*., 2017, Vecchio *et al*., 2015).

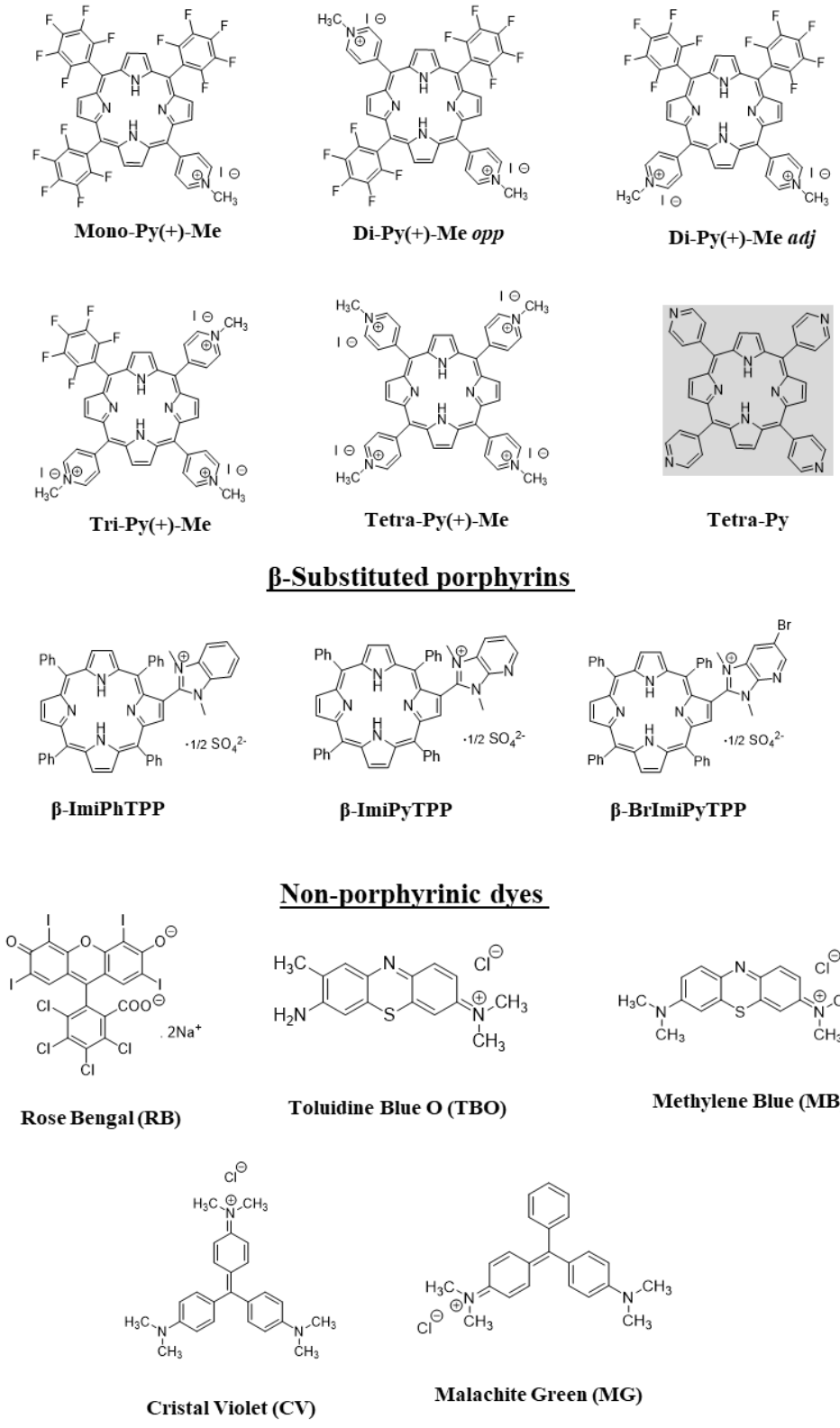

Figure 2.2: Structures and acronyms/abbreviations of the PSs used in this study.

2.3. Materials and Methods

2.3.1. Photosensitizers: stock solutions and UV-Vis spectra

Stock solutions of each porphyrin were prepared at 500 µM in dimethyl sulfoxide (DMSO) and stored in the dark. Stock solutions of non-porphyrinic dyes were prepared at 500 µM in phosphate buffer solution (PBS) and stored in the dark.

The porphyrins [5-(1-methylpyridinium-4-yl)-10,15,20-tris(pentafluorophenyl)-porphyrin mono-iodide (**Mono-Py(+)-Me**), 5,15-bis(1-methylpyridinium-4-yl)-10,20-bis(pentafluorophenyl)porphyrin di-iodide (**Di-Py(+)-Me *opp***) 5,10-bis(1-methylpyridinium-4-yl)-15,20-bis(pentafluorophenyl)-porphyrin di-iodide (**Di-Py(+)-Me *adj***), 5,10,15-tris(1-methylpyridinium-4-yl)-20-(pentafluorophenyl)porphyrin tri-iodide (**Tri-Py(+)-Me**) and 5,10,15,20-tetrakis(1-methylpyridinium-4-yl)porphyrin tetra-iodide (**Tetra-Py(+)-Me**), the formulation (**Form**) of the non-separated porphyrins Mono-Py(+)-Me (19%), Di-Py(+)-Me *opp* and Di-Py(+)-Me *adj* (20%) Tri-Py(+)-Me (44%) and Tetra-Py(+)-Me (17%) and the neutral 5,10,15,20-tetra-(4-pyridil)porphyrin (**Tetra-Py**) were synthetized according with the literature (Simões *et al*. 2016; Marciel *et al* 2018; Martins *et al* 2018). The preparation of the mono-cationic porphyrins **β-ImiPhTPP**, **β-ImiPyTPP** and **β-BrImiPyTPP** bearing an imidazole ring at the β-pyrrolic position were synthetized according with a procedure developed in our laboratory (Moura *et al* 2019), Crystal Violet (**CV**) was purchased from Merck, Rose Bengal (**RB**) from Fluka AG, Malachite Green (**MG**) from Riedel-de-Haën™, Methylene Blue (**MB**) and Toluidine Blue O (**TBO**) from Acros organics.

2.3.2. Light sources

The potentiation of aPDT effect between the PS and KI was evaluated by exposing the bacterial suspension in the presence of each combination to a set of fluorescent PAR lamps which is constituted by 13 fluorescent lamps OSRAM 21 of 18 W each, PAR white radiation (380–700 nm) at an irradiance of 25 $W.m^{-2}$. All the irradiances were measured with a Power Meter Coherent FieldMaxII-Top combined with a Coherent PowerSens PS19Q energy sensor.

2.3.3. Bacterial strains and growth conditions

The genetically transformed bioluminescent *E. coli* Top10 (Alves *et al*. 2011) was grown on Tryptic Soy Agar (TSA, Merck) supplemented with 50 mg mL^{-1} of ampicillin (Amp) and with 34 mg mL^{-1} of chloramphenicol (Cm). Before each assay, one isolated colony was transferred to 10 mL of tryptic soy broth medium (TSB, Merck) previously supplemented with Amp and Cm and was grown overnight at 25 °C under stirring (120 rpm). An aliquot was transferred into 10 mL TSB under the same growth conditions till stationary growth phase was achieved. An optical density at 600 nm (OD_{600}) of 1.6 ± 0.1 corresponded to ≈10^8 colony forming units (CFU) mL^{-1}.

The correlation between CFU mL^{-1} and the bioluminescent signal (in RLUs) of bioluminescent *E. coli* strain was evaluated. A fresh overnight bacterial culture was serially diluted (10^{-1} to 10^{-9}) in PBS. Non-diluted and diluted aliquots were pour-plated on TSA medium (0.5 mL) and, simultaneously, were read on a luminometer (0.5 mL) (TD-20/20 Luminometer, Turner Designs, Inc., Madison, WI, USA) to determine the bioluminescence signal.

2.3.4. Antimicrobial Photodynamic Therapy (aPDT) Procedure

Bioluminescent *E. coli* culture was grown overnight and was tenfold diluted in PBS (pH 7.49), to a final concentration of ∼10^8 CFU mL^{-1}, which corresponds approximately to 10^8 RLU. The bacterial suspension was equally distributed in 50 mL sterilized and acid-washed beakers.

2.3.4.1. Bioluminescence monitoring

All the experiments were carried out under PAR white light (380-700 nm) and the *E. coli* bioluminescence signal was measured in the luminometer at different times of light exposure. The assays were finished whenever the detection limit of the luminometer was achieved (*c.a* 2.3 log). Light control (LC), dark control (DC) and KI control, were also evaluated as described below.

2.3.4.2. Evaluation of the inorganic salt effect on Tetra-Py(+)-Me photodynamic action

The first experiments were performed in order to assess the effect of different inorganic salts in the inactivation of *E. coli* through aPDT approach using the tetracationic porphyrin **Tetra-Py(+)-Me,** extensively studied in bacterial photoinactivation processes (Alves *et al*., 2008, Tavares *et al*., 2011, Simões *et al*., 2016). The selected inorganic salts were KI, NaI, KCl, NaCl and NaBr and the assays were conducted with 50 mM of each salt and 5.0 μM of **Tetra-Py(+)-Me**. All the inorganic salts were purchased from Sigma-Aldrich (St. Louis, MO) and stock solutions were prepared at 500 mM in PBS immediately before each experiment.

The assays were carried out by exposing the bioluminescent *E. coli* suspension to **Tetra-Py(+)-Me** at 5.0 μM with each salt added from the stock solution to achieve the final concentrations of 50 mM. Simultaneously, the following different controls were performed: one light control (LC) that contained a bacterial suspension exposed to the same light conditions as the samples, and dark controls (DC) that comprised a bacterial suspension incubated with the PS at 5.0 μM and with the distinct salts at 50 mM. DC were protected from light during all the procedure. The samples and controls were protected from light with aluminium foil and remained in the dark for 15 min to promote the porphyrin binding to *E. coli* cells before irradiation. Then, both samples and controls were exposed to the PAR white light at 25 $W.m^{-2}$ under stirring (120 rpm) and placed on a tray; the beaker bottoms were covered with water to maintain the samples at constant temperature (25 °C). Finally, aliquots of 0.8 mL of samples and controls were collected at different times of light exposure and the bioluminescence signal was measured in the luminometer. Three independent experiments with two replicates were performed and the results were averaged.

2.3.4.3. Evaluation of the antimicrobial effect in the presence of different PSs and KI

The assays were carried out by exposing a final volume of 10 mL of a bioluminescent *E. coli* suspension to each PS at 5.0 μM and combinations of each PS at

5.0 µM and KI concentrations at 50 and 100 mM and for **RB**, **CV**, **MG** also at 25 mM. The samples were protected from light with aluminium foil and incubated in the dark for 15 min. Light and dark controls were also carried out simultaneously with the aPDT procedure: the light controls (LC) comprised a bacterial suspension and a bacteria suspension with KI at 100 mM exposed to the same light protocol; and the dark control (DC) comprised a bacterial suspension incubated with the PSs at 5.0 µM and KI at the higher concentration tested (100 mM) protected from light. The aPDT treatment was performed as described above. Three independent experiments with two replicates were performed and the results were averaged.

2.3.5. Detection of iodine formation

In a 96 wells microplate, appropriate volumes of each PS at 5.0 µM (1µL) and combinations of each PS at 5 µM (1µL) and KI at 100 mM (2 µL) were added to each well and irradiated with PAR white light at 25 $W.m^{-2}$. The generation of iodine was monitored by reading the absorbance at 340 nm at irradiation times 0, 5, 10, 15, 30, 45, 60, 75, 90, 105 and 120 min. As positive control it was used Lugol's solution diluted to 1.1000.

Another simple assay to detect iodine was also performed, for the different combinations of PS and KI, in the presence of amylose due to the well-known formation of a strong blue complex when these two species are present (Luallen, 2017). So, to the beakers containing a starch solution at a concentration of 2 mg L^{-1}, it was added each PS at 5 µM and KI at 100 mM. The samples were incubated in the dark for 15 min and afterwards were exposed continuously and under stirring (120 rpm) to the same light source used in the aPDT assays. The colour change was registered and photographed at different times of irradiation for each sample. At the same time, the following control assays were performed: PS + light; KI + light, PS + KI under dark.

2.3.6. Statistical analysis

Three independent experiments with two replicates per assay for each condition were done. The statistical analysis was performed with GraphPad Prism. Normal distributions were checked by the Kolmogorov–Smirnov test and the homogeneity of

variance was verified with the Brown Forsythe test. ANOVA and Dunnet's multiple comparison tests were applied to assess the significance of the differences between the tested conditions. A value of $p < 0.05$ was considered significant.

2.4. Results

The effect of KI for each series of PSs towards *E. coli* was evaluated using the same concentration of PS (5.0 μM) and KI concentrations of 50 and 100 mM (unless other concentrations were mentioned) under PAR white light at an irradiance of 25 $W.m^{-2}$. These KI concentrations were selected considering the ones referred in similar studies and knowing that higher concentrations can limit the combined protocol application in clinic area due to osmotic stress. The PS, **TetraPy(+)-Me,** was selected to confirm the benefic effect of KI among other inorganic salts (NaI, NaCl, KCl, NaBr). This well-known tetracationic porphyrin is extensively studied in bacterial photoinactivation processes and is considered an excellent reference when the efficacy of different cationic porphyrins are compared (Alves *et al*., 2008, Tavares *et al*., 2011, Simões *et al*., 2016). Low light doses ranging from 1.5 to 36 J/cm^2 emitted by a fluorescent lamp set (380-700 nm) were selected based on their efficacy to inactivate a large range of microorganisms (Marciel *et al*., 2017, Moura *et al*., 2019). Additionally, this light source was able to accomplish the required overlap between PS absorption and light setup emission spectrum (Cieplik *et al*., 2015, Costa *et al*., 2010).

2.4.1. Evaluation of the salt effect on Tetra-Py(+)-Me photodynamic efficiency.

The results presented in Figure 2.3 show that the photoinactivation pattern of *E. coli* in the presence of **Tetra-Py(+)-Me** is strongly dependent on the anion used.

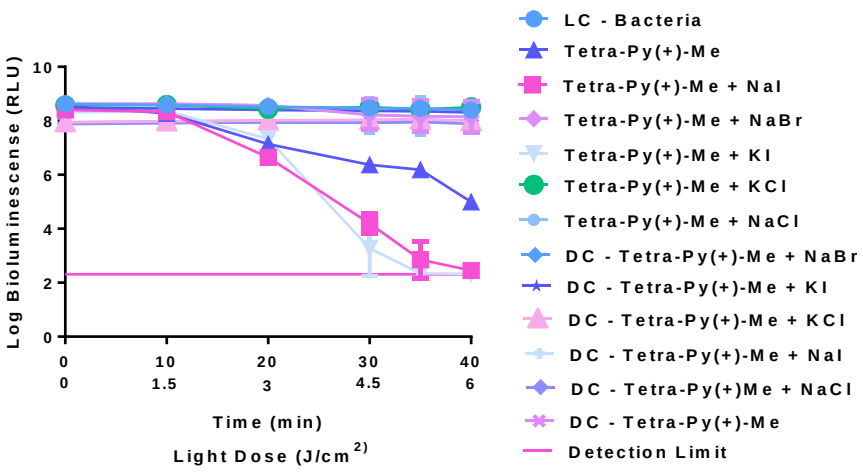

Figure 2.3. Survival of bioluminescent *E. coli* during aPDT with **Tetra-Py-(+)-Me** at 5.0 µM and 50 mM of KI, NaI, KCl, NaCl and NaBr after irradiation with PAR white light (380–700 nm) at an irradiance of 25 W m^{-2} for 40 min. The values are expressed as the three independent experiments; error bars indicate the standard deviation and in some cases are collapsed with the symbols.

The results clearly indicate that when combinations of **Tetra-Py(+)-Me** with KI and NaI were used, a reduction of the bioluminescence signal of *c.a.* 4 log was observed after 30 min of irradiation. In the case of NaBr, KCl and NaCl no potentiation on the aPDT effect was detected. Light and dark controls showed no significant variation in the bioluminescence produced by *E. coli*.

2.4.2. Evaluation of the KI effect on the photodynamic action of *meso* tetraarylporphyrins bearing one to four positive charges

The effects of KI at 50 and 100 mM in the photodynamic action of **Mono-Py(+)-Me**, **Di-Py(+)-Me *opp***, **Di-Py(+)-Me *adj***, **Tri-Py(+)-Me** and **Tetra-Py(+)-Me** towards *E. coli* are summarized in Figure 2.4.

In the cases of the LCs (Bacteria and bacteria + KI irradiated) and DC (bacteria + PS + KI in the dark) no decrease in *E. coli* bioluminescent signal was detected. These results indicate that the viability of this recombinant bioluminescent bacterium was not affected by irradiation, by the presence of the salt or by any of the tested combinations of PS + KI in the dark.

The results shown in Figure 2.4 A for the monocationic porphyrin (**Mono-Py(+)-Me**) demonstrated that its low efficacy is strongly improved by the presence of KI; the poor activity of this PS towards *E. coli* was previously related with its low water solubility leading to aggregation and, consequently, to low $^1O_2$ generation. Under the conditions used in these assays this porphyrin maintained its low efficacy causing a decrease on *E. coli* bioluminescence signal of 0.9 log ($p<0.0001$) after 240 min of irradiation. However, the addition of KI at 50 mM and 100 mM potentiated the effect of this mono-cationic porphyrin, causing bioluminescent signal reductions of *c.a.* 3.5 and 5.5 log ($p<0.0001$) after 150 min of irradiation.

The dicationic porphyrins **Di-Py(+)-Me *opp*** and **Di-Py(+)-Me *adj*** without the presence of the coadjuvant promoted similar effects on the reduction (*c.a.* 6 log after, respectively, 150 and 120 min of irradiation) of *E. coli* bioluminescence signal (Figure 2.4 B and 2.4 C). However, when these two isomers were combined with KI the results obtained were significantly different. The combination of **Di-Py(+)-Me *adj*** with KI at 50 mM and 100 mM produced similar results in the photoinactivation of bioluminescent *E. coli* and no improvement in aPDT efficiency was detected (Figure 2.4 C). In fact, in the last irradiation time, there were no significant differences in the *E. coli* bioluminescence signal promoted by **Di-Py(+)-Me *adj*** and the two combinations of **Di-Py(+)-Me *adj*** + KI. In the case of **Di-Py(+)-Me opp** (Figure 2.4 B) the presence of KI (at 50 and 100 mM) led to a significant reduction on its efficacy. The maximum inactivation achieved for the combination of this PS with 100 mM of KI was 1.7 log ($p<0.0001$).

The **Tetra-Py(+)-Me** and **Tri-Py(+)-Me** were the most efficient porphyrins in the photoinactivation of bioluminescent *E. coli*, which is also in accordance with the literature (Simões *et al*. 2016). These porphyrins, when acting by themselves, showed to be potent PSs for the inactivation of bioluminescent *E. coli*, demanding short irradiation times (*c.a.* 70 min) to achieve total photoinactivation of this Gram-negative bacterium (Figure 2.4 D and E). The combination of these PSs with KI at 50 and 100 mM increased dramatically the effect of these PSs in the photoinactivation of bioluminescent *E. coli* (Figure 2.4 D and E). In the case of **Tri-Py(+)-Me**, it was observed an abrupt decrease in *E. coli* viability after 30 and 10 min of irradiation when the combinations of this PS with 50 mM and 100 mM

of KI were used, respectively (Figure 2.4 D). This sharp decrease was also observed for the combination of **Tetra-Py(+)-Me** and KI; after 30 and 10 min of irradiation no bioluminescent signal was detected for combinations **Tetra-Py(+)-Me** +KI 50 mM and **Tetra-Py(+)-Me** +KI 100 mM, respectively.

These results prompted us to study the effect of KI in the aPDT efficiency of the porphyrinic formulation (**Form**) described as an excellent alternative to the highly efficient **Tri-Py(+)-Me,** as it was mentioned above. The results summarized in Figure 2.4 F show that this formulation at 5μM in the absence of the coadjuvant and after 60 min of irradiation, promoted a decrease in the bioluminescence signal of *E. coli* of 4 log ($p<0.0001$) (Figure 2.4 F). When the assays were repeated in the presence of KI at 50 mM a more pronounced decrease in *E. coli* viability was detected after 40 min of irradiation, reaching the detection limit of the luminometer after 60 min. This rapid decrease in the viability of this bacterium occurred even sooner, after only 20 min of irradiation, when KI was used at 100 mM.

In order to check if the presence of positive charges is a required feature for the combination of KI with this series of porphyrins, the efficacy of the neutral 5,10,15,20-tetra(4-pyridyl)porphyrin (**Tetra-Py**) was evaluated in the presence of this salt at 50 mM and 100 mM. In Figure 2.4 G are summarized the results obtained and it was verified that the low efficacy of this neutral porphyrin was not improved by the presence of the salt, suggesting that when an increment effect was observed in the presence of KI in this series of porphyrins, the presence of at least one positive charge is mandatory.

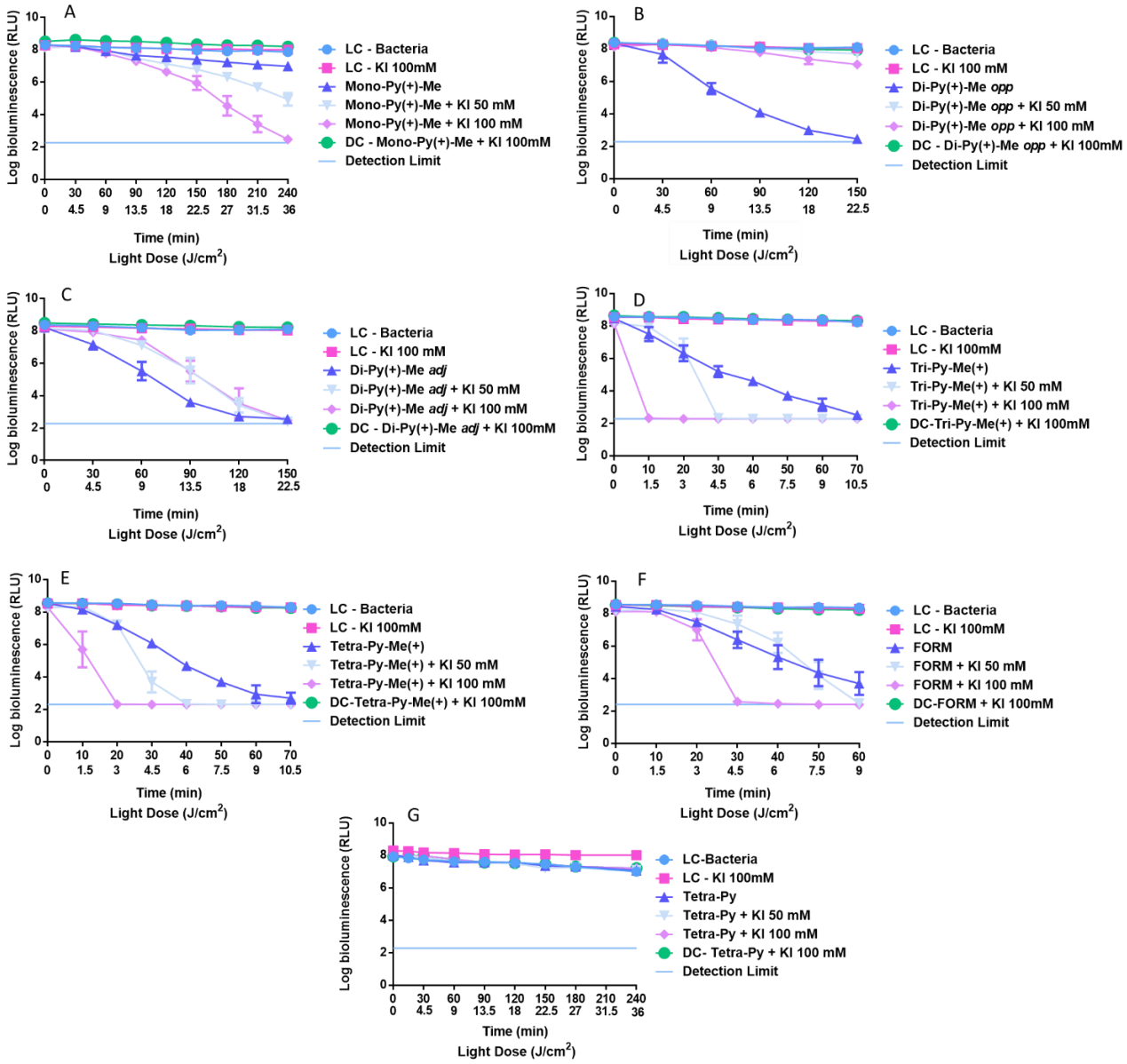

Figure 2.4. Survival of bioluminescent *E. coli* during aPDT assays in the presence of **Mono-Py(+)-Me** (**A**), **Di-Py(+)-Me *opp*** (**B**), **Di-Py(+)-Me *adj*** (**C**), **Tetra-Py(+)-Me** (**D**), **Tri-Py(+)-Me** (**E**), **Form** (**F**) and **Tetra-Py** (**G**) at 5.0 μM alone and combined with KI at 50 and 100 mM. The values are expressed as the three independent experiments; error bars indicate the standard deviation.

2.4.3. Evaluation of the KI effect on the photodynamic action of porphyrin derivatives bearing cationic imidazole units at the β-pyrrolic position

The results obtained in the photoinactivation of bioluminescent *E. coli* with the monocationic porphyrins **β-ImiPhTPP**, **β-ImiPyTPP** and **β-BrImiPyTPP** bearing an imidazole moiety at the β-pyrrolic position, both in the absence and in the presence of KI

are presented in Figure 2.5. The low activity of these porphyrins at 5.0 µM in the photoinactivation of bioluminescent *E. coli* was improved in the presence of KI, although the inactivation increment was different. The combination of **β-ImiPhTPP** and **β-BrImiPhTPP** with KI at 100 mM promoted a significant positive effect in the photoinactivation of *E. coli* with an increment on the bioluminescent reduction of 1.3 and 1.1 log for **β-ImiPhTPP** and **β-BrImiPyTPP** ($p<0.0001$), respectively, after 240 min of irradiation when compared with the effect of these PSs in the absence of KI (Figure 2.5 A and C).

A different profile was observed for porphyrin derivative **β-ImiPyTPP** (Figure 2.5 B). The best results were obtained with the combination of this PS with 100 mM of KI, promoting a significant decrease in *E. coli* viability (Figure 2.5 B). The bioluminescence signal reduction reached the method detection limit after 240 min; when compared with the effect of these PS in the absence of KI an increment on the bioluminescent reduction of 5.3 log in cell viability was observed ($p<0.0001$).

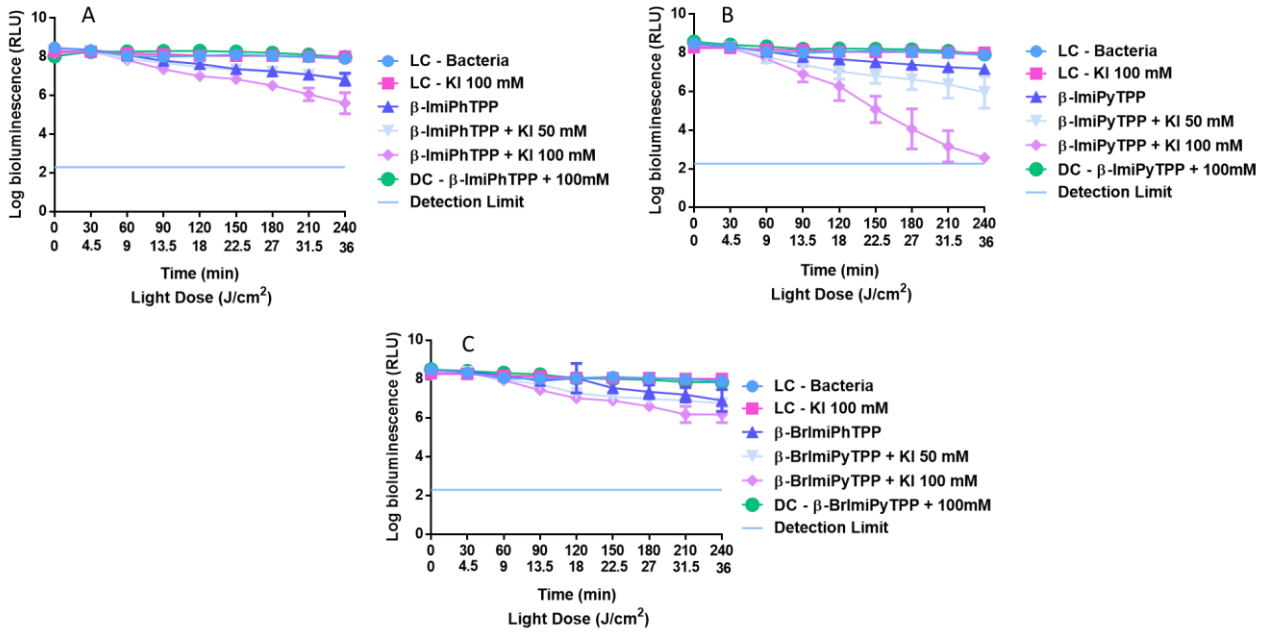

Figure 2.5. Survival of bioluminescent *E. coli* during aPDT assays in the presence of mono-cationic porphyrins **β-ImiPhTPP**, **β-ImiPyTPP** and **β-BrImiPyTPP** at 5.0 µM alone or combined with KI at 50 and 100 mM. The values are expressed as the three independent experiments; error bars indicate the standard deviation.

2.4.4. Evaluation of the KI effect in the photodynamic action of non-porphyrinic dyes

In Figure 2.6 are summarized the effects of KI at 50 and 100 mM in the photodynamic inactivation of *E. coli* when using **RB** (A), **TBO** (B), **MB** (C), **CV** (D) and **MG** (F). Combinations of **RB** (Figure 2.6 A) and **MB** (Figure 2.6 C) at 5.0 µM and KI showed to have a potential effect in the photodynamic inactivation of *E. coli*, causing marked reductions in the *E. coli* viability when compared with the results obtained with these dyes alone. The PS **RB**, when acting alone, promotes a decrease of 1.3 log ($p<0.0001$) in *E. coli* viability after 150 min of irradiation. When combined with KI, an efficient decrease in bioluminescent signal of *E. coli* was observed, even when KI at 25 mM was used. At this concentration, the combination of **RB** 5.0 µM + KI 25 mM, caused a sharp decrease in *E. coli* viability after 90 min of irradiation, reaching the detection limit of the luminometer after 120 min. This marked effect was also observed when **RB** was combined with 50 mM of KI, but it was with the combination of **RB** 5.0 µM+ KI 100 mM that this effect became more noteworthy; after 20 min of irradiation it was observed a decrease of 6 log ($p<0.0001$) in *E. coli* viability and after 30 min no bioluminescent signal was observed.

A similar profile was observed with combinations of **MB** at 5.0 µM and KI. In the absence of KI, **MB** caused a decrease in the bioluminescence signal of *E. coli* of 5.5 log ($p<0.0001$) after 180 min of irradiation, but when combinations of this PS with KI were used, an efficient decrease in the viability of this bacterium was also observed, after 30 and 60 min of irradiation, with KI at 100 mM and 50 mM, respectively.

In the cases of **TBO**, **CV** and **MG**, a potentiation of their photodynamic action mediated by the presence of KI was not observed. In fact, **TBO** when acting alone at 5.0 µM revealed to be an excellent PS for the inactivation on bioluminescent *E. coli*, promoting a remarkable decrease in the bioluminescent signal of 6 log ($p<0.0001$) after 60 min of irradiation. In the presence of KI, this reduction was only observed after 90 min of irradiation.

CV when acting alone caused a decrease in the bioluminescent signal of 3.2 log ($p<0.0001$), however, in the presence of KI at 25, 50 and 100 mM the decrease did not go beyond 1.4, 2.2 and 2.7 log ($p<0.0001$), respectively. In the case of **MG** no significant

effect was observed in the *E. coli* viability either when this dye was used alone or combined with KI.

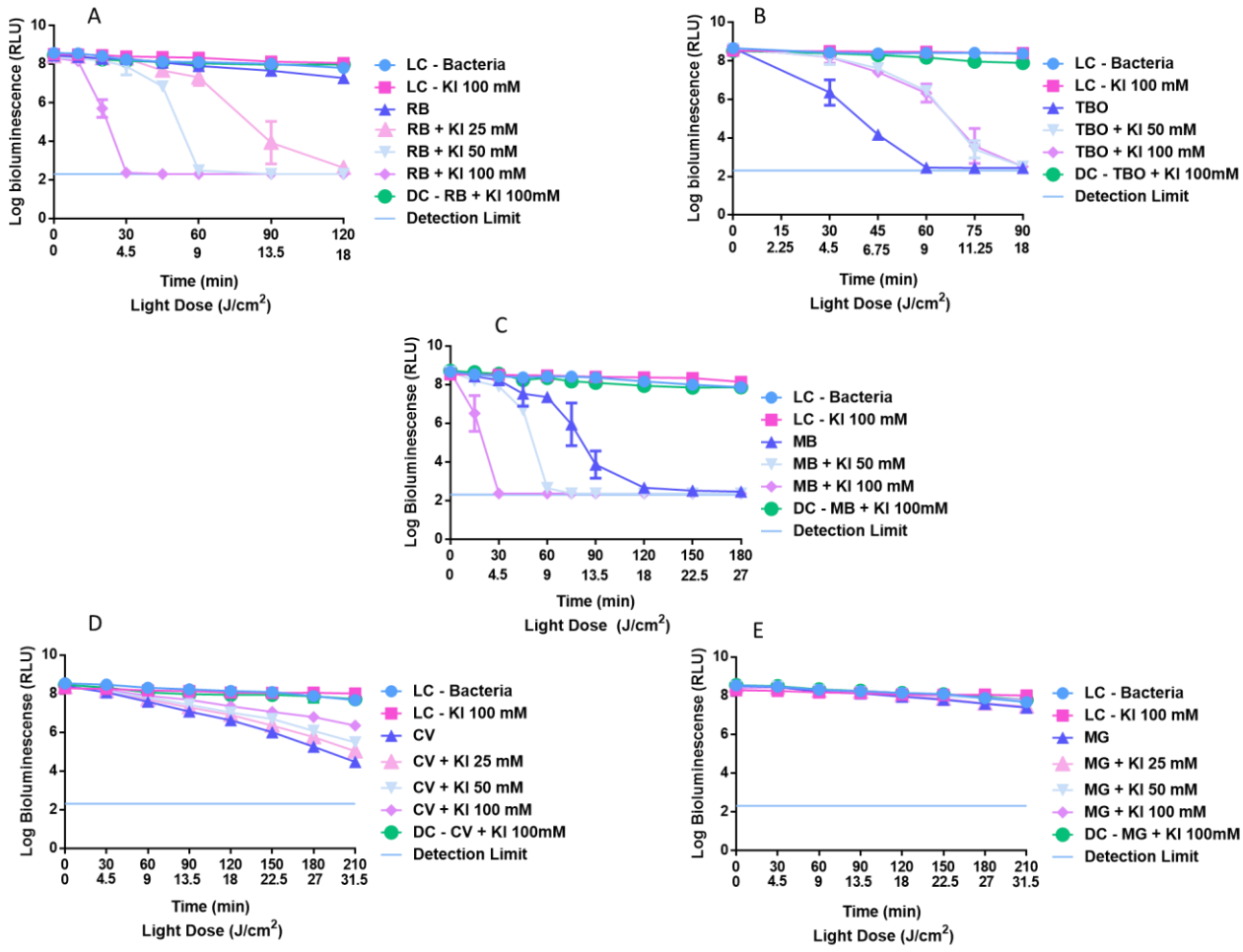

Figure 2.6. Survival of bioluminescent *E. coli* during aPDT assays in the presence of non-porphyrinic PSs at 5.0 µM **RB** (A), **TBO** (B), **MB** (C), **CV** (D) and **MG** (E) alone and combined with KI at 25, 50 and 100 mM. The values are expressed as the three independent experiments; error bars indicate the standard deviation.

2.4.5. Detection of iodine formation mediated by the PS

In order to clarify if the photodynamic improvement was related with the iodine generation from KI by the PS, the different PSs (5.0 µM) were irradiated both in the absence and in the presence of that coadjuvant at 100 mM. To verify the generation of

iodine, the absorbance at 340 nm was read after 0, 5, 10, 15, 30, 45, 60, 75, 90, 105 and 120 minutes of irradiation. The results obtained are summarized in Figure 7.

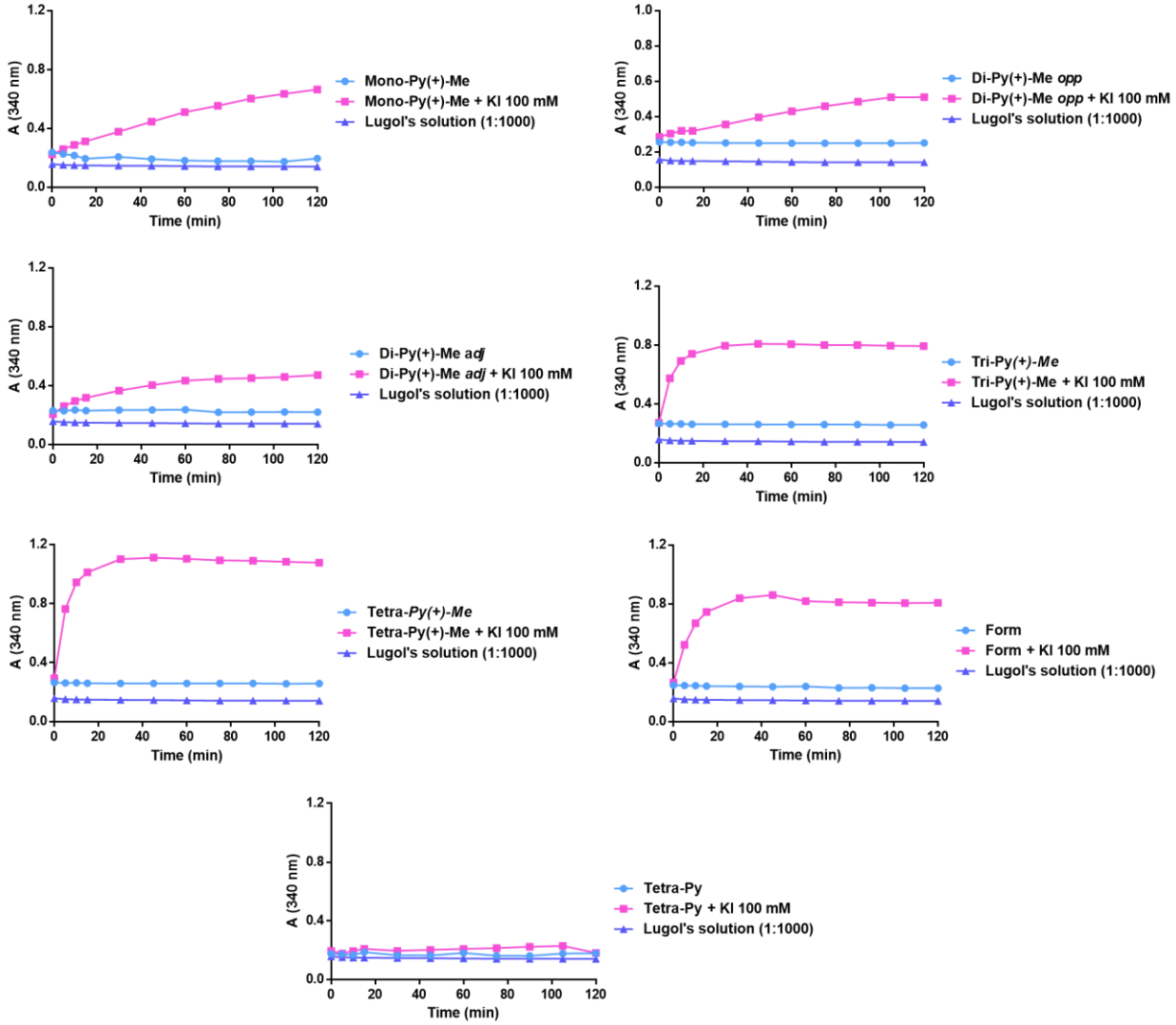

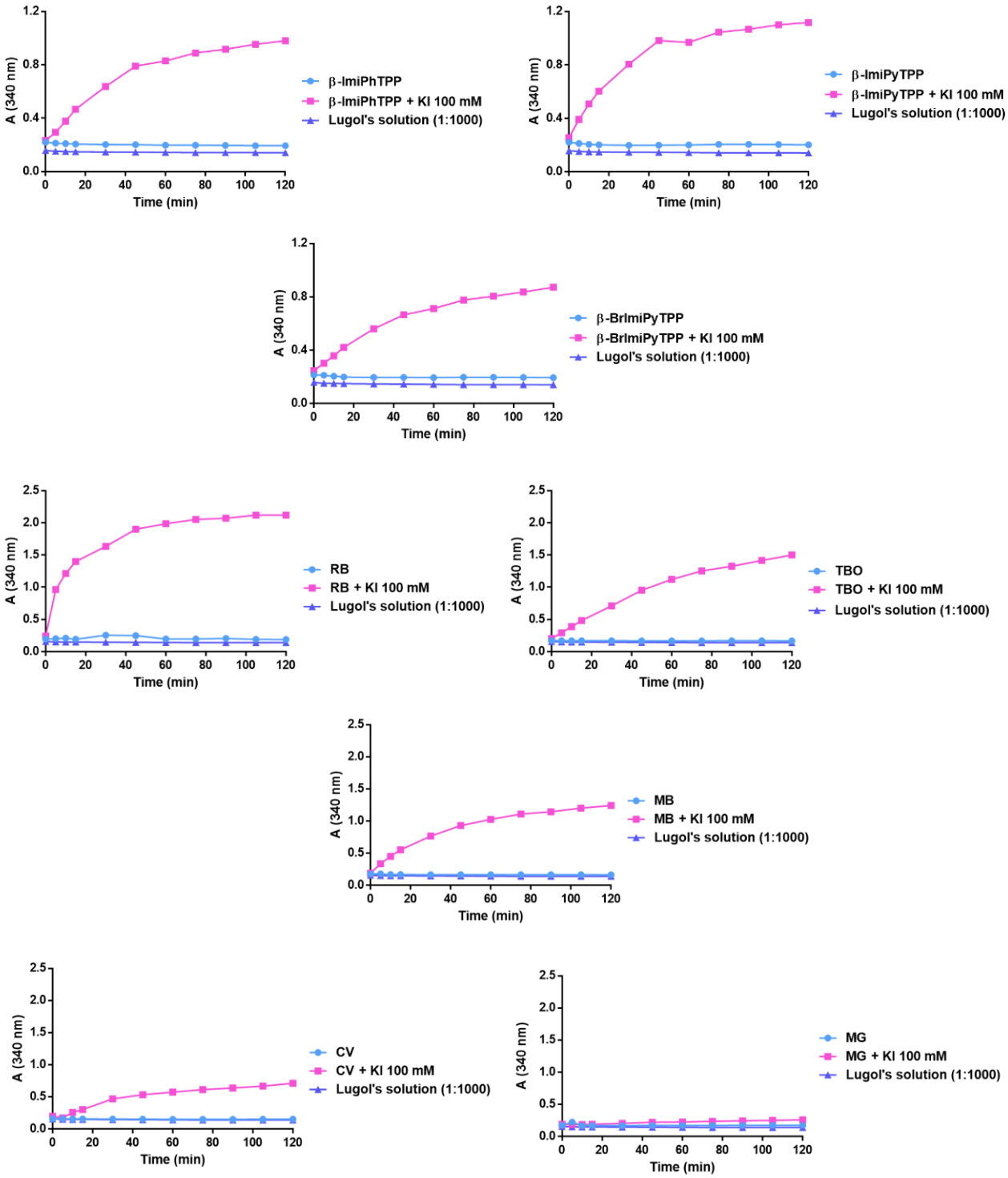

Figure 2.7. Monitoring of the formation of iodine at 340 nm after different irradiation periods in the presence of each PS at 5.0 µM and combinations of each PS at 5.0 µM and KI at 100 mM.

The results show that the combination of KI with **Tri-Py(+)-Me**, **Tetra-Py(+)-Me** and **Form** causes a higher production of I_2, leading to a sharp increase in absorbance at

340 nm in the first 20 minutes of irradiation. On the other hand, the combination of KI with **Mono-Py(+)-Me**, **Di-Py(+)-Me *adj*** , **Di-Py(+)-Me *opp*** only was able to induce a gradual increase of the absorbance at 340 nm, thus indicating the lower ability to produce I_2. The combination of **Tetra-Py** + KI did not produce I_2.

The gradual increase in the absorbance at 340 nm was also observed in the case of mono-cationic porphyrins **β-ImiPhTPP**, **β-ImiPyTPP** and **β-BrImiPyTPP**. However, in the case of **β-ImiPyTPP**, the absolute value of absorbance at 340 nm after 40 min of irradiation was higher than the values observed for the other PSs, indicating the formation of higher amounts of I_2 in this case.

In the case of the non-porphyrinic dyes, the combination of KI with **MB** and **RB** demonstrated a higher ability to produce I_2, with a sharp increase in the absorbance at 340 nm, after 30 min of irradiation. However, combinations of **TBO** + KI and **CV** + KI only produced a gradual increase in the absorbance, indicating the lower capability to produce I_2. Combination of **MG** + KI did not promote the formation of I_2.

The visual appearance of the starch solutions after different irradiation periods are presented in Figure 2.8 and the results corroborated that the time required for the formation of the complex between amylose and iodine was dependent on the PS used. In the presence of **Tri-Py(+)-Me**, **Tetra-Py(+)-Me** and **Form**, the formation of the dark colour appeared just after 2-4 min of irradiation, while for **Di-Py(+)-Me *adj*** the iodine-amylose complex was observed after 45 min of irradiation. The formation of the coloured complex was not observed for the neutral **Tetra-Py** after 240 min of irradiation and for **Mono-Py(+)-Me** and **Di-Py(+)-Me *opp*** after 75 min of irradiation a slight darkening of the solution was observed.

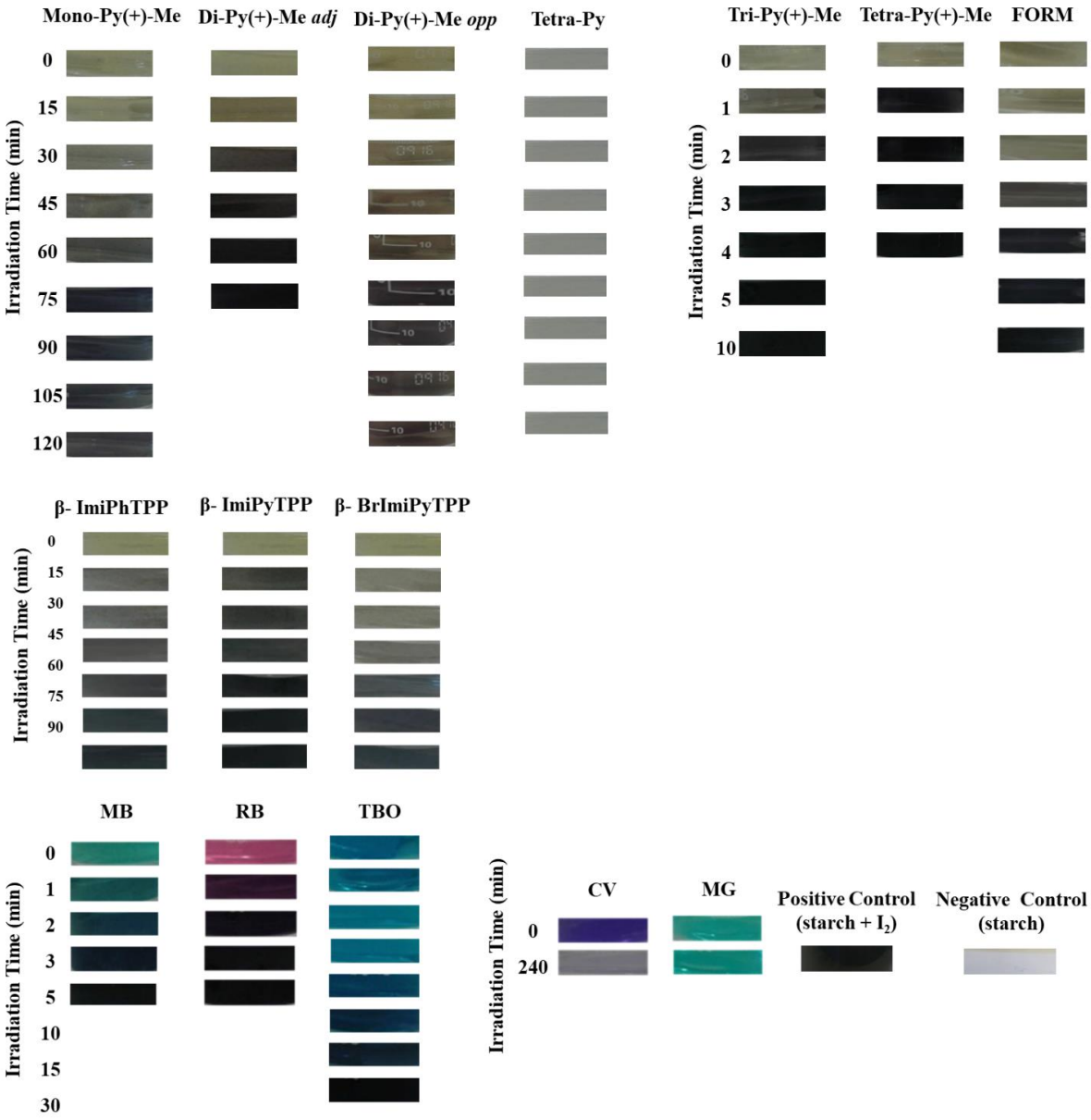

Figure 2.8. Visual appearance of the starch solutions after different irradiation periods in the presence of each PS at 5.0 µM and KI at 100 mM.

For the mono-cationic porphyrins **β-ImiPhTPP**, **β-ImiPyTPP** and **β-BrImiPyTPP** the formation of the deep coloured complex was only observed in the presence of **β-ImiPyTPP** after 60 min of irradiation.

In the assays performed with the non-porphyrinic dyes the combinations **MB**+KI and **RB**+KI promoted the formation of the dark complex after 2-5 min of irradiation and the combination **TBO**+KI after 30 min of irradiation. The combinations of **CV** and **MG** with KI were not able to produce the iodine-amylose complex even after 240 min of irradiation.

2.5. Discussion

Several studies have shown that aPDT combined with some inorganic salts, namely potassium iodide (Vecchio *et al*. 2015; Zhang *et al*. 2015; Huang *et al*. 2016; Wen *et al*. 2017; Huang *et al*. 2018) can be potentiated. However, there is not any evidence until now that this potentiation can be observed for all types of PSs, namely cationic porphyrins. In order to gain a more comprehensive knowledge about the potentiation of aPDT by KI, a broad range of PSs were tested in this study.

We started our study by selecting the most effective salt, using as PS the widely studied tetracationic porphyrin 5,10,15,20-tetrakis(1-methylpyridinium-4-yl)porphyrin tetra-iodide (**Tetra-Py^{+}-Me**), which is frequently used as standard in aPDT studies. This can be considered a reference for all porphyrinic PSs, since this PS is extensively studied in bacterial photoinactivation processes (Alves *et al*., 2008, Tavares *et al*., 2011, Simões *et al*., 2016). The efficacy of bacterial inactivation by the combination of this PS and the salts KI and NaI was clearly higher than when the PS was used alone, showing that these combinations promoted an increase of the antimicrobial photodynamic efficiency of the PS. On the other hand, no effect was observed with the combinations of **Tetra-Py(+)-Me** with NaBr, KCl and NaCl during the irradiation time. The loss of efficiency of this porphyrin in these cases could be explained by the fact that bromide and chloride ions retarded the $^{1}O_2$ generation, and consequently its action as PS (Keum, Kim, and Li 2003; Krumova and Cosa 2016). Therefore, it was obvious that for this PS and under the tested conditions, only salts containing I^- as counterion were capable of potentiate the antimicrobial photodynamic inactivation. Similar results were earlier observed when other PSs were tested (Hamblin 2016). As the combinations PS + KI and PS + NaI were both effective to

inactivate the *E. coli*, the potentiation of the others PSs was performed in the presence of the most studied salt KI.

Besides the difficulty of explaining which of the two proposed pathways of decomposition of peroxyiodide produced by the reaction of $^1O_2$ and (see Figure 2.1) are responsible for the extra microbial killing when KI is present, it was assumed, as proposed previously in other studies, that some information can be taken by the profile of inactivation. If the inactivation curve shows a sharp decrease, free iodine is the main killing species, but if there is a more gradual increase in killing, then there is a contribution from short-lived reactive iodine species (Huang *et al*. 2018). Considering the above, we tried to explain the results obtained with the two series of cationic porphyrins, including the neutral **Tetra-Py,** and with the non-porphyrinic PSs. In Table 2.1 are summarized the results obtained concerning the inactivation profile observed for each combination of KI and PS at 5.0 µM in the photoinactivation of bioluminescent *E. coli*.

	Mono-Py(+)-Me	Di-Py(+)-Me *opp*	Di-Py(+)-Me *adj*	Tri-Py(+)-Me	Tetra-Py(+)-Me	FORM	Tetra-Py	β-ImiPhTPP	β-ImiPyTPP	β-BrImiPhTPP	RB	MB	TBO	CV	MG
KI potentiate aPDT?	✓	✗	✗	✓	✓	✓	✗	✓	✓	✓	✓	✓	✗	✗	✗
KI causes a sharp decrease in the *E. coli* survival?	✗	-	-	✓	✓	✓	-	✗	✗	✗	✓	✓	-	-	-

✗ : No ; ✓ : Yes ;

Table 2.1. Results obtained in the photoinactivation of bioluminescent *E. coli* using combinations of tested PSs at 5.0 µM and KI.

These results allow to classify the PSs studied as: 1) PSs in which its efficiency was potentiated by KI and it was observed a gradual decrease in the *E. coli* survival rate profile (**Mono-Py(+)-Me**, **β-ImiPhTPP**, **β-ImiPyTPP** and **β-BrImiPyTPP**); 2) PSs in which its

efficiency was potentiated by KI and it was observed an abrupt decrease in the *E. coli* survival rate profile (**Tri-Py(+)-Me, Tetra-Py(+)-Me**, **Form**, **RB** and **MB**) and 3) PSs in which its efficiency was not potentiated by KI (**Di-Py(+)-Me *opp***, **Di-Py(+)-Me *adj***, **Tetra-Py**, **TBO**, **CV** and **MG**).

Based on the explanations given in previous works, we can assume that the mechanism of action of the combinations of KI and the PSs **Mono-Py(+)-Me**, **MB**, **β-ImiPhTPP**, **β-ImiPyTPP** and **β-BrImiPyTPP** is probably related to the preferential decomposition of the peroxyiodide to the iodine radicals ($I_2^{\cdot-}$) that, due to their short diffusion distance, cause a gradual decrease in the photoinactivation profile. In the case of **Tri-Py(+)-Me**, **Tetra-Py(+)-Me**, **Form** and **RB** the preferential decomposition of the peroxyiodide leads to the formation of free iodine (I_2/I_3^-), which contributes significantly for the abrupt increase observed in the photoinactivation profile of the *E. coli*. This fact was confirmed by the formation of iodine, visible by spectroscopy (Figure 2.7) and by the colour alteration during the irradiation in the presence of starch (Figure 2.8): PSs that cause a sharp decrease in the *E. coli* survival rate profile revealed higher ability to produce I_2. On the other hand, the belatedly detection of I_2 was observed for PSs that cause a gradual decrease in the *E. coli* survival rate profile.

In the cases of PSs in which the efficiency was not potentiated by KI, or was even reduced, we need also to look at other factors that can likewise contribute to this behaviour.

The different behaviour observed with the dicationic PSs **Di-Py(+)-Me *opp*** (the efficacy was lost in the presence of KI) and **Di-Py(+)-Me *adj*** (no potentiation with KI) (Figure 2.4 B and 2.4 C**)** is probably related with their structural features since both isomers have similar capability to generate $^1O_2$ with high efficiency, as it was described by Simões *et. al* in 2016. Consequently, it can be assumed that both compounds are able to promote the formation of peroxyiodide and its decomposition to iodine radical species ($I_2^{\cdot-}$). However, for **Di-Py(+)-Me *opp*** these radicals, with a short diffusion distance, probably were not generated close to the target cells and the depletion of $^1O_2$ by the previous reaction was responsible by losing its previous efficacy. On the other hand, for **Di-Py(+)-Me *adj*** the formation of toxic radicals in close proximity to the target cells can justify the

maintenance of its efficacy. However, the toxicity under these conditions was comparable to the previous one in the absence of iodide. The different charge distribution in the two di-cationic porphyrins can explain the different behavior in the presence of KI. A study of Alves *et al.* (Alves *et al*. 2011) showed the massive importance of the charge distribution in these two PS efficacies. In this work, the photodynamic inactivation of *E. coli* and *Enterococcus faecalis* using the two isomeric di-cationic porphyrins with different charge distribution showed that the porphyrin with adjacent cationic groups was significantly more active (for both bacteria) than the one with the cationic groups located in opposite *meso* positions. This fact was justified by the distortion of the macrocycle induced by the electrostatic repulsion between the neighbouring charged groups in the porphyrin with adjacent cationic groups (Kessel *et al*., 2003). So, in the case of porphyrinic PSs with cationic groups located in opposite *meso* positions, accompanied by the preferential decomposition of the peroxyiodide to the iodine radicals, as it was observed with **Di-Py(+)-Me *opp***, the addition of KI can even impair the aPDT efficacy. With the porphyrin derivatives **Di-Py(+)-Me *adj***, **Mono-Py(+)-Me** and **β-ImiPyTPP** the asymmetric distribution of the charge allows the radicals to reach the bacterial cells more effectively. However, the potentiation of the aPDT processes mediated by **Mono-Py(+)-Me** and **β-ImiPyTPP** in the presence of KI but not by **Di-Py(+)-Me *adj*** can also be due to the higher production of free iodine by the two first porphyrins when compared with porphyrin.**Di-Py(+)-Me *adj.***

Neutral **Tetra-Py** revealed to be inefficient to photoinactivate *E. coli*, even when KI was used. This can be explained by the fact that this is a neutral PS, and consequently, is not capable to interact with the external membrane of the cell wall of this Gram-negative bacterium. Thus, even when $^1O_2$ is produced in great amounts, the cytotoxic species will never be close enough to the bacterial cells to cause damage. It is also important to refer that this porphyrin tends to aggregate in aqueous media, making it difficult to act as a PS.

CV is known to have an efficient non-radiative deactivation route producing triplet species, such as $^1O_2$, with low yield and acting mainly through an electron-transfer mechanism (Type I), which causes its bleaching (Docampo *et al*. 1983; Indig *et al*. 2000).

The results clearly indicate its low efficiency in the photoinactivation of *E. coli*, either when acting alone or combined with KI. These results are justified by its poor $^1O_2$ production rates allied to its photodegradation when irradiated. Such as in the case of **CV**, it was not surprising that **MG** did not produced any effect in the photoinactivation of bioluminescent *E. coli*, since this PS dye did not produce $^1O_2$, acting only by the Type I mechanism (Zhuo 2016). These two PSs dyes show the importance that $^1O_2$ generation has in the potentiation of aPDT processes mediated by KI. The **TBO** acts mainly by Type II mechanism and, when acting alone inactivate efficiently the bacteria, as **MB** and **RB.** However, when combined with KI, no potentiation was observed. There is, however, a study in the literature reporting the potentiation of the effect of **TBO** by KI, but in this study the **TBO** was tested at 100 μM (Ghaffari *et al*., 2018). In our case, the concentration of **TBO** was 20 times lower (5.0 μM). These different experimental conditions can justify the differences observed in these two studies. Nevertheless, using NaN_3 as potentiation agent, the aPDT effect of **TBO** was more effective when compared with the result without the NaN_3 (Kasimova *et al*., 2014). **MB** used as the reference for all non-porphyrin dyes, once is the most commonly studied antimicrobial PS in the literature and has received regulatory approval to mediate photodynamic therapy (PDT) of several infectious diseases, acts mainly through Type II mechanism (Marotti *et al*., 2010, de Oliveira *et al*., 2014). Moreover, its aPDT potentiation when combined with KI was already described (Vecchio *et al*., 2015). Besides that, and according with our results, **MB** can be designated as a PS reference for evaluate the potentiation of these dyes by KI.

It remains unanswered which factor determines whether the mechanism follows *via* formation of iodine radical species ($I_2^{\cdot-}$) or *via* formation of free iodine (I_2/I_3^-). To answer this question, we cannot neglect other factors that can also contribute for the efficiency of these PSs, such as $^1O_2$ production, charge number and distribution, aggregation behavior, affinity for the cell membrane.

It is undeniable that the ability of KI to potentiate the aPDT process mediated by some cationic PSs, allows a drastic reduction of the aPDT treatment time as well as the reduction of the PS concentration. However, this potentiation is limited to some PSs and

the addition of KI can even impair some PSs. This work helped to elucidate that for the series of compounds studied, the PSs capable to decompose the peroxyiodide into iodine (easily detectable by monitoring the formation of I_2 through spectroscopy or by the visual appearance of a blue colour in the presence of starch) are the promising ones in terms of complementing their efficacy with the action of iodine. Although these studies confirm that the generation of $^1O_2$ is an important fact in this process, the PS structure, aggregation behavior and affinity for the cell membrane are also important features to take into account.

2.6. References

Abrahamse, H., and Hamblin, M.R., 2016. New photosensitizers for photodynamic therapy. Biochemical Journal, 473 (4), 347–364.

Alves, E., Carvalho, C.M.B., Tomé, J.P.C., Faustino, M.A.F., Neves, M.G.P.M.S., Tomé, A.C., Cavaleiro, J.A.S., Cunha, Â., Mendo, S., and Almeida, A., 2008. Photodynamic inactivation of recombinant bioluminescent *Escherichia coli* by cationic porphyrins under artificial and solar irradiation. Journal of Industrial Microbiology and Biotechnology, 35 (11), 1447–1454.

Alves, E., Costa, L., Cunha, Â., Faustino, M.A.F., Neves, M.G.P.M.S., and Almeida, A., 2011. Bioluminescence and its application in the monitoring of antimicrobial photodynamic therapy. Applied Microbiology and Biotechnology, 92 (6), 1115–1128.

Alves, E., Faustino, M.A.F., Tomé, J.P.C., Neves, M.G.P.M.S., Tomé, A.C., Cavaleiro, J.A.S., Cunha, Â., Gomes, N.C.M., and Almeida, A., 2011. Photodynamic antimicrobial chemotherapy in aquaculture: Photoinactivation studies of *Vibrio fischeri*. PLoS ONE, 6 (6).

Chambers, H. F., and DeLeo, F.R., 2009. Waves of Resistance: *Staphylococcus aureus* in the Antibiotic Era. Nature Reviews Microbiology, 7 (9), 629–641.

Cieplik, F., Pummer, A., Regensburger, J., Hiller, K.A., Späth, A., Tabenski, L., Buchalla, W., and Maisch, T., 2015. The impact of absorbed photons on antimicrobial photodynamic efficacy. Frontiers in Microbiology, 6 (7), 706.

Costa, L., Carvalho, C.M.B., Faustino, M.A.F., Neves, M.G.P.M.S., Tomé, J.P.C., Tomé, A.C., Cavaleiro, J.A.S., Cunha, Â., and Almeida, A., 2010. Sewage bacteriophage inactivation by cationic porphyrins: Influence of light parameters. Photochemical and Photobiological Sciences, 9 (8), 1126–1133.

Costa, L., Tomé, J.P.C., Neves, M.G.P.M.S., Tomé, A.C., Cavaleiro, J.A.S., Faustino, M.A.F., Cunha, Â., Gomes, N.C.M., and Almeida, A., 2011. Evaluation of resistance development and viability recovery by a non-enveloped virus after repeated cycles of aPDT. Antiviral Research, 91 (3), 278–282.

Dai, T., Huang, Y.Y., and Hamblin, M.R., 2010. Photodynamic therapy for localized infections – state of the art. NIH Public Access, 6 (617), 170–188.

DeLeo, F. R., Otto, M., Kreiswirth, B.N., and Chambers, H.F., 2010. Community-associated methicillin-resistant *Staphylococcus aureus*. The Lancet, 375 (9725), 1557–1568.

Oliveira, B. P., Lins, C.C. dos S.A., Diniz, F.A., Melo, L.L.M., and Castro, C.M.M.B., 2014. In Vitro antimicrobial photoinactivation with methylene blue in different microorganisms. Brazilian Journal of Oral Sciences, 13 (1), 53-57.

Docampo, R., Moreno, S.N.J., Muniz, R.P.A., Cruz, F.S., and Mason, R.P., 1983. Light-enhanced free radical formation and trypanocidal action of gentian violet (crystal violet). Science, 220 (4603), 1292–1295.

Economou, V., and Gousia, P., 2015. Agriculture and food animals as a source of antimicrobial-resistant bacteria. Infection and Drug Resistance, 8, 49–61.

Freire, F., Ferraresi, C., Jorge, A.O.C., and Hamblin, M.R., 2016. Photodynamic therapy of oral Candida infection in a mouse model. Journal of Photochemistry and Photobiology B: Biology, 159, 161–168.

Gao, R., Hu, Y., Li, Z., Sun, J., Wang, Q., Lin, J., Ye, H., Liu, F., Srinivas, S., Li, D., Zhu, B., Liu, Y.H., Tian, G.B., and Feng, Y., 2016. Dissemination and Mechanism for the MCR-1 Colistin Resistance. PLoS Pathogens, 12 (11), 1–1

Gardete, S., and Tomasz, A. 2014. Mechanisms of vancomycin resistance in *Staphylococcus aureus*. The Journal of Clinical Investigation, 124 (7), 2836–40.

Ghaffari, S., Sarp, A.S.K., Lange, D., and Gülsoy, M., 2018. Potassium iodide potentiated photodynamic inactivation of *Enterococcus faecalis* using Toluidine Blue: Comparative analysis and post-treatment biofilm formation study. Photodiagnosis and Photodynamic Therapy, 24, 245–249.

Giuliani, F., Martinelli, M., Cocchi, A., Arbia, D., Fantetti, L., and Roncucci, G., 2010. In vitro resistance selection studies of RLP068/Cl, a new Zn(II) phthalocyanine suitable for antimicrobial photodynamic therapy. Antimicrobial Agents and Chemotherapy, 54 (2), 637–642.

Gsponer, N. S., Agazzi, M.L., Spesia, M.B., and Durantini, E.N., 2016. Approaches to unravel pathways of reactive oxygen species in the photoinactivation of bacteria induced by a dicationic fulleropyrrolidinium derivative. Methods, 109, 167–174.

Hamblin, M. R., 2016. Antimicrobial photodynamic inactivation: a bright new technique to kill resistant microbes. Current Opinion in Microbiology, 33, 67–73.

Hamblin, M. R. 2017. Potentiation of antimicrobial photodynamic inactivation by inorganic salts. Expert Review of Anti-Infective Therapy, 15 (11), 1059–1069.

Hancock, R. E., Farmer, S.W., Li, Z., and Poole, K., 1991. Interaction of aminoglycosides with the outer membranes and purified lipopolysaccharide and OmpF porin of *Escherichia coli*. Antimicrobial Agents and Chemotherapy, 35 (7), 1309–1314.

Helander, I. M., Alakomi, H.L., Latva-Kala, K., and Koski, P., 1997. Polyethyleneimine is an effective permeabilizer of Gram-negative bacteria. Microbiology, 143 (10), 3193–3199.

Huang, L., Bhayana, B., Xuan, W., Sanchez, R. B., McCulloch, B. J., Lalwani, S., and Hamblin, M.R., 2018. Comparison of two functionalized fullerenes for antimicrobial photodynamic inactivation: Potentiation by potassium iodide and photochemical mechanisms. Journal of Photochemistry and Photobiology B: Biology, 186, 197–206.

Huang, L., El-Hussein, A., Xuan, W., and Hamblin, M.R., 2018. Potentiation by potassium iodide reveals that the anionic porphyrin $TPPS_4$ is a surprisingly effective

photosensitizer for antimicrobial photodynamic inactivation. Journal of Photochemistry and Photobiology B: Biology, 178, 277–286.

Huang, Y. Y., Wintner, A., Seed, P.C., Brauns, T., Gelfand, J.A., and Hamblin, M.R., 2018. Antimicrobial photodynamic therapy mediated by methylene blue and potassium iodide to treat urinary tract infection in a female rat model. Scientific Reports, 8 (1), 7257.

Huang, L., St. Denis, T.G., Xuan, Y., Huang, Y.Y., Tanaka, M., Zadlo, A., Sarna, T., and Hamblin, M.R., 2012. Paradoxical potentiation of methylene blue-mediated antimicrobial photodynamic inactivation by sodium azide: Role of ambient oxygen and azide radicals. Free Radical Biology and Medicine, 53 (11), 2062–2071.

Huang, L., Szewczyk, G., Sarna, T., and Hamblin, M.R., 2017. Potassium Iodide Potentiates Broad-Spectrum Antimicrobial Photodynamic Inactivation Using Photofrin. ACS Infectious Diseases, 3 (4), 320–328.

Huang, Y. Y., Choi, H., Kushida, Y., Bhayana, B., Wang, Y., and Hamblin, M.R., 2016. Broad-spectrum antimicrobial effects of photocatalysis using titanium dioxide nanoparticles are strongly potentiated by addition of potassium iodide. Antimicrobial Agents and Chemotherapy, 60 (9), 5445–5453.

Indig, G. L., Anderson, G. S., Nichols, M.G., Bartlett, J.A., Mellon, W.S., and Sieber, F., 2000. Effect of molecular structure on the performance of triarylmethane dyes as therapeutic agents for photochemical purging of autologous bone marrow grafts from residual tumor cells. Journal of Pharmaceutical Sciences, 89 (1), 88–99.

Jori, G., Camerin, M., Soncin, M., Guidolin, L., and Coppellotti, O., 2011. Antimicrobial Photodynamic Therapy: Basic Principles. the Royal Society of Chemistry, 11, 1–18.

Jori, G., Fabris, C., Soncin, M., Ferro, S., Coppellotti, O., Dei, D., Fantetti, L., Chiti, G., and Roncucci, G., 2006. Photodynamic therapy in the treatment of microbial infections: Basic principles and perspective applications. Lasers in Surgery and Medicine, 38 (5), 468–481.

Kashef, N., Huang, Y. Y., and Hamblin, M. R., 2017. Advances in antimicrobial photodynamic inactivation at the nanoscale. Nanophotonics, 6 (5), 853–879.

Kasimova, K. R., Sadasivam, M., Landi, G., Sarna, T., and Hamblin, M.R., 2014. Potentiation of photoinactivation of Gram-positive and Gram-negative bacteria mediated by six phenothiazinium dyes by addition of azide ion. Photochemical and Photobiological Sciences, 13 (11), 1541–1548.

Kessel, D., Luguya, R., and Vicente, M. G. H., 2003. Localization and photodynamic efficacy of two cationic porphyrins varying in charge distributions. Photochemistry and photobiology, 78 (5), 431–435.

Keum, Y. S., Kim, J. H., and Li, Q. X. 2003. Relationship between Singlet Oxygen Formation and Photolysis of Phloxine B in Aqueous Solutions, 10, 219–223.

Krumova, K., and Cosa, G., 2016. "Overview of reactive oxygen species," in Singlet Oxygen: Applications in Biosciences and Nanosciences, Vol. 1, eds S. Nonell and C. Flors (Washington, DC: Royal Society of Chemistry), 1–21.

Levine, D. P. 2006. Vancomycin : A History. Clinical Infectious Disease, 42 (Suppl 1), S5–S12.

Lounatmaa, K., Helander, I. M., and Latva-Kala, K., 1998. Permeabilizing action of polyethyleneimine on 90 Printed in Great Britain Permeabilizing action of polyethyleneimine on Salmonella typhimurium involves disruption of the outer membrane and interactions with Iipopolysaccharide. Microscopy, 144, 385–390.

Luallen, T. 2017. Utilizing Starches in Product Development. Starch in Food: Structure, Function and Applications: Second Edition, 545–579.

Marciel, L., Teles, L., Moreira, B., Pacheco, M., Lourenço, L.M.O., Neves, M.G., Tomé, J.P.C., Faustino, M.A.F., and Almeida, A., 2017. An effective and potentially safe blood disinfection protocol using tetrapyrrolic photosensitizers. Future Medicinal Chemistry, 9 (4), 365–379.

Marciel, L., Mesquita, M.Q., Ferreira, R., Moreira, B., Neves, M.G.P.M.S., Faustino, M.A.F., and Almeida, A., 2018. An efficient formulation based on cationic porphyrins to photoinactivate *Staphylococcus aureus* and *Escherichia coli*. Future Science, 10, 1821–1833.

Martins, D., Mesquita, M.Q., Neves, M.G.P.M.S., Faustino, M.A.F., Reis, L., Figueira, E., and Almeida, A., 2018. Photoinactivation of *Pseudomonas syringae pv. actinidiae* in kiwifruit plants by cationic porphyrins. Planta, 248 (2), 409–421.

Marotti, J., Sperandio, F.F., Fregnani, E.R., Aranha, A.C.C., de Freitas, P.M., and de Paula Eduardo, C., 2010. High-Intensity Laser and Photodynamic Therapy as a Treatment for Recurrent Herpes Labialis. Photomedicine and Laser Surgery, 28 (3), 439–444.

Merchat, M., Bertolini, G., Giacomini, P., Villanueva, A., and Jori, G., 1996. Meso-substituted cationic porphyrins as efficient photosensitizers of gram-positive and gram-negative bacteria. Journal of Photochemistry and Photobiology B: Biology, 32 (3), 153–157.

Minnock, A., Vernon, D.I., Schofield, J., Parish, J.H., and Brown, S.B., 2000. Mechanism of Uptake of a Cationic Water-Soluble Pyridinium Zinc Phthalocyanine across the Outer Membrane of *Escherichia coli* Mechanism of Uptake of a Cationic Water-Soluble Pyridinium Zinc Phthalocyanine across the Outer Membrane of *Escherichia coli*, 44 (3), 522–527.

Moura, N. M. M., Esteves, M., Vieira, C., Rocha, G.M.S.R.O., Faustino, M.A.F., Almeida, A., Cavaleiro, J.A.S., Lodeiro, C., and Neves, M.G.P.M.S., 2019. Novel β-functionalized mono-charged porphyrinic derivatives: Synthesis and photoinactivation of *Escherichia coli*. Dyes and Pigments, 160, 361–371.

Nitzan, Y., Gutterman, M., Malik, Z., and Ehrenberg, B., 1992. Inactivation of Gram-Negative Bacteria By Photosensitized Porphyrins. Photochemistry and Photobiology, 55 (1), 89–96.

O'Neill, J., 2016. "Tackling drug-resistant infections globally: final report and recommendations," in The Review on Antimicrobial Resistance, ed. A. Ro (London: HM Government and the Wellcome Trust), 84.

Ormond, A.B. and Freeman, H.S., 2013. Dye sensitizers for photodynamic therapy. Materials, 6 (3), 817–840.

Reynoso, E., Quiroga, E.D., Agazzi, M.L., Ballatore, M.B., Bertolotti, S.G., and Durantini, E.N., 2017. Photodynamic inactivation of microorganisms sensitized by cationic

BODIPY derivatives potentiated by potassium iodide. Photochemical and Photobiological Sciences, 16 (10), 1524–1536.

Simões, C., Gomes, M.C., Neves, M.G.P.M.S., Cunha, Â., Tomé, J.P.C., Tomé, A.C., Cavaleiro, J.A.S., Almeida, A., and Faustino, M.A.F., 2016. Photodynamic inactivation of *Escherichia coli* with cationic meso-tetraarylporphyrins - The charge number and charge distribution effects. Catalysis Today, 266, 197–204.

Soukos, N. S., Ximenez-Fyvie, L. A., Hamblin, M. R., Socransky, S. S., and Hasan, T., 1998. Targeted antimicrobial photochemotherapy. Antimicrobial Agents and Chemotherapy, 42 (10), 2595–2601.

St Denis, T. G., T., Vecchio, D., Zadlo, A., Rineh, A., Sadasivam, M., Avci, P., Huang, L., Kozinska, A., Chandran, R., Sarna, T., and Hamblin, M., 2013. Thiocyanate Potentiates Antimicrobial Photodynamic Therapy: In Situ Generation of the Sulfur Trioxide Radical Anion by Singlet Oxygen. Free Radical Biol Med, 65, 800–810..

Tavares, A., Carvalho, C.M.B., Faustino, M.A., Neves, M.G.P.M.S., Tomé, J.P.C., Tomé, A.C., Cavaleiro, J.A.S., Cunha, Â., Gomes, N.C.M., Alves, E., and Almeida, A., 2010. Antimicrobial Photodynamic Therapy: Study of Bacterial Recovery Viability and Potential Development of Resistance after Treatment. Marine Drugs, 8 (12), 91–105.

Tavares, A., Dias, S.R.S., Carvalho, C.M.B., Faustino, M.A.F., Tomé, J.P.C., Neves, M.G.P.M.S., Tomé, A.C., Cavaleiro, J.A.S., Cunha, Â., Gomes, N.C.M., Alves, E., and Almeida, A., 2011. Mechanisms of photodynamic inactivation of a Gram-negative recombinant bioluminescent bacterium by cationic porphyrins. Photochemical and Photobiological Sciences, 10 (10), 1659–1669.

Vecchio, D., Gupta, A., Huang, L., Landi, G., Avci, P., Rodas, A., and Hamblin, M.R., 2015. Bacterial photodynamic inactivation mediated by methylene blue and red light is enhanced by synergistic effect of potassium iodide. Antimicrobial Agents and Chemotherapy, 59 (9), 5203–5212.

Wang, R., Van Dorp, L., Shaw, L.P., Bradley, P., Wang, Q., Wang, X., Jin, L., Zhang, Q., Liu, Y., Rieux, A., Dorai-Schneiders, T., Weinert, L.A., Iqbal, Z., Didelot, X., Wang, H.,

and Balloux, F., 2018. The global distribution and spread of the mobilized colistin resistance gene mcr-1. Nature Communications, 9 (1), 1–9.

Wen, X., Zhang, X., Szewczyk, G., El-Hussein, A., Huang, Y. Y., Sarna, T., *et al*., 2017. Potassium iodide potentiates antimicrobial photodynamic inactivation mediated by rose bengal in in vitro and in vivo studies. Antimicrob. Agents Chemother. 61:e00467-17.

Wu, X., Huang, Y. Y., Kushida, Y., Bhayana, B., and Hamblin, M. R., 2016. Broad- spectrum antimicrobial photocatalysis mediated by titanium dioxide and UVA is potentiated by addition of bromide ion via formation of hypobromite. Free Radic. Biol. Med. 95, 74–81.

Yoshimura, F., and Nikaido, H., 1985. Diffusion of beta-lactam antibiotics through the porin channels of *Escherichia coli* K-12. Antimicrob. Agents Chemother. 27, 84–92.

Zhang, Y., Dai, T., Wang, M., Vecchio, D., Chiang, L. Y., and Hamblin, M. R., 2015. Potentiation of antimicrobial photodynamic inactivation mediated by a cationic fullerene by added iodide: in vitro and in vivo studies. Nanomedicine 10, 603–614.

Zhuo, J., 2016. Photoactive chemicals for antimicrobial textiles. Antimicrob. Tex. 11, 197–223.

Advances in the photoinactivation by a cationic porphyrinic formulation with potassium iodide: effectiveness on planktonic and biofilm forms of bacteria, viruses and fungi.

Cátia Vieira[1], Adriele Santos[1,2], Mariana Q. Mesquita[3], Ana T. P. C. Gomes[1], M. Graça P. M. S. Neves[2], M. Amparo F. Faustino[2]*, Adelaide Almeida[1]*

[1] Department of Biology and CESAM, University of Aveiro, 3810-193 Aveiro, Portugal

[2]Department of Clinical Analysis and Biomedicine, State University of Maringá, 87020-900, Maringá - Paraná, Brazil.

[3] Department of Chemistry and QOPNA, University of Aveiro, 3810-193 Aveiro, Portugal

Keywords: Antimicrobial Photodynamic Therapy, Cationic Formulation of Porphyrins, Potassium Iodide, *Escherichia. coli*, Methicillin resistant *Staphylococcus aureus*, *Candida albicans*, T4 bacteriophage, biofilms, planktonic

CHAPTER III

3.1. Abstract:

The world-wide increasing rate of antibiotic resistance as well as the capacity of microorganisms to form biofilms, have led to a higher incidence of mortal infections that require alternative methods for their control. Antimicrobial photodynamic therapy (aPDT) emerged as an effective solution against resistant strains. The present work aims to evaluate the photodynamic therapy efficiency of a PS formulation (FORM) and its potentiation effect by KI on a broad-spectrum of microorganisms under PAR white light (25 W/m^2). FORM is constituted by five cationic porphyrins and is associated with low production costs and synthesis time. The assays were performed with different concentrations of FORM and 100 mM of KI on planktonic and biofilm forms of gram-positive (*Staphylococcus aureus* resistant to methicillin - MRSA) and gram-negative bacteria (*Escherichia coli* resistant to chloramphenicol and ampicillin), of the fungi *Candida albicans* and on a T4 like bacteriophage as a mammalian virus model. The results indicate that FORM is an efficient PS to inactivate not only gram-negative and gram-positive bacteria, but also fungi and viruses, both in planktonic and biofilm forms, at low concentrations (below 5 μM). KI enhanced the effect of the FORM on all microorganisms on the planktonic form, allowing the reduction of PS concentration and the time of treatment. The combined treatment of FORM at low concentrations (below 5 μM) with KI also destroy effectively the already well-established biofilms of *E. coli, S. aureus* and *C. albicans* and avoids the formation of biofilms, avoiding the microbial regrowth over at least 24 h after treatment. The longer-lives iodine species resulting from KI avoid the microbial regrowth after aPDT.

3.2. Introduction

The emerging problems with resistance against antimicrobials and the formation of complex and highly structured microbial biofilms, bring the need for the development of novel, effective and inexpensive methods to circumvent microbial diseases (Alves, Faustino, *et al.* 2011, Alves, Faustino, Neves, Angela, *et al.* 2014). Antimicrobial photodynamic therapy (aPDT) emerged as an effective solution against multidrug resistant strains and against biofilm formation and biofilm destruction. This therapeutic approach involves the use of a photosensitizer molecule (PS) that it is excited by light and can react with molecular oxygen producing reactive oxygen species (ROS) such as singlet oxygen ($^1O_2$) and/or hydroxyl radicals, superoxide and hydrogen peroxide. These ROS can react with biological molecules (nucleic acids, proteins and lipids) causing microbial death (Hamblin 2018). aPDT presents several advantages when compared with the use of traditional antimicrobials showing to be efficient independently of the antimicrobial resistance profile (Jori *et al.* 2011) and be able to prevent further development of resistance even after several cycles of treatment (Giuliani *et al*., 2010; Tavares *et al*., 2010; Costa *et al*., 2011) as well as to prevent microbial biofilms formation and even promoting biofilms destruction. In fact, this approach has been efficiently applied to inactivate several microorganisms, such as Gram-negative and Gram -positive bacteria (Tavares *et al.* 2010, Liu *et al.* 2015), fungi (Donnelly *et al.* 2008), viruses (Costa, Faustino, *et al.* 2012) and even to degrade the complex matrix of microbial biofilms and kill the resident bacteria (Beirão *et al.* 2014, Hu *et al.* 2018). However, microbial biofilms are less susceptible to aPDT and requires higher PS concentrations to be efficiently photinactivated (Beirão *et al.* 2014). Biofilms are the default mode-of-life for many microbial species and are a key virulence factor for a wide range of microorganisms that cause chronic infections. In fact, approximately 80% of infectious diseases affecting humans are due to biofilm formation (Høiby 2017). The complex nature of biofilms; the presence of an extracellular polymeric matrix, physical and chemical heterogeneity; and drug tolerance to conventional treatments and to immunologic host defense, imposes great remarkable therapeutic challenges (Costerton *et al.* 1999, Høiby 2017).

Although the efficacy of aPDT has been proved to be an alternative to the conventional antimicrobials, there is still room for new improvements namely to translate the approach to the field. Some important aspects are related with the development of synthetic strategies able to afford efficient PS at low cost and aPDT protocols where the amount of the PS or the treatment time is reduced and effective against a wide microbial range. Nowadays, several groups are pursuing new strategies to efficiently obtain new PS as well planning new aPDT protocols to prevent adverse effects associated with its application (Takasaki *et al.* 2009) and to inactivate microorganisms capable to form biofilms. Another important aspect that needs to be prevented is the potential microbial regrowth after aPDT protocol, whereas ROS are only generated during the irradiation time, hampering the total inactivation of microorganisms *in vivo* (Huang, Wintner, *et al.* 2018).

During the past two decades, many highly efficient PS have been produced, but the chances to reach the market remain extremely low, not only due to the existing legal framework but also due to the laborious and expensive processes involved in PS synthesis. Consequently, the development of new efficient PS with a cost–benefit ratio which will allow their introduction in the market, are needed. However, the synthetic access to some highly efficient PS requires laborious laboratorial processes mainly related with chromatographic purifications. Recently a PS formulation (Form), based on a non-separated mixture of five tetraarylporphyrins porphyrins, was equally effective in the photoinactivation of *E. coli*, *Pseudomonas syringae* and *S. aureus* bacteria, as the best PS included in the FORM (the highly efficient Tri-Py(+)-Me) used separately (Marciel *et al.* 2018, Martins *et al.* 2018). The effective reduction of Gram-positive and Gram-negative bacteria with Form provided promising indications toward its use, which would lead to a substantial decrease in costs and production time, paving its potential to field exploitation.

The use of combinations of PS and potassium iodide during aPDT arises also as a solution for the exploitation of photoinactivation to the market. KI has been used as an antiseptic and disinfectant for many years since it presents a broad-spectrum antimicrobial effect (Gottardi, 1991). More recently, several studies have shown that the

addition of this salt at lower concentrations can potentiate the aPDT effect on bacteria and fungi in the free and biofilm forms and to reduce the incidence of regrowth after treatment due to the production of free iodine/triiodide, a longer-live specie than singlet oxygen that may remain active even after the irradiation time (Vecchio *et al*. 2015; Zhang *et al*. 2015; Freire *et al*. 2016; Y. Y. Huang *et al*. 2016; Hamblin 2017; L. Huang *et al*. 2017; Reynoso *et al*. 2017; Wen *et al*. 2017; L. Huang *et al*. 2018a; L. Huang *et al*. 2018b; Y.-Y. Huang *et al*. 2018). The mechanism of aPDT potentiation by KI has been already described. KI reacts with oxygen singlet affording free iodide (I_2/I_3^-), hydrogen peroxide (H_2O_2) and iodine radicals ($I_2^{\bullet-}$). Several *in vitro* and *in vivo* studies have been shown the potentiation of different PS. The potentiation of a fullerene, rose Bengal (RB), and methylene blue (MB)by KI has been performed *in vivo* mouse infections such as *Acinetobacter baumannii* and *Pseudomonas aeruginosa* skin infections, *Candida albicans* oral infection and a burn infection with MRSA (Vecchio *et al.* 2015, Zhang *et al.* 2015, Wen *et al.* 2017, Huang, Wintner, *et al.* 2018). Also, it was shown that MB at the high concentration of 100 μM combined with KI at 100 mM allowed to inactivate 2.3 logs of *C. albicans* biofilms (Freire *et al.* 2016). Recently, the combination of the FORM + KI was already tested in the photoinactivation of *E. coli*, showing a remarkable efficacy when compared to the photoinactivation of this bacterium just in the presence of FORM (Vieira *et al.* 2018). FORM is composed by Mono-Py(+)-Me (19%), Di-Py(+)-Me opp and Di-Py(+)-Me adj (20%) Tri-Py(+)-Me (44%) and Tetra-Py(+)-Me (17%) (Figure 3.1).

The aim of this work is evaluate the photodynamic effect of combinations of the effective FORM with KI in the inactivation of a wide range of microorganisms: planktonic forms of a Gram-negative bacterium (*E. coli*), a Gram-positive bacterium (*S. aureus*), a fungus (*C. albicans*) and a virus (a T4-like bacteriophage) as well in the destruction of *E. coli*, *S. aureus* and *C. albicans* biofilms and in the prevention of *E. coli* and *S. aureus* biofilms formation.

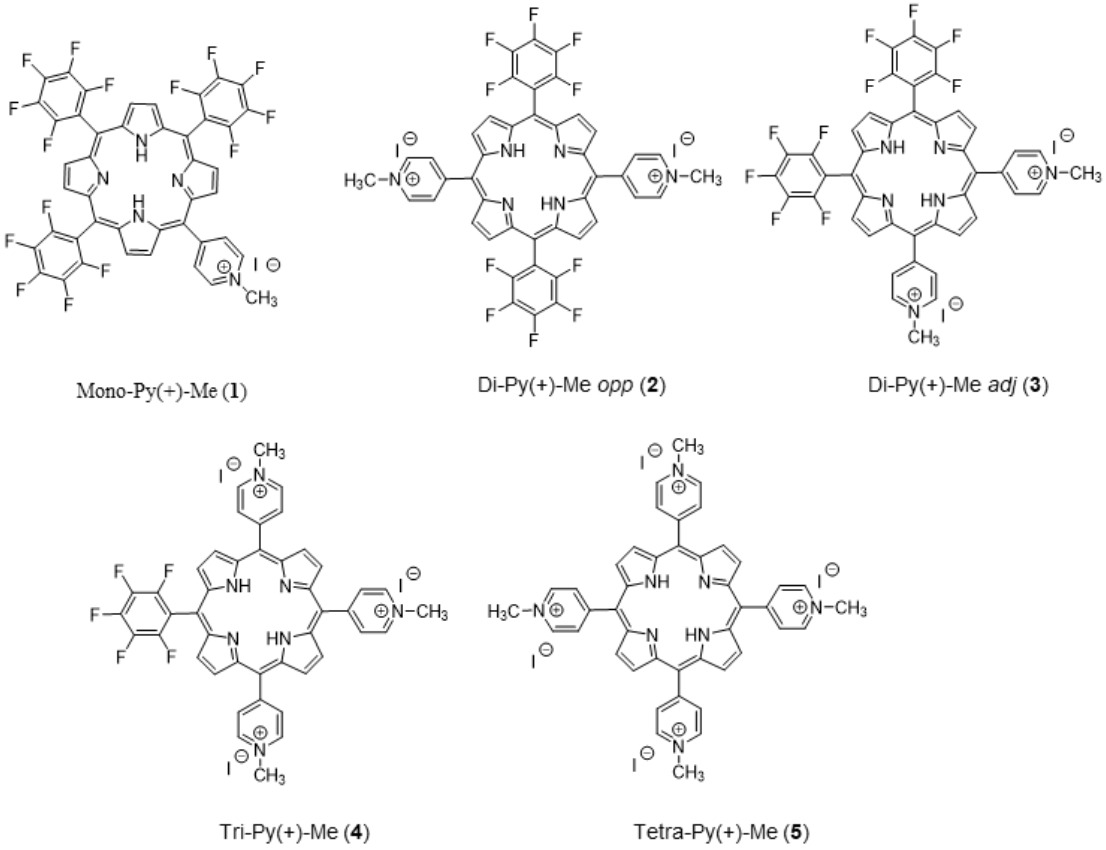

Figure 3.1. Structures of porphyrin derivatives present in FORM

3.3. Material and methods

3.3.1. Photosensitizer and KI solution

FORM is a non-separated mixture of the *meso*-tetraarylporphyrins composed by 5-(1-methylpyridinium-4-yl)-10,15,20-tris(pentafluorophenyl)porphyrin mono-iodide [Mono-Py(+)-Me **1**] (19%), 5,15-bis(1-methylpyridinium-4-yl)-10,20-bis(pentafluorophenyl)porphyrin di-iodide [Di-Py(+)-Me *opp* **2**], 5,10-bis(1-methylpyridinium-4-yl)-15,20-bis(pentafluorophenyl)porphyrin di-iodide [Di-Py(+)-Me *adj* **3**] (2 + 3 20%), 5,10,15-tris(1-methylpyridinium-4-yl)-20-(pentafluorophenyl)porphyrin tri-iodide [Tri-Py(+)-Me **4**] (44%) and 5,10,15,20-tetrakis(1-methylpyridinium-4-yl)porphyrin tetra-iodide [Tetra-Py(+)-Me **5**] (17%) (Simões *et al.* 2016, Marciel *et al.* 2018, Martins *et al.* 2018) (Figure 3.1). The this formulation was prepared as described in the literature ((Simões *et al.* 2016, Marciel *et al.* 2018, Martins *et al.* 2018, Vieira *et al.* 2018).

Stock solution of FORM was prepared at 500 µM in dimethyl sulfoxide (DMSO) and kept in the dark. Before each assay, the stock of FORM solution was sonicated during 30 min at room temperature (Ultrasonic bath, Nahita 0.6 L, 40 kHz).

Potassium iodide (KI) was purchased from Sigma-Aldrich (St. Louis, MO) and its solutions were prepared at 500 mM in sterile PBS immediately before each experiment.

3.3.2. Characterization of microbial strains

In this study a gram-negative bacterium, a gram-positive bacterium, a yeast and a virus were used: *Staphylococcus aureus* DSM 25693, a methicillin-resistant (MRSA) strain, producing the staphylococcal enterotoxins S, E, A, C, H, G, and I, that was isolated from a biological low respiratory tract sample of a hospitalized individual (Gonçalves *et al*., 2014); the recombinant bioluminescent *Escherichia coli*, previously transformed (with luxCD-ABE genes from marine bioluminescent bacteria *Vibrio fischeri*) by our research group (Alves *et al.* 2008); *Candida albicans* (ATCC 10231) and the T4-like bacteriophage KC755108 (Silva *et al.* 2014)., Phage KC755108 was isolated from the Corte das Freiras aquaculture of Ria de Aveiro (Aveiro, Portugal, 40°37'54.94' N & 8°40'9.76' W) using the recombinant *E. coli* bioluminescent as host, according to (Silva *et al*., 2014).

3.3.3. Microbial grown conditions

S. aureus strain was kept on Tryptic Soy Agar (TSA, Merck) at 4 °C and, prior to each aPDT assay a colony was transferred to 30 mL of Brain-Heart Infusion (BHI, Liofilchem, Italy) at 37 °C for 18 h under stirring (120 rpm), until the stationary phase of approximately 10^8 colony forming units per mL (CFU mL^{-1}). Afterward, 300 µL of the formerly grown solution was transferred to fresh 30 mL BHI and incubated at the referred conditions. This last process was repeated.

The *E. coli* was grown on TSA (Merck) previously supplemented with 50 mg mL^{-1} of ampicillin (Amp) and with 34 mg mL^{-1} of chloramphenicol (Cm). Fresh cultures were obtained by inoculating one isolated colony from the petri dish into 30 mL of tryptic soy broth medium (TSB, Merck) supplemented with Amp and Cm and after incubated overnight at 37 °C under a constant agitation of 120 rpm. A 300 µL aliquot was

transferred into 30 mL of TSB under the same prior growth conditions to reach stationary phase of approximately 10^8 colony forming units per mL (CFU mL^{-1}), and this step was repeated.

The yeast *C. albicans* was maintained on Yeast Extract Glucose Chloramphenicol Agar (YGCA, Merck) at 4 °C. Before each essay, a colony was transferred to 30 mL of YG [Yeast extract (10g/L) + Glucose (20g/L)] and incubated for 24h at 37 °C with constant stirring (120 rpm). After, 300 µL aliquots were transferred from the previous grown yeast to new 30 mL YG and was incubated at the previous grown conditions. This step was repeated.

Phage KC755108 stocks are stored at 4 ° C with 1% chloroform (TSA, Merck). The phage suspension titer was determined by the double-layer agar method using TSA before each essay. The plates were incubated at 25 °C for 18-24 h and the number of lysis plaques was counted. The results were expressed as plaque forming units per millilitre (PFU mL^{-1}).

3.3.4. Light source

In aPDT assays were used a set of 13 white fluorescent lamps (PAR radiation, OSRAM 21 lamps of 18 W each, 380–700 nm) with an irradiance of 25 W m^{-2}. The irradiances were measured with a Power Meter Coherent FieldMax-II Top combined with a Coherent PowerSens PS19Q energy sensor.

3.3.5. Photodynamic inactivation essays

Different concentrations of FORM were tested in the aPDT assays with KI at 100 mM (FORM + KI) and without KI (FORM). Additionally, darks and lights controls were carried out during the aPDT assays: Light control (LC), containing only the microbial suspension, maintained under radiation, was used to evaluate the light effect on microbial viability; KI light control (KI), comprising the microorganism suspension only with KI at 100 mM, and exposed to light, to assess the KI effect during the irradiation time; dark control (DC) containing microbial suspension, PS (in the highest concentration

tested for each microorganism) and KI (at 100 mM) protected with aluminium foil was also performed to evaluate the PS + KI toxicity in the dark.

3.3.6. Planktonic cells Treatment

The microbial cultures at stationary phase were 10-fold diluted in phosphate buffered saline (PBS) and the suspensions were distributed in sterilized glass beakers. The appropriate volume of FORM or FORM + KI were added to the samples in order to achieve a final concentration of: 5.0 µM and 2.5 µM of FORM for *E. coli*; 5.0 µM, 1.0 µM and 0.5 µM of FORM for *S. aureus*; 1 µM and 0.5 µM of FORM for *C. albicans* and; 1.5 µM 1.0 µM, 0.5 µM and 0.1 µM of FORM for T4-like bacteriophage.

Afterwards, 15 min of dark incubation was performed, under stirring and at room temperature, in order to promote the binding of the PS to the microorganisms. The glass beakers of samples and light controls were exposed in parallel to the white light, under stirring, during different irradiation times. The dark control was also kept under stirring at room temperature, but protect from light for equal irradiation times used for each microorganism.

To evaluate the aPDT effect, the counts of CFU mL^{-1} (for bacteria and yeast) and PFU mL^{-1} (for the virus) was determined. Aliquots of the samples and controls were collected at predefined times of light exposure (depending on both microorganism and PS concentration), serially diluted in PBS and pour plated in duplicate in TSA (*E. coli* and *S. aureus*) or YGC agar (*C. albicans*). The petri plates of *E. coli* and *S. aureus* were incubated for 24 h at 37 °C and the *C. albicans* plates were incubated at the same temperature for 72 h. The bacteriophage suspensions were serially diluted in PBS and plated with its host by the Double-Layer Agar (DLA) technique according to previous studies (Costa *et al* 2008). The petri plates were incubated at 25 °C for 18 - 24 h. Colonies and phage plaques were counted and the concentration of viable cells or bacteriophages was expressed as Log CFU mL^{-1} or Log PFU mL^{-1}, respectively. Three independent assays for each condition and each microorganism were performed.

3.3.7. Formed Biofilm Cells Treatment

The bacterial and fungal cultures at stationary phase were diluted 1:100 in fresh TSB (for *E. coli* and *S. aureus*) or YG (*C. albicans*) and, aliquots of 100 µL of these suspensions, were transferred to polypropylene 96-well microplates and incubated under stirring (120 rpm) at 37 °C for 24 h to development of microbial biofilm. Afterwards, the liquid medium, containing planktonic cells, was carefully discharged, and the biofilms gently washed twice with 100 µL of sterile PBS. Solutions of FORM at 0.5 µM, 1 µM, 5 µM, 10 µM and 20 µM (for *E. coli* and *S. aureus*) and 0.1 µM, 0.5 µM, 1 µM, 5 µM, 10 µM and 20 µM (for *C. albicans*) with KI at 100 mM were prepared in PBS. Posteriorly, 200 µL of each PS solution were transferred to the wells containing biofilm developed and previously washed. Light control (LC), dark control (DC), KI control (KI) and PS control (with only FORM at 20 µM) were also performed.

The 96-well microplate containing the samples was firstly incubated in the dark during 30 min, at room temperature, to allow the PS binding to the microbial cells. Afterwards, the irradiation was performed at 25 W m^{-2} for 60 min. The 96-well microplate was sonicated during 10 min (ultrasonic bath, SONOREX SUPER BK 102H, 35 kHz), in order to detach sessile cells, and the wells suspensions were serially diluted in PBS. Three replicate aliquots of all dilutions were drop-plated on TSA (*E. coli* and *S. aureus*) and YGC agar (*C. albicans*). After 24 h (*E. coli* and *S. aureus*) or 72 h (*C. albicans*) of incubation at 37 °C, colonies were counted, and the concentration of viable cells was expressed as CFU mL^{-1}.

3.3.8. Biofilm Formation Cells Treatment

The aPDT effect on biofilm formation of *E. coli* and *S. aureus* was tested with different concentrations of FORM: 0.5 µM and 1.0 µM of FORM with KI at 100 mM for *E. coli* and; 0.05 µM and 0.1 µM of FORM with KI at 100 mM *for S. aureus*.

The bacterial cultures at stationary phase were diluted in fresh PBS (~10^7 CFU mL^{-1}). Then an appropriate volume of FORM + KI was added to the diluted cultures and 200 µL of these solutions were added to 96-well polystyrene microtiter plates. Afterwards, 30 min of incubation was performed under dark and at room temperature in order to

promote the binding of the PS to microorganisms. Microplate was then irradiated with white light (25 W m^{-2}) for 60 min. After photosensitization a 100 µL aliquot of each well was removed, serial diluted in PBS, drop-plated in TSA plates and incubated at 37 °C for 24 h. The microtiter plate with the remaining content was dark incubated at 37 °C, under stirring (120 rpm) for 24 h. After incubation, the wells contents were aspirated, diluted and plated as described above and, each well was gently washed with PBS to remove the non-adherent cells. Then 200 µL of PBS was added to each well and the microtiter plate was submitted to ultrasonic bath (SONOREX SUPER BK 102H, of 35 kHz for 10 min) to detach sessile cells. Serial dilutions were performed in PBS and 10 µL droplets of each dilution were plated on TSA plates and incubated as described above. The results were expressed as log CFU cm^{-2}. Light control (LC), dark control (DC), KI control (KI) and PS control (with only FORM at 20µM) were also performed.

3.3.9. Statistics

Statistical analysis was performed with GraphPad Prism 6. Normal distributions were checked by the Kolmogorov–Smirnov test and the homogeneity of variance was verified with the Brown Forsythe test. Three independent experiments with two replicates per assay for each condition were done with planktonic forms of microorganisms. The differences between the results were assessed by ANOVA and Dunnet's multiple comparison tests. Two independent experiments with three replicates per assay were performed to bacterial biofilms, and its data was analysed by one-way analysis of variance (ANOVA) and Tukey HSD post hoc test. The value of $p < 0.05$ was considered significant.

3.4. Results and Discussion

3.4.1. Photoinactivation of planktonic cells with combinations of FORM and KI

The effect of FORM at different low concentrations and its combination with KI at 100 mM were evaluated towards planktonic forms of a Gram-negative bacterium (*E. coli*)

a Gram-positive bacterium (*S. aureus*), a fungus *(C. albicans)* and a virus (a T4-like bacteriophage) under a low intensity of a safe PAR white light at an irradiance of 25 W m-^{2}. The KI concentration was selected considering our previous study where KI at 100 mM showed to potentiate the FORM aPDT effect (Vieira *et al.* 2018). For all experiments LCs (microorganism), LCs + KI (microorganism + KI at 100 mM) and DCs (microorganism + FORM + KI at 100 mM in the dark) were evaluated and in all cases the viability of microorganisms was not affected. These results indicate that the irradiation, the presence of salt and the combinations of the FORM with KI in the dark, does not affect the viability of the microorganisms.

The photodynamic effect of combinations of FORM at 2.5 and 5.0 µM and KI at 100mM was evaluated toward *E. coli* planktonic cells during 120 minutes of irradiation. The results obtained are presented in Figure 3.2 and showed that, after 120 min of irradiation, *E. coli* was inactivated in approximately 5 and 1.8 logs using FORM at 5.0 µM and 2.5 µM, respectively ($p<0.05$). These results are consistent with previous studies, where the FORM acts as an efficient PS in the photoinactivation of *E. coli* (Marciel *et al.* 2018, Vieira *et al.* 2018).

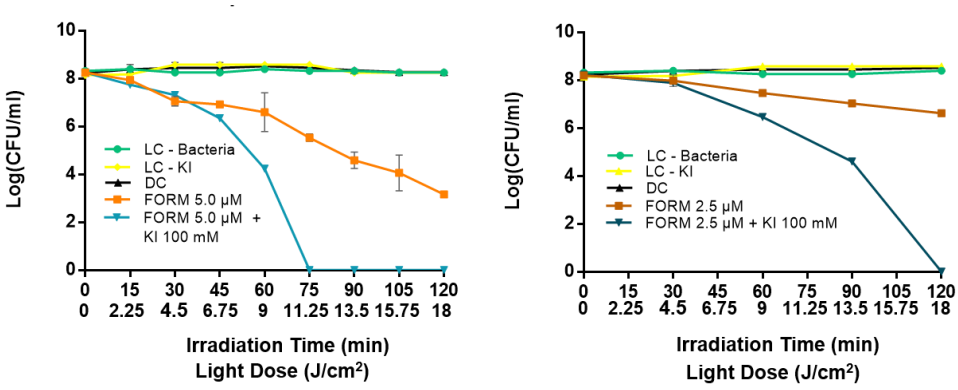

Figure 3.2 - Photodynamic inactivation of planktonic forms of *E. coli* by combination of KI and FORM at 5.0 µM, and 2.5 µM during 120 of irradiation with white light (25 W m^{-2}). Error bars represent the standard deviation. The values are expressed as the three independent experiments; error bars indicate the standard deviation.

Even so, the use of the combination FORM at 5.0 µM + KI 100 mM allowed to reduce significantly the time required to inactivate efficiently *E. coli* to 75 min (reduction of 8.3 log at this time against more than 120 min without KI), confirming the enormous potential of this combination to potentiate the aPDT effect of FORM. (Vieira *et al.* 2018). This potentiated effect was also achieved when the combination FORM at 2.5 µM + KI 100 mM was used; in this case it was possible to photoinactive, till the detection limit of the method (reduction of 8.4 log at this time), *E. coli* after 120 min of irradiation with lower concentration of the PS.

The same approach was used to study the effect of the combination of FORM with KI in the inactivation of *S. aureus*. Since Gram-positive bacteria are more suspceptible to aPDT than Gram-negative, due to their differences on the external membrane (Minnock *et al.* 2000), and based on the results previously obtaind for *S. aureus* with FORM (Marciel *et al.* 2018), in this case the FORM was tested at 5.0, 1.0 and 0.5 µM (Figure 3.3).

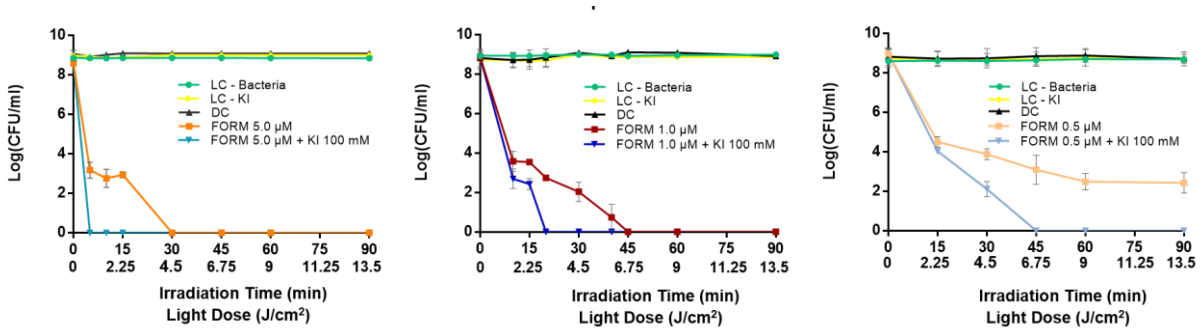

Figure 3.3 - Photodynamic inactivation of planktonic forms of *S. aureus* by combination of KI and FORM at 5.0 µM, 1.0 µM and 0.5 µM during 90 min of irradiation with white light (25 W m^{-2}). Error bars represent the standard deviation. The values are expressed as the three independent experiments; error bars indicate the standard deviation.

The results showed that FORM, was capable to photinactivate *S. aureus* till the detection limit when used at 5.0 and 1.0 µM and after 30 and 45 min, respectivly (reduction of 8.9 log). These results coroborate our previus results (Marciel *et al.* 2018). When the FORM was combined with KI, is was observed a potentiated effect of the aPDT for *S. aureus*. With combinations of FORM at 5.0 and 1.0 µM and KI, this bacterium was

inactivated to the detection limit of the method earlier (after 5 min and 20 min of irradiation, respectively) with a redution of aproximately 9 logs for both cases. When FORM was used at 0.5 µM, *S. aureus* was inactivated in *c.a* 5 logs after 90 min of irradiation, and the combination of FORM at this concetrations with KI allowed to inactivate *S. aureus* to the detection limit of the method (reduction of 8.6 log), reducing the treatment time for 45 min.

Comparing ours results with those obtained by other groups focused on the use of combinations of PSs with KI in the inactivation of bacteria, we can say that our achievements are in line with these results, since FORM + KI allowed the total inactivation of *E. coli* and *S. aureus* more effectively than the PS alone, and, in general, the inactivation was obtained using lower concetrations and lower radiance exposure than those used in previous studies for both Gram positive and Gram negative bacteria. Fullerene derivatives were described as efficient PSs of Gram-negative bacterium *Acinetobacter baumannii*, Gram-positive methicillin-resistant *S. aureus* when combined with KI, *in vitro* and *in vivo* using a mouse model with an infected skin abrasion (Zhang *et al.* 2015). In the *in vitro* assays, these results were achived with combinations of 20 µM of the PS and 10mM of KI with radiance exposure of 20-120 J/cm^2. The sudy effect of the combination Methylene Blue and of KI in the photoinactivation of *E. coli* and *S. aureus* had shown that the addition of KI increased the bacterial killing in 4 and 2 logs for *S. aureus* and *E. coli*, respectively, in a dose-dependent manner (Vecchio *et al.* 2015). In this case, Methylene Blue was *in vitro* tested in a range of concentration of 0 – 100 µM, with best resultes achieved for 10 µM of PS and 100 mM with radiance exposure between 0 -7 J/cm^2 (Vecchio *et al.* 2015). Rose Bengal (Wen *et al.* 2017) and fullerenes (L. Huang *et al*. 2018b) in the inactivation of of Gram-negative and Gram-positive bacteria and BODIPY dyes in the photoinactivation of *S. aureus* and *E. coli* (Reynoso *et al.* 2017) were also reported. For both bacteria, the total inativation of was achieved in higher concentration of the PS when compared to the ones used in combinations of FORM + KI to inactivate *E. coli* and *S.aureus*.

In the case of porphyrin based PSs, the potentiated effect with KI was also studied for Photofrin (Huang *et al.* 2017) and for the cationic porphyirin 5,10,15,20-tetrakis(1-methylpyridinium-4-yl)porphyrin tetratosylate ($TMPyP_4$) and the tetraanionic 5,10,15,20-tetrakis(4-sulfonatophenyl)porphyrin dihydrochloride ($TPPS_4$) in the photoinactivation *E. coli* (L. Huang *et al*. 2018a). In both cases, a potentiated effect was observed when KI was added. In particular, 10 μM hematoporphyrin equivalent (Photofrin) irradiated with 415 nm light (10 J/cm^2) was able to inactivativete (>6 logs killing) five different Gram-negative species (*Escherichia coli*, *Pseudomonas aeruginosa*, *Klebsiella pneumoniae*, *Proteus mirabilis* and *A. baumannii*), while no killing effect was obtained without KI (Huang *et al.* 2017). Our achiements with FORM + KI allowed an effcicient inactivation of *E. coli* with 5 μM of the PS and with an radiance exposure of 13.5 J/cm^2, therefore, the same result with half of PS concentration. Moreover, FORM is a mix of porphyrins with a controllable composition, unlike Photofrin, which is a great advantage since a controlled composition of a drug may lead to more predictable and reliable results. The $TPPS_4$ alone did not photoinactivate the Gram-negative *E. coli*, but surprisingly when 100 mM of KI was added, the inactivation of this bacterium ocurred (total inactivation at 0.2 μM + 10 J/cm^2 of 415 nm light). This porphyrin combined with KI was also more effective than $TMPyP_4$ in the photoinactivations of Gram-positive bacterium and methicillin-resistant *S. aureus* (L. Huang *et al*. 2018). Our achievements are in line with these results, since FORM + KI allowed the total inactivation of *E. coli* and *S. aureus* with lower concentrations and irrradiance time.

The results obtained in the photodynamic effect of combination FORM + KI in the fungus *C. albicans* also points out for the reduction of the aPDT treatment time with lower concentrations of FORM (Figure 3.4).

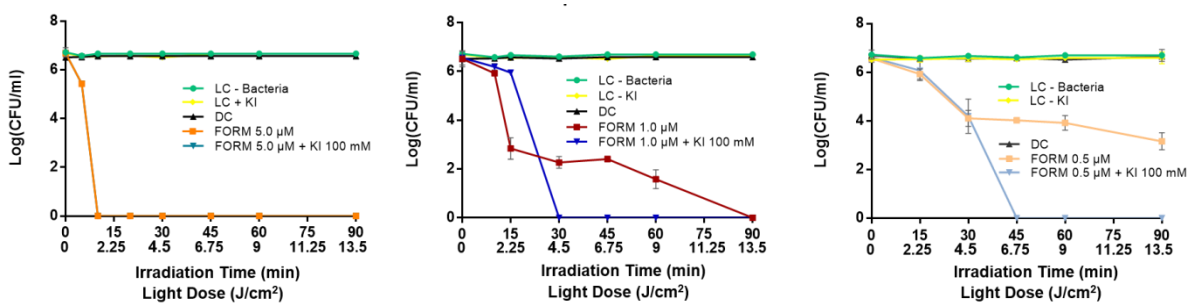

Figure 3.4 - Photodynamic inactivation of planktonic forms of *C. albicans* by combination of KI and FORM at 5.0 µM, 1.0 µM and 0.5 µM during 90 min of irradiation with white light (25 W/m^2), respectively. Error bars represent the standard deviation. The values are expressed as the three independent experiments; error bars indicate the standard deviation.

The use of FORM at 5.0 µM allowed the photoinactivation of the yeast in 6.1 logs, reaching the detention limit of the method, after 10 min of irradiation. The addition of KI promotes a similar profile to the one observed for FORM at 5.0 µM, not being observed the expected potentiation effect. This fact can be justified by the total inactivation of *C. albicans* by the ROS species produced by the FORM before the formation of the iodide species produced by the combination of FORM + KI. When FORM was tested at 1.0 and 0.5 µM, the effectiveness of the inactivation also decreased (inactivation of 5.1 logs and 2.8 logs after 60 min and 90 min of treatment, respectively). At these low concentrations of PS, the addition of KI improved significanly the killing effect of FORM ($p<0.05$), by inactivating the yeast to the detention limit of the method after 30 and 45 min of treatment at 1.0 and 0.5 µM, respectively (reductions of 6.7 for both cases). These results showed by the first time the enormous advantage of the use of FORM and combinations of FORM + KI in the inactivation of *C. albicans*, where low light doses, low PS concetrations and reduced time, photoinactivate the yeast efficiently, to the detection limit of the method.

When these results are compared to the literature, this results are more noteworthy, even when the PS FORM was tested alone but also when tested with KI. When *C. albicans* was tested with Tetra-Py(+)-Me at 5 µM, which is included in the FORM, total inactivation was only observed after 270 min of irradiation time (with a light dose of 64.8 J/cm^2) (Beirão *et al.* 2014), but with the FORM, without KI, the total inactivation ocurred at 5.0 µM and after 10 min.

Fullerene derivatives when combined with KI were efficient PSs against *C. albicans in vitro* (20 µM of the PS and 10 mM of KI with 20-120 J/cm^2) and *in vivo* using a mouse model with an infected skin abrasion (Zhang *et al.* 2015), but in our study lower concentrations of FORM inactivated also effectively the fungus. MB and new methylene blue (NMB) were also applied in the inactivation of oral *C. albicans* infection in a mouse model (Freire *et al.* 2016) and BODIPY dyes in the inactivation of *C. albicans in vitro* (Reynoso *et al.* 2017), but, in both cases, the total inativation was achieved with higher PS concentrations when compared to the ones used in combinations of FORM + KI. In the case of porphyrin based PS, the $TPPS_4$ combined with KI was also more effective than the PS alone in the inactivations of *C. albicans* (L. Huang *et al*. 2018a).

T4-like bacteriophages are non-enveloped virus and consequently less susceptible to aPDT than enveloped viruses (Costa, Faustino, *et al.* 2012). The FORM at 2.0, 1.0 and 0.5 µM as well the combination of FORM at the same concentrations with KI were used to study the photinactivation profile of T4-like bacteriophages (Figure 3.5).

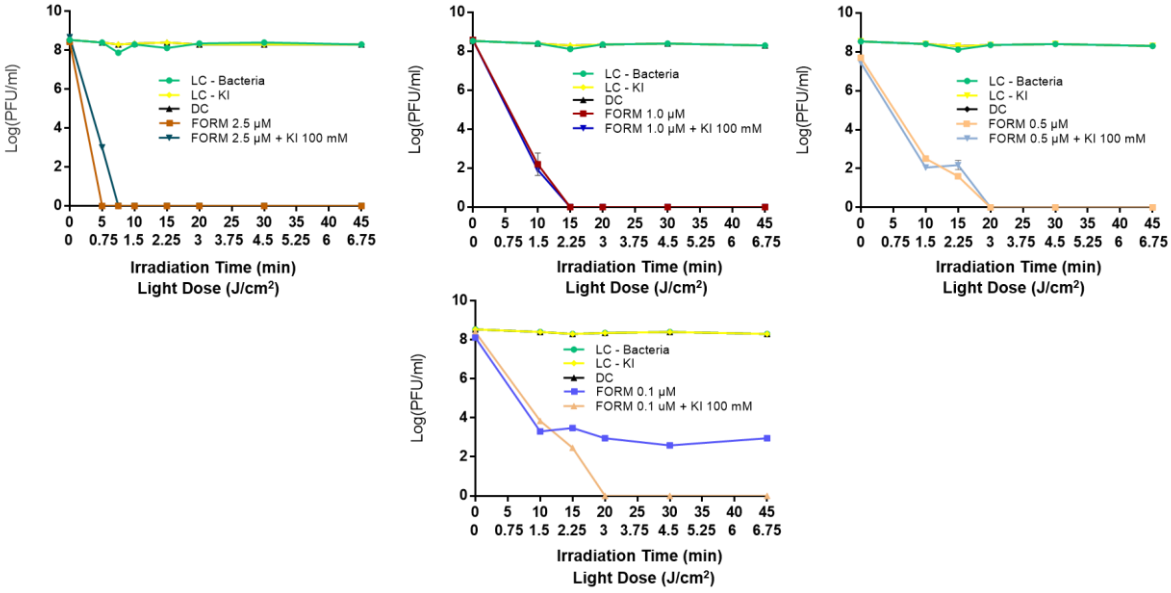

Figure 3.5 - Photodynamic inactivation of bacteriophage T4 by combination of KI and FORM at 0.1, 0.5, 1.0 and 2.5 µM during 45 min of irradiation with white light (25 W/m^2). Error bars represent the standard deviation. The values are expressed as the three independent experiments; error bars indicate the standard deviation.

In this case, the photoinactivation profile observed was quite different to the one observed for the bacteria and the fungus. Although FORM tested at different concentrations was able to inactivate efficiently the phage, the potentiated effect of combination FORM + KI was only observed for the lowest concetration of the FORM (0.1 µM). When FORM was tested at 0.1 µM, a reduction of 4.6 log was observed after 20 min of irradiation. The combination of FORM with KI inactivated to the detention limit of the method bacteriophage T4 (8.4 log), after 20 min of treatment. For the higher concentrations of FORM no significant differences were observed when FORM was used alone or combined with KI. As it was postulated for *C. albicans*, this fact can be justified by the total inactivation of the phage by the ROS species produced by the FORM before the formation of the iodide species produced by the combination of FORM + KI.

Nevertheless, our results showed that the FORM was more effective to inactivate this phage that some isolated porphyrins, such as Tetra-Py(+)-Me and Tri-Py(+)-Me-PF, which are also included in the FORM. The inactivation profile of T4-like phage with these isolated porphyrins occurs after longer periods of treatment (270 min and 180 min under 40 W/m^2, respectively) (Costa *et al.* 2008). Comparing our results with results obtained in similar studies using other cationic porphyrins, in general, FORM is more effective in the inactivation of non-enveloped viruses (reductions of 3 and 4 logs for MS2 phage and hepatitis A virus against reduction of 8.4 log for T4 like phage with FORM) (Almeida *et al.* 2011).

3.4.2. Photoinactivation of biofilms with combinations of FORM and KI

The ability of microorganisms to produce biofilms on surfaces is believed to contribute substantially to the pathogenesis of infection and for that reason it is urgent to find effective antimicrobial technologies for the destruction of this microbial three-dimensional structure (Hu *et al.* 2018).

In order to evaluate the aPDT effect of combination of FORM and KI on biofilms, different concentrations of FORM with KI at 100 mM were also evaluated towards biofilms forms of the Gram-negative bacterium *E. coli*, the Gram-positive bacterium *S. aureus and* the fungus *C. albicans.* Knowing that biofilms are less susceptible to aPDT than

their counterpart planktonic forms, FORM was tested at 20 µM under PAR white light at an irradiance of 25 W/m^2 during 60 min. The potentiated effect of combination of FORM + KI was also evaluated at 20 µM of FORM and at lower PS concentrations 10, 5.0, 1.0 µM of FORM, with 100 mM of KI. Also in this case, for all experiments LCs (microorganism), LCs + KI (microorganism + KI at 100 mM) and DCs (microorganism + FORM + KI at 100 mM in the dark) were evaluated and in all cases the viability of the biofilms forms was not been affected. These results indicate that the irradiation, the presence of salt and the combinations of the FORM with KI in the dark, does not affect the viability of the biofilms.

The results obtained for the photoinactivation of the different biofilms with FORM and FORM + KI are presented in Figure 3.6. FORM at 20 µM was not capable to destroy the biofilm matrix of *E. coli*, *S. aureus* and *C. albicans* (p>0,005), proving the difficulty in inactivate this microbial three-dimensional structure. However, when combinations of this FORM with KI was used to destroy the biofilms, it was observed a drastic aPDT effect. For *E. coli* and *S. aureus* biofilms, when KI was combined with FORM at 20 µM, 10 µM, 5.0 µM and 1.0 µM, the cells of the biofilms were inactivated aproximately in 7.5 log, reaching the limit of detention of the method. Although combination of KI with FORM at 0.5 µM did not totally inactivate *E. coli* and *S. aureus* in biofilm forms, it allowed a reduction of the viability of the cells in aproximately 1 log and 2 logs, respectively.

C. albicans biofilms showed to be more susceptible to aPDT with combinations of FORM + KI than bacterial biofilms, since concentrations of FORM 0.5 µM and KI at 100 mM was enough for destroy *C. albicans* biofilms to the detention limit of method after 60 min of treatment (9 J/cm^2). The same susceptibility for aPDT was also observed in the plancktonic cells: the photonactivation till de detection limit of *C. albicans* occurs after 5 min of irradiation with 5.0 µM of FORM and the same results was achieved with combination FORM 5.0 µM + KI. This result was not achieved for the other microrganims. These results indicate that *C. albicans* biofilms destruction with the FORM is easier than the destruction of bacterial biofilms. Comparing these results with those obatained with other PS, the same finding was obtained (Beirão *et al.* 2014), which suggest that it is esier to destroy fungi biofilms than bacterial biofilms with aPDT. Several PS with different structural features (porphyrinic and non porphyrinic) has being also imployed in the aPDT

of biofilms *in vitro*, but also in animal models, corresponding to aPDT of preclinical infections (Cieplik *et al.* 2018, Hu *et al.* 2018). In most cases it is described the use of high doses of irradiation and/or high concentrations of PS to achieve total destruction of bacterial and yeast biofilms. The tetra cationic porphyirin Tetra-Py(+)-Me at 20 µM (one of the five porphyrins presents on FORM) showed that it is capable to inactivated *C. albicans* biofilms to the detention limit after 180 min of irradiation (43.2 J/cm^2) (Beirão *et al.* 2014). *P. aeruginosa* and *S. aureus* were less susceptible to aPDT, with rates of decrease of 2.8 logs and 6.3 logs, respectively (Beirão *et al.* 2014). Our achievement are in line with these results but showed that it is possible to destroy *S. aureus* and *C. albincans* biofilms successfully with lower light doses and lower PS concentration when the FORM is used as PS. Phenothiazine photosensitizers Methylene Blue and Toluidine Blue were also studied in the photoinactivation of *S. aureus* and *E. coli* biofilms (Vilela *et al.* 2012). These PSs showed to be efficient against *S. aureus* and *E. coli* biofilm-structured in which the best results were achieved with approximately 300 µM methylene blue, with microbial reductions of 0.8–1.0 log; 150 µM toluidine blue, with a light source of 105 mW/cm^2 for a period of *c.a.* 3 min. Again, the combination of FORM + KI allowed significant improvement in the destruction of *S. aureus* and *E. coli* biofilm-structured, since the concentration of PS was more than 100 times lower. The *in vivo* inactivation of *C. albicans* biofilms promoted by methylene blue at 100 µM + KI at 100 mM and new methylene blue (NMB) 100 µM + KI at 100 mM was also reported in immunosuppressed mouse model of oral candidiasis infection (Freire *et al.* 2016). In this case, the higher destruction of such biofilms (*in vitro* studies) was attained with Methylene Blue + KI (2.31 log) with 31 mW/cm^2 during 3 min (5.58 J/cm^2) and NMB without KI (1.77 log) with 31 mW/cm^2 during 10 min (18.6 J/cm^2) These conditions were chosen for treating the *in vivo* model of oral *Candida* infection and, after 5 days of treatment, the disease was practically eradicated, especially using MB + KI with 263.15 mW/cm^2 during 3 min (47.37 J/cm^2). Despite the structural differences between these PSs and FORM, it is undeniable the potential of FORM combined with KI, allowing the destruction of *C. albicans* biofilms with lower light doses (9 J/cm^2) and lower PS concentrations (200 times lower).

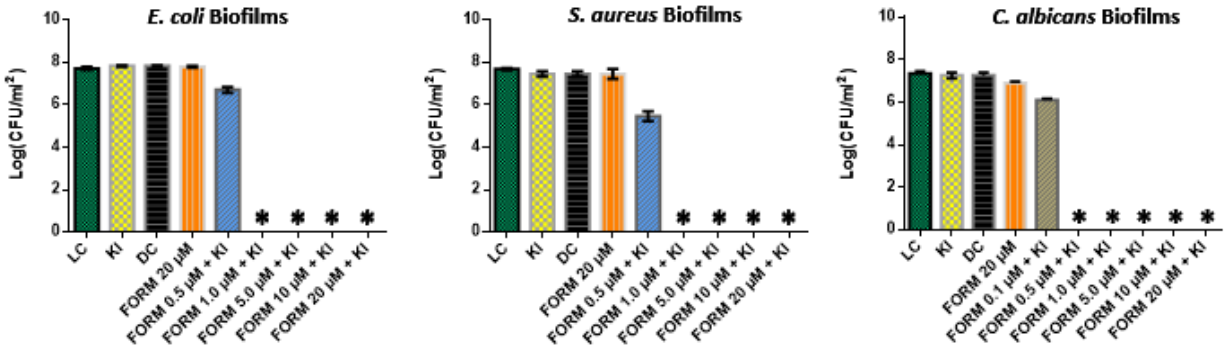

Figure 3.6 - Photodynamic inactivation of biofilms of *E. coli*, *S. aureus* or *C. albicans* by FORM at 1 µM, 0.5 µM and/or 0.1 with or without KI; All the essays were performed with white light (25 W/m^2) and 60 min of irradiation (9 J/cm^2). Error bars represent the standard deviation. The values are expressed as the three independent experiments; error bars indicate the standard deviation. Samples which reached the totally inactivation are represented by (*).

3.4.3. Prevention of biofilms development through aPDT with combinations of FORM and KI

Althought aPDT consists on a valuable technique to destroy well-stablished microorganisms in their complex organized biofilm forms and planktonic forms, the regrowth of the bacteria can happen after the aPDT protocol, difficulting the treatment of infections and its application to prevent the formation of biofilms.

The promissing results obtained with the combination of FORM + KI in the photoinactivation of plancktonic and biofilms forms of *E. coli* and *S. aureus*, led us to study the effect of this combination in the prevention of biofilms development after aPDT protocol. In this case, each microorganism was incubated with lower concentrations of FORM (0.1 and 1.0 µM) and FORM (1.0, 0.1, 0.05 µM) + KI at 100 mM than the ones used on planktonic forms and then subjected to aPDT protocol (60 min of irradiation under PAR white light at an irradiance of 25 W/m^2). The viability of each microorganism was evaluated immediately after the aPDT protocol and after 24 h of incubation at 37 ^{o}C in the dark. LCs (microorganisms exposed to light) were also evaluated and in all cases the viability of the microorganisms was not effect. The results obtained fo *E. coli* and *S. aureus* are presented in Figures 3.7 and 3.8, respectively.

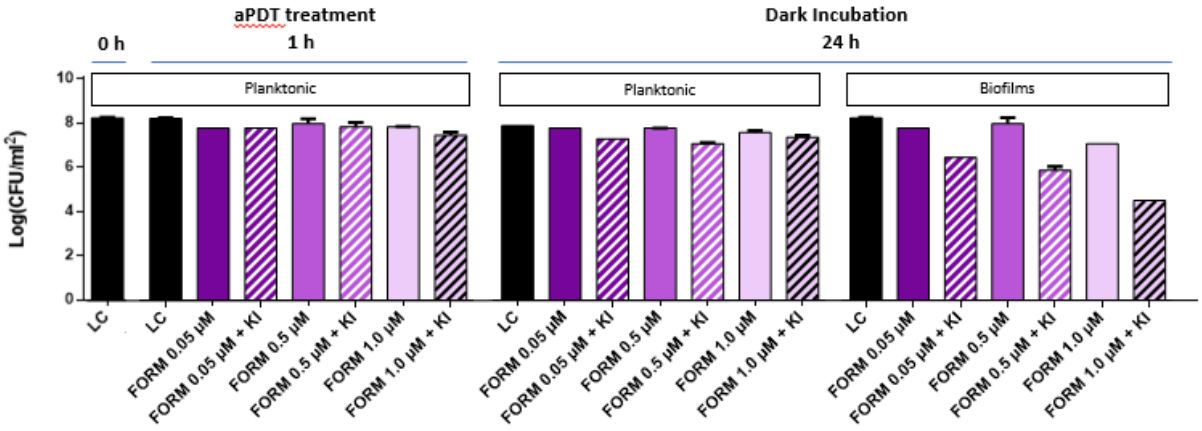

Figure 3.7 – Inactivation of *E. coli* planktonic cells and prevention of biofilms formation by FORM at 1.0 µM, 0.5 µM and 0.05 µM with or without KI; Samples were firstly submited to an aPDT treatment (60 of irradiation with white light (25 W/m^2) with sub-inibitory concentrations of FORM and KI. The efficacy of the treatment was evaluated. Afterwards, samples were incubated in the dark for 24 h. The evaluation of non-adherent cells and biofilms forms were perforrmed. Error bars represent the standard deviation. The values are expressed as the three independent experiments; error bars indicate the standard deviation. Samples which reached the totally inactivation are represented by (*). Due to the high quantity of data, the results of DCs and LCs – KI are not represented.

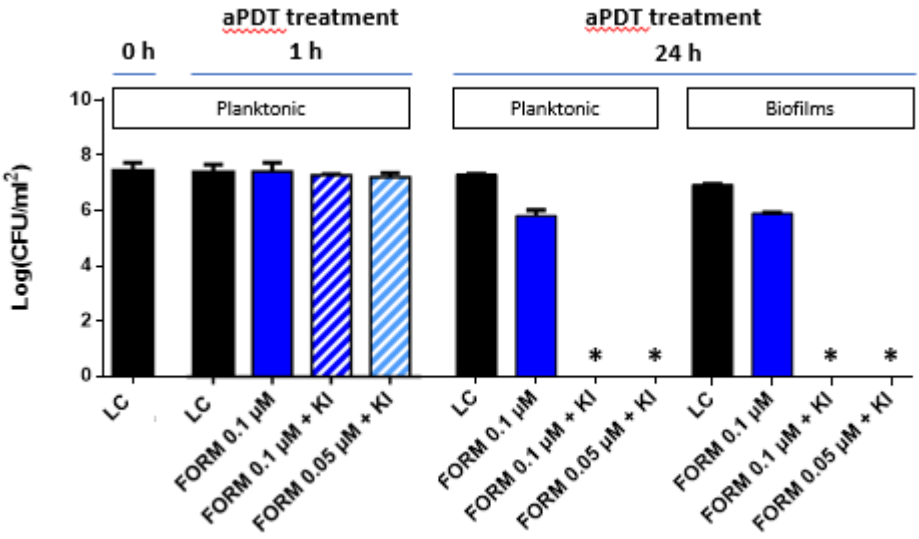

Figure 3.8 - Inactivation of *S. aureus* non-adherent cells and prevention of biofilms formation by FORM at 0.1 µM and 0.05 µM with or without KI; Samples were firstly submited to an aPDT treatment (60 of irradiation with white light (25 W/m^2) with sub-inibitory concentrations of FORM and KI. The efficacy of the treatment was evaluated. Afterwards, samples were incubated in the dark for 24 h. The evaluation of non-adherent cells and biofilms forms were perforrmed. Error bars represent the standard deviation. The values are expressed as the three independent experiments; error bars indicate the standard deviation. Samples

which reached the totally inactivation are represented by (*). Due to the high quantity of data, the results of DCs and LCs – KI are not represented.

The use of FORM at 0.1 and 1.0 µM in the treatment of planktonic cells of *E. coli* did not produce any inactivation effect on this bacterium. These results as expected as the PS was used at low concentrations and since the short-lived ROS formed by PS are only produced during the the irradiation protocol (Huang, Wintner, *et al.* 2018). The same profile was observed after 24 h of the aPDT protocol, where neither the plancktonic cells were inactivated nor the formation of biolfim was avoided. Also when combinations of FORM at 1.0, 0.1 and 0.05 µM + KI 100 mM were used, no significant photodynamic effect was observed for the *E. coli* plancktonic forms. Even after the period of incubation in dark (24 h), the reduction in the *E. coli* plancktonic cells that did not adhere to form biofilm was not significant for all the tested combinations. However, the cells of the *E. coli* that formed biofilms suffer a decrease of 1.8 logs ($p<0.05$) for the combination FORM 0.05 µM + KI 100 mM, of 2.4 logs ($p<0.05$) and 3.7 logs ($p<0.05$) for the combination of FORM 0.1 µM + KI and FORM 1.0 µM + KI with, respectively. This fact clearly shows that, despite FORM at these concentrations are not capable to inactivate the planktonic cells even after 24 h of the aPDT protocol, the *E. coli* viability was affected in such way that its biofilm formation capacity was reduced. It was also clear that the decrease in the ability to form biolfilms was dependent on the FORM concentration, which led us to believe that higher concentrations of FORM, por example 5 µM, combined with KI, may lead to the total inhibition of the ability in the *E. coli* biofilm formation. Moreover, it is also expected that the increase in the FORM concentration as well as the application of several cycles of irradiation, will lead to total inhibition of biofilm development by *E. coli* cells. These experiments are already ongoing in our laboratory.

The results obtained in the prevention of the *S. aureus* biofilm formation show, once again, the high susceptibility of these Gram-positive bacteria to aPDT. In this case, neither FORM nor combinations of FORM with KI affect the viability of *S. aureus* imediatatly after the aPDT. The viability of the plancktonic non-adherent cells and biofilm forms of *S. aureus* treated with FORM at 0.1 µM and incubated in the dark (after aPDT protocol) suffered a tiny decrase o *c.a.* 1 log ($p>0.05$), when compared to the control.

However, when both combinations of FORM + KI were used, even using low FORM concentrations, it was observed the total photinactivation of the non-adherent cells and the *S. aureus* biolfilm formation was avoided. This extended photodynamic effect during the dark incubation period of 24 h after aPDT performed in the presence of KI seems be due to the iodine long-lived species produced by the combination of the FORM + KI, that continue to inactivate the *E. coli* after the irradiation (Wen *et al*. 2017; Y. Y. Huang *et al*. 2018). This effect was also referred by Huang (2018) where the use of Methlylene Blue combined with KI avoided the regrowth of *E. coli* (Y. Y. Huang *et al*. 2018).

These results of this study show that the combination of FORM with KI, besides kill the bacteria, affect bacterial metabolic activity even at low PS concentration, inhibiting the biofilm formation, probably influencing the virulence characteristics, the quorum sensing and the exopolissacharides (EPS) production.

3.5. Conclusion

In conclusion, FORM combined with KI represents a prevailing antibacterial, antifungal and antiviral PS, destroying, in low concentrations, planktonic and pre-formed biofilm and also preventing the development of biofilms. These features could be usefull to the translation of this aPDT protocol to the field

3.6. References

Almeida, A., Cunha, A., Faustino, M.A.F., Neves, M.G.P.M.S., and Tome, A.C., 2011. Porphyrins as Antimicrobial Photosensitizing Agents, 11, 83-160.

Alves, E., Carvalho, C.M.B., Tomé, J.P.C., Faustino, M.A.F., Neves, M.G.P.M.S., Tomé, A.C., Cavaleiro, J.A.S., Cunha, Â., Mendo, S., and Almeida, A., 2008. Photodynamic inactivation of recombinant bioluminescent *Escherichia coli* by cationic porphyrins under artificial and solar irradiation. Journal of Industrial Microbiology and Biotechnology, 35 (11), 1447–1454.

Alves, E., Faustino, M.A.F., Neves, M.G.P.M.., Angela, C., Helena, N., and Adelaide, A., 2014. Potential applications of porphyrins in photodynamic inactivation beyond the medical scope. Journal of Photochemistry and Photobiology, 22, 34-57.

Alves, E., Faustino, M.A.F., Tomé, J.P.C., Neves, M.G.P.M.S., Tomé, A.C., Cavaleiro, J.A.S., Cunha, Â., Gomes, N.C.M., and Almeida, A., 2011. Photodynamic antimicrobial chemotherapy in aquaculture: Photoinactivation studies of *Vibrio fischeri*. PLoS ONE, 6 (6).

Beirão, S., Fernandes, S., Coelho, J., Faustino, M.A.F., Tomé, J.P.C., Neves, M.G.P.M.S., Tomé, A.C., Almeida, A., and Cunha, A., 2014. Photodynamic inactivation of bacterial and yeast biofilms with a cationic porphyrin. Photochemistry and Photobiology, 90 (6), 1387–1396.

Cieplik, F., Deng, D., Crielaard, W., Buchalla, W., Hellwig, E., Al-Ahmad, A., and Maisch, T., 2018. Antimicrobial photodynamic therapy–what we know and what we don't. Critical Reviews in Microbiology, 44 (5), 571–589.

Costa, L., Alves, E., Carvalho, C.M.B., Tomé, J.P.C., Faustino, M.A.F., Neves, M.G.P.M.S., Tomé, A.C., Cavaleiro, J.A.S., Cunha, Â., and Almeida, A., 2008. Sewage bacteriophage photoinactivation by cationic porphyrins: A study of charge effect. Photochemical and Photobiological Sciences, 7 (4), 415–422.

Costa, L., Faustino, M.A.F., Neves, M.G.P.M.S., Cunha, Â., and Almeida, A., 2012. Photodynamic inactivation of mammalian viruses and bacteriophages. Viruses, 4 (7), 1034–1074.

Costerton, J.W., Stewart, P.S., and Greenberg, E.P., 1999. Bacterial Biofilms: A Common Cause of Persistent Infections. Science, 284, 1318.

Donnelly, R.F., McCarron, P.A., and Tunney, M.M., 2008. Antifungal photodynamic therapy. Microbiological Research, 163 (1), 1–12.

Freire, F., Ferraresi, C., Jorge, A.O.C., and Hamblin, M.R., 2016. Photodynamic therapy of oral Candida infection in a mouse model. Journal of Photochemistry and Photobiology B: Biology, 159, 161–168.

Hamblin, M.R., 2017. Potentiation of antimicrobial photodynamic inactivation by inorganic salts. Expert Review of Anti-Infective Therapy, 15 (11), 1059–1069.

Hamblin, M.R., 2018. Upconversion in photodynamic therapy: Plumbing the depths. Dalton Transactions, 47 (26), 8571–8580.

Høiby, N., 2017. A short history of microbial biofilms and biofilm infections. APMIS, (6), 272–275.

Hu, X., Huang, Y.Y., Wang, Y., Wang, X., and Hamblin, M.R., 2018. Antimicrobial photodynamic therapy to control clinically relevant biofilm infections. Frontiers in Microbiology, 9, 1–24.

Huang, L., Bhayana, B., Xuan, W., Sanchez, R.P., McCulloch, B.J., Lalwani, S., and Hamblin, M.R., 2018. Comparison of two functionalized fullerenes for antimicrobial photodynamic inactivation: Potentiation by potassium iodide and photochemical mechanisms. Journal of Photochemistry and Photobiology B: Biology, 186, 197–206.

Huang, L., El-Hussein, A., Xuan, W., and Hamblin, M.R., 2018. Potentiation by potassium iodide reveals that the anionic porphyrin TPPS4 is a surprisingly effective photosensitizer for antimicrobial photodynamic inactivation. Journal of Photochemistry and Photobiology B: Biology. 178, 277–286.

Huang, L., Szewczyk, G., Sarna, T., and Hamblin, M.R., 2017. Potassium Iodide Potentiates Broad-Spectrum Antimicrobial Photodynamic Inactivation Using Photofrin. ACS Infectious Diseases, 3 (4), 320–328.

Huang, Y.-Y., Wintner, A., Seed, P.C., Brauns, T., Gelfand, J.A., and Hamblin, M.R., 2018. Antimicrobial photodynamic therapy mediated by methylene blue and potassium iodide to treat urinary tract infection in a female rat model. Scientific Reports, 8 (1), 7257.

Huang, Y.Y., Choi, H., Kushida, Y., Bhayana, B., Wang, Y., and Hamblin, M.R., 2016. Broad-spectrum antimicrobial effects of photocatalysis using titanium dioxide nanoparticles are strongly potentiated by addition of potassium iodide. Antimicrobial Agents and Chemotherapy, 60 (9), 5445–5453.

Jori, G., Camerin, M., Soncin, M., Guidolin, L., and Coppellotti, O., 2011. Antimicrobial Photodynamic Therapy: Basic Principles. The Royal Society of Chemistry, 11, 1–18.

Liu, Y., Qin, R., Zaat, S.A.J., Breukink, E., and Heger, M., 2015. Antibacterial photodynamic therapy: overview of a promising approach to fight antibiotic-resistant bacterial infections. Journal of Clinical and Translational Research, 1 (3), 140–167.

Marciel, L., Mesquita, M.Q., Ferreira, R., Moreira, B., Neves, M.G.P.M.S., Faustino, M.A.F., and Almeida, A., 2018. An efficient formulation based on cationic porphyrins to photoinactivate *Staphylococcus aureus* and *Escherichia coli*. Future Science, 10, 1821–1833.

Martins, D., Mesquita, M.Q., Neves, M.G.P.M.S., Faustino, M.A.F., Reis, L., Figueira, E., and Almeida, A., 2018. Photoinactivation of *Pseudomonas syringae pv. actinidiae* in kiwifruit plants by cationic porphyrins. Planta, 248 (2), 409–421.

Minnock, A., Vernon, D.I., Schofield, J., Parish, J.H., and Brown, S.B., 2000. Mechanism of Uptake of a Cationic Water-Soluble Pyridinium Zinc Phthalocyanine across the Outer Membrane of *Escherichia coli* Mechanism of Uptake of a Cationic Water-Soluble Pyridinium Zinc Phthalocyanine across the Outer Membrane of *Escherichia coli*. Antimicrobial Agents and Chemotherapy, 44 (3), 522–527.

Reynoso, E., Quiroga, E.D., Agazzi, M.L., Ballatore, M.B., Bertolotti, S.G., and Durantini, E.N., 2017. Photodynamic inactivation of microorganisms sensitized by cationic BODIPY derivatives potentiated by potassium iodide. Photochemical and Photobiological Sciences, 16 (10), 1524–1536.

Silva, Y.J., Costa, L., Pereira, C., Cunha, Â., Calado, R., Gomes, N.C.M., and Almeida, A., 2014. Influence of environmental variables in the efficiency of phage therapy in aquaculture. Microbial Biotechnology, 7 (5), 401–413.

Simões, C., Gomes, M.C., Neves, M.G.P.M.S., Cunha, Â., Tomé, J.P.C., Tomé, A.C., Cavaleiro, J.A.S., Almeida, A., and Faustino, M.A.F., 2016. Photodynamic inactivation of *Escherichia coli* with cationic meso-tetraarylporphyrins - The charge number and charge distribution effects. Catalysis Today, 266, 197–204.

Takasaki, A.A., Aoki, A., Mizutani, K., Schwarz, F., Sculean, A., Wang, C.-Y., Koshy, G., Romanos, G., Shikawa, I., and Zumi, Y., 2009. Application of antimicrobial photodynamic therapy in periodontal and peri-implant diseases. Periodontology 51, 109–140.

Tavares, A., Carvalho, C.M.B., Faustino, M.A., Neves, M.G.P.M.S., Tomé, J.P.C., Tomé, A.C., Cavaleiro, J.A.S., Cunha, Â., Gomes, N.C.M., Alves, E., and Almeida, A., 2010. Antimicrobial Photodynamic Therapy: Study of Bacterial Recovery Viability and

Potential Development of Resistance after Treatment. Marine Drugs, 8 (12), 91–105.

Vecchio, D., Gupta, A., Huang, L., Landi, G., Avci, P., Rodas, A., and Hamblina, M.R., 2015. Bacterial photodynamic inactivation mediated by methylene blue and red light is enhanced by synergistic effect of potassium iodide. Antimicrobial Agents and Chemotherapy, 59 (9), 5203–5212.

Vieira, C., Gomes, A.T.P.C., Mesquita, M.Q., Moura, N.M.M., Neves, M.G.P.M.S., Faustino, M.A.F., and Almeida, A., 2018. An Insight Into the Potentiation Effect of Potassium Iodide on aPDT Efficacy. Frontiers in Microbiology, 9, 1–16.

Vilela, S.F.G., Junqueira, J.C., Barbosa, J.O., Majewski, M., Munin, E., and Jorge, A.O.C., 2012. Photodynamic inactivation of *Staphylococcus aureus* and *Escherichia coli* biofilms by malachite green and phenothiazine dyes: An in vitro study. Archives of Oral Biology, 57 (6), 704–710.

Wen, X., Zhang, X., Szewczyk, G., El-Hussein, A., Huang, Y.Y., Sarna, T., and Hamblin, M.R., 2017. Potassium iodide potentiates antimicrobial photodynamic inactivation mediated by Rose bengal in in vitro and in vivo studies. Antimicrobial Agents and Chemotherapy, 61 (7), e00467-17.

Zhang, Y., Dai, T., Wang, M., Vecchio, D., Chiang, L.Y., and Hamblin, M.R., 2015. Potentiation of antimicrobial photodynamic inactivation mediated by a cationic fullerene by added iodide: In vitro and in vivo studies. Nanomedicine, 10 (4), 603–614.

Chapter IV: General Conclusions and Future Perspectives

4.1. **Conclusions**

In In this work a series of experiments were performed to gain a more comprehensive knowledge about the aPDT potentiation by KI on *E. coli* inactivation, namely the importance of the PS structural characteristics to this process. Additionally, it was evaluated the combined effect of KI and FORM, which was selected based on the previous study, on aPDT against planktonic and biofilms forms of a broad-spectrum of microorganisms, as well to prevent the biofilm formation of gram-negative and gram-positive bacteria.

The main conclusions of this work are summarized in the following topics:

Chapter II - An Insight into the Potentiation Effect of Potassium Iodide on aPDT Efficacy:

The non-toxic salt KI efficiently potentiated the aPDT effect of some cationic PSs on *E. coli* inactivation allowing the reduction of the treatment time. The PSs were divided in three categories, according to their enhancer effect by KI:

- Tri-Py(+)-Me, Tetra-Py(+)-Me, FORM, RB and MB – PSs whose efficiency potentiated by KI was accompanied by an abrupt decrease in the *E. coli* survival rate.
- β-ImiPhTPP, β-ImiPyTPP, and β-BrImiPyTPP – PSs whose efficiency potentiated by KI accompanied by a gradual decrease in the *E. coli* viability concentration.
- Di-Py(+)-Me opp, Di-Py(+)-Me adj, Tetra-Py, TBO, CV, and MG – PSs whose efficacy was not improved by the presence of the coadjuvant.
- The most promising PSs to be applied in combination with KI, were those capable to decompose the peroxyiodide into iodine (demonstrated in this study by spectroscopy and by the visual appearance of a blue color in the presence of amylose).
- Our study confirmed that the generation of $^1O_2$ is an important factor in the aPDT potentiation effect by KI, and showed that are also others features to be taken in account such as:

- PS structure (charge number and charge position)
- Aggregation properties
- Affinity for the cell membrane

Chapter III - Advances in the photoinactivation by a cationic porphyrinic formulation with potassium iodide: effectiveness on planktonic and biofilm forms of bacteria, fungi and viruses.

Planktonic

- FORM was an efficient PS to inactivate the planktonic forms of *E. coli, S. aureus*, *C. albicans* and a T4 like bacteriophage.
- The combination of KI with FORM potentiated the inactivation of the planktonic forms of all microorganisms, allowing to reduce the PS concentration and the treatment time.
    - For *E. coli*, FORM at 5.0 µM was incapable to totally inactivate the bacteria even after 120 min of treatment. However, aPDT in the presence of KI allowed to inactivate *E. coli* to the detention limit of the method, reducing the treatment time to 120 min, and the PS concentration from 5.0 µM to 2.5 µM.
    - For *S. aureus* and *C. albicans*, the coadjuvant allowed a reduction of treatment time from more than 120 min to 45 min and of the PS concentration from 5.0 µM. to 0.5 µM.
    - For bacteriophage T4, the addition of KI permitted to reduce the treatment time from more than 45 min to 20 min and the concentration of PS from 2.5 µM to 0.1 µM.

- At the higher tested concentrations of FORM, the addition of KI produces a similar inactivation profile of *C. albicans* and bacteriophage T4 to the one observed for FORM (at 5.0 µM of FORM to the yeast, and at 2.5 µM, 1.0 µM, and 0.5 µM to the virus). It is possible that both microorganisms were

inactivated by the ROS species produced by the FORM before the formation of the iodide species produced by the combination of FORM + KI.

Biofilms

- The FORM at 20 μM failed to destroy bacterial biofilms after 60 min of aPDT treatment.
- The combination of KI with FORM allowed the destruction of biofilms forms of both bacteria and also the reduction of the FORM concentrations.
    - For *E. coli* and *S. aureus*, the destruction of biofilms forms was achieved when KI was combined with FORM at 20 μM, 10 μM, 5.0 μM and 1.0 μM.
    - *C. albicans* biofilms were even more susceptible to aPDT than the gram-negative bacterium and the gram-positive bacterium biofilms. The biofilms were destroyed with the combination of KI and FORM at 20 μM, 10 μM, 5.0 μM and 1.0 μM.
- The combination of KI with FORM was useful on impacting and preventing the formation of biofilms of *E. coli* and *S. aureus*.
    - Although the combination of KI with FORM at 1.0 μM and 0.1 μM were incapable to inactivate the planktonic cells even after 1 h of aPDT, the inactivation of *E. coli* in the biofilm form was reduced in 1.3 logs and 2.1 logs after 24 h of dark incubation.
    - The prevention of *S. aureus* formation was achieved with the combination of FORM at 0.1 μM and 0.05 μM.
    - The extended photodynamic effect during the dark incubation period of 24 h after aPDT in the presence of KI may be due to iodine long-lived species produced by the combination of the FORM + KI, that continue to inactivate the *E. coli* and *S. aureus* after the irradiation period.

4.2. Future perspectives:

The potentiation of aPDT by KI has specially awakened the scientific community interest, since it allows the reduce of the treatment time and PS concentration, turning aPDT in a more feasible approach.

Since KI has already been approved for clinical use, in the future we aim to:

- Test the effect of higher concentrations of FORM, por example 5 μM, combined with KI, in the inhibition of *E. coli* biofilm formation.
- Assess the ability of the combination of FORM and KI to prevent the formation of *C. albicans* biofilms.
- Perform *in vivo* studies with the combination of FORM + KI.
- Determine if FORM + KI have influence on the virulence characteristics, the quorum sensing and the exopolissacharides (EPS) production during the biofilms formation.

CHAPTER V Appendix